2011

Sensory Organ Morphogenesis in Caenorhabditis Elegans

Grigorios Oikonomou

Sensory Organ Morphogenesis in *Caenorhabditis elegans*

A Thesis Presented to the Faculty of

The Rockefeller University

in Partial Fulfillment of the Requirements for

the degree of Doctor of Philosophy

by

Grigorios Oikonomou

June 2011

Sensory Organ Morphogenesis in *Caenorhabditis elegans*

Grigorios Oikonomou, Ph.D.

The Rockefeller University 2011

Sensory organs are the gates through which information flows into the nervous system. In most animals, such organs consist of sensory neurons, which can transform stimuli into changes in their membrane potential, and glial cells, which establish a niche important for the morphogenesis and function of the neurons. Although similar glial compartments are seen throughout the nervous system, their morphogenesis is poorly understood. In the work presented here, I use the main sensory organ of *Caenorhabditis elegans*, the amphid, as a model system for understanding how glia form these compartments.

First, by the interpretation of electron microscopy reconstructions of the developing amphid, I was able to uncover a role for *daf-6*/Patched, an established regulator of amphid morphogenesis, in restricting the size of the sensory compartment.

Second, I sought to identify genes acting in the opposite direction, in expanding the sensory compartment, by cloning and characterizing suppressors of *daf-6*. Through this approach I discovered that *lit-1*/Nlk acts within glia, in counterbalance to *daf-6*, to promote sensory compartment expansion. Although LIT-1 has been shown to regulate Wnt signaling, my genetic studies demonstrate a novel, Wnt-independent role for LIT-1 in sensory compartment size control. The LIT-1 activator MOM-4/TAK1 is also important for compartment morphogenesis and both proteins line the glial sensory

compartment. LIT-1 compartment localization is important for its function and requires neuronal signals. Furthermore, the conserved LIT-1 C-terminus is necessary and sufficient for this localization. Two-hybrid and co-immunoprecipitation studies demonstrate that the LIT-1 C-terminus binds both actin and the Wiskott-Aldrich syndrome protein (WASP), an actin regulator. I show that actin also lines the sensory compartment, and that WASP is important for compartment expansion, potentially by functioning in the same pathway as LIT-1. These results suggest that the *daf-6* and *lit-1* glial pathways constitute a rheostat used to control sensory compartment size.

Finally, I also identify a role for the retromer complex, a module involved in the recycling of transmembrane proteins and membrane material from the endosomes to the Golgi apparatus, in amphid morphogenesis. Similar to *lit-1*, mutations of retromer components suppress *daf-6*, suggesting that the retromer could also act in promoting sensory compartment expansion.

για την Κατερίνα μου

Acknowledgements

First, I would like to thank my advisor **Shai Shaham**. Shai is an extraordinary scientist with a deep and contagious enthusiasm for understanding how the world – anything in the world– works. He is also a charismatic and extremely patient teacher, who always kept both his door, and his mind, open for me. I cannot overstate the importance of his guidance and constant encouragement for the success of my research, and my development as a scientist.

It was a great honor and pleasure to have **Drs. Cori Bargmann** and **Hermann Steller** serve on my academic committee. Their keen insights during our annual meetings were critical for the development of my research project. Their contribution, however, has extended far beyond this: they have always maintained a genuine interest in my progress as a student, and have been extremely generous with their advice and support for my career. I am also extremely grateful to **Dr. Fred Cross**; a critical part of my project was conducted in his lab and he has also been a most inspiring teacher. I would like to thank **Dr. Jeremy Nance** for graciously accepting to serve as my external committee member.

Shai has built an extraordinary lab, filled with professional, dedicated and simply nice people to work with. I am particularly indebted to my early guide in the lab **Elliot Perens**, and my long-term collaborator and talented electron microscopist **Yun Lu**. The advice, encouragement and guidance of all members of the Shaham lab has been generously offered to me since the day I joined the lab and is continuing to this day. I want to thank **Aakanksha**, **Carine**, **Carl**, **Elyse**, **Jennifer**, **Limor**, **Margherita**, **Mary**, **Maxime**, **Melanie**, **Menachem**, **Mike**, **Peter**, **Sean**, **Satoshi**, **Sharon** and **Taulant** for making the lab such a great place to do science. I am particularly grateful to my baymate **Max Heiman** for generously sharing his knowledge and expertise, and to **Maya Tevlin** for her advice and encouragement.

Shigeki Watanabe and **Dr. Erik Jorgensen** from the University of Utah were enthusiastic and gracious collaborators; I am thankful for their contributions and tenacity.

I want to thank the Dean's Office, **Sid**, **Emily**, **Kristen**, **Cris** and **Marta** for their constant help and support with all complications of academic life.

I am deeply indebted to all the **teachers** who opened my eyes to the world; too many to list, but always fondly remembered.

Tsouk, **Dani**, **Pan** and **Villy**; you know.

Ο πατέρας μου **Απόστολος**, η μητέρα μου **Νικολίτσα** και ο αδερφός μου **Νικόλαος**, μου πρόσφεραν περισσότερη αγάπη, στοργή και στήριξη από ότι μου άξιζαν. The addition of **Patricia** and **Andrew** to my family has made me even more embarrassed of my good fortune.

In the fall of 2005, I met my wife Catherine and the greatest adventure began. For more reasons than I can tell, I thank you **Cat**.

Table of Contents

List of Figures

List of Tables

Chapter 1

Introduction

Summary

In order for organisms to survive and thrive, they must be able to detect changes in their environment and respond accordingly. Most animals achieve this through a network of specialized cells, namely neurons and glia, which make up the nervous system. Sensory organs are the gates through which information flows into the nervous system from the environment. Within sensory organs, glia form compartments that isolate the receptive endings of sensory neurons. Such glial compartments encase many neuronal specializations in addition to sensory receptive endings, such as axons, synapses and neuromuscular junctions, and are important for neuronal physiology and function. In my graduate work, I sought to further our understanding of glial compartment morphogenesis within sensory organs using as a model system the development of the amphid, the main sensory organ of the nematode *Caenorhabditis elegans*. In this chapter I will try to summarize the observations that led to the development of my research project, and provide the necessary background for the interpretation of my findings.

1.1. Glial compartments surround neuronal specializations

The nervous system of most animals consists of two broad categories of cells, neurons and glia. Neuronal cells are physiologically and morphologically specialized for intercellular communication by electrical signaling. The dendrites of sensory neurons are able to transform a variety of chemical and physical stimuli into changes in their membrane potential and propagate these changes to the cell body. These changes are then further propagated through afferent axonal processes and reach other neuronal cells broadly referred to as interneurons or projections neurons. The propagation of the electrical signal from one neuron to another, across the extracellular space, is achieved through a specialized structure, the synapse. In synapses, the change of membrane potential in the presynaptic terminal stimulates the release of neurotransmitters that cross the synaptic cleft, bind to receptors found in the postsynaptic terminal, and induce a change in the membrane potential of the postsynaptic neuron. Interneurons and projection neurons are able to integrate and process signals from many different sources. After integration and processing of the information provided by the periphery, the appropriate response is generated. This response consists in the activation of a motor neuron or another kind of efferent neuron resulting in movement of the animal, secretion of a hormone, alteration of the arousal state, or a host of other adaptations to the original stimulus (Figure 1.1).

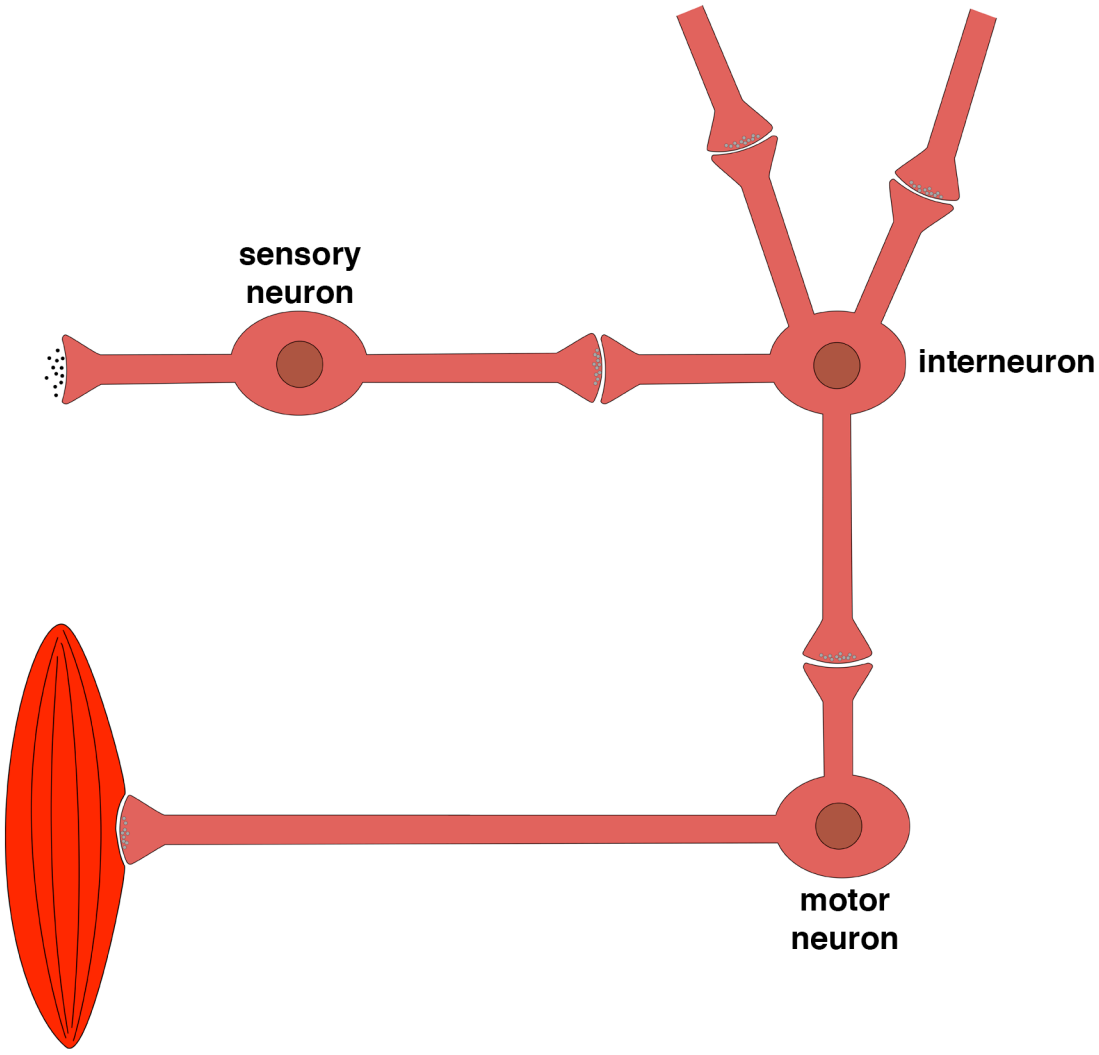

Figure 1.1. A diagrammatic representation of the nervous system. In response to a chemical stimulus, a sensory neuron transmits an electrical signal to an interneuron. After integration and processing of inputs from different sources, the interneuron activates a motor neuron that stimulates a muscle.

In all but the most rudimentary nervous systems, neurons neither exist, nor act alone; they are accompanied by glia. Glial cells can be loosely defined as cells that are not themselves neurons but are physically associated with neurons, and are often lineally related to them (Shaham, 2005). In vertebrates, four kinds of glia are traditionally described: Schwann cells in the periphery, astrocytes and oligodendrocytes in the central nervous system (CNS), and microglia, the resident macrophages of the CNS. A striking property of glia is the ability to create physical compartments that surround neuronal specializations. In the simplistic, bird's eye view of neuronal function presented above, these glial compartments are prominent in every step. Modified Schwann cells, or other cells with glial properties, surround and isolate the dendritic endings of sensory neurons. Schwann cells in the periphery and oligodendrocytes in the CNS surround axonal processes, wrapping them in tight membrane sheets called myelin. Astrocytes in the CNS extend processes that ensheath synapses by wrapping around the presynaptic and postsynaptic terminals, with each astrocyte ensheathing thousands of synapses. Astrocytes are also associated with the blood-brain barrier that isolates the CNS. Finally, Schwann cells surround most neuromuscular junctions in the periphery (Figure 1.2).

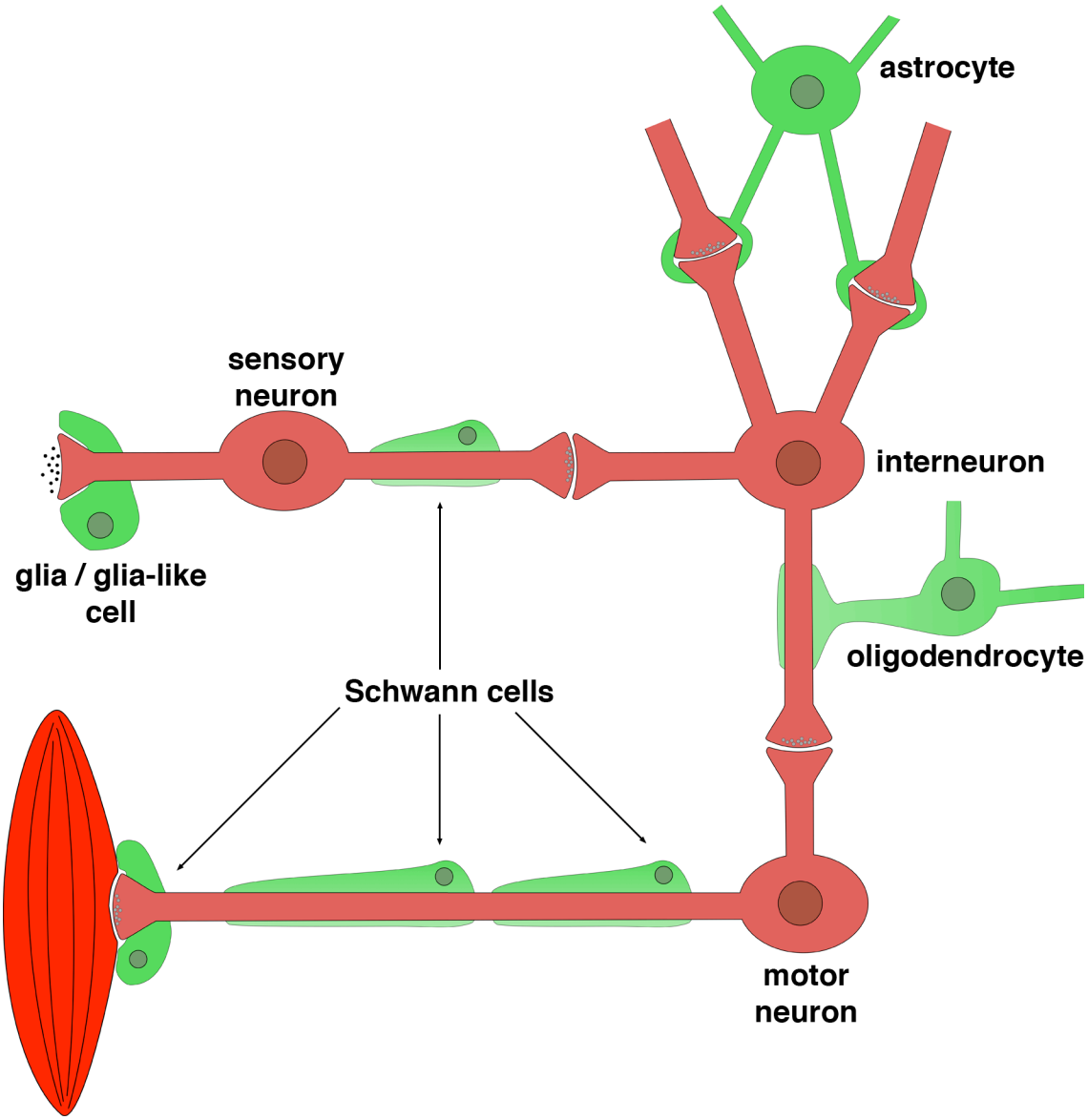

Figure 1.2. A representation of the nervous system that takes into account the glia. Glial cells form compartments around receptive endings of sensory neurons, axons, neuronal synapses and neuromuscular junctions.

We know a lot about what neurons do, less about how glia affect their function, and even less about how most of the glial compartments that enclose neurons are formed. In the next few sections of the introduction, I will discuss various examples of glial compartments and what we know about their morphogenesis.

1.2. Glial compartments in sensory organs

1.2.1. Glia in the sensory organs of *C. elegans*

Anatomy

Most studies of sensory organ morphogenesis in *C. elegans* have been performed within the context of the amphid, a bilateral sensory organ located at the head of the animal (Figure 1.3A). Each amphid consists of twelve sensory neurons and two glial cells, referred to as sheath and socket cells (Ward et al., 1975). Amphid neurons are bipolar, projecting an axon into the nerve ring (the main neuropil of the animal) and a dendrite anteriorly, to the tip of the nose (Figure 1.3B). The two amphid glia also extend anterior processes collateral to the dendrites. At the nose tip, sheath and socket glia form discrete single-cell tubular channels joined by adherens junctions (Figure 1.3C). The resulting two-cell compartment is open to the environment anteriorly and is referred to as the amphid sensory compartment, the amphid channel, or the amphid pocket. Of the twelve dendrites, eight extend non-motile, microtubule-based sensory cilia that travel the length of the channel to become exposed to the environment. These specialized receptive endings are sites of localization for receptors that recognize chemical and mechanosensory stimuli (Bargmann, 2006). The receptive endings of three other amphid

sensory neurons enter the compartment, but then divert and expand wing-like cilia into blind pockets within the sheath glial cell where the detection of volatile chemicals takes place. The remaining amphid sensory neuron, which senses temperature, is also embedded within the sheath glia, but its dendritic terminus does not track through the amphid compartment. All of the dendrites form tight junctions with the sheath glia, which, combined with the junctions between socket and sheath, ensure the isolation of the sensory compartment from the rest of the animal. The socket portion of the compartment is lined with cuticle and serves as a conduit for cilia to sample the animal's environment (Ward et al., 1975). The sheath glial cell, however, is an active secretory cell (Ward et al., 1975), releasing extracellular matrix proteins, at least some of which are required for sensory neuron function (Bacaj et al., 2008), into the sheath glia channel. An electron-dense, filamentous material surrounds the anterior portion of the sheath channel (Perkins et al., 1986).

Figure 1.3. The amphid sensory organ. (A) Schematic of an adult *C. elegans* hermaphrodite. The amphids are located in the head. (B) Each amphid consists of twelve neurons (in red; only one is drawn here for simplicity) and two glial cells, the sheath (AMsh, in green) and the socket (in blue). (C) Processes from the neurons and glia come together at the tip of the nose. The glial cells align to form the amphid sensory compartment (or amphid channel, or amphid pocket), through which some amphid neuron dendrites extend sensory cilia that adopt distinct morphologies: single cilia (neurons ASE, ASG, ASH, ASI, ASJ, ASK), double cilia (neurons ADF, ADL), wing cilia (neurons AWA, AWB, AWC) and the finger cilia of AFD. Tight junctions between the dendrites and the sheath glia, as well as between the sheath and socket glia, establish a niche for the sensory cilia. This niche is filled with matrix material secreted by the sheath glia. Thus, the site where the nervous system of the animal meets the environment is under the direct control of glia. The electron-dense dark material surrounding the anterior portion of the channel could be analogous to the terminal web of secretory cells. Adapted from Perkins et al., 1986.

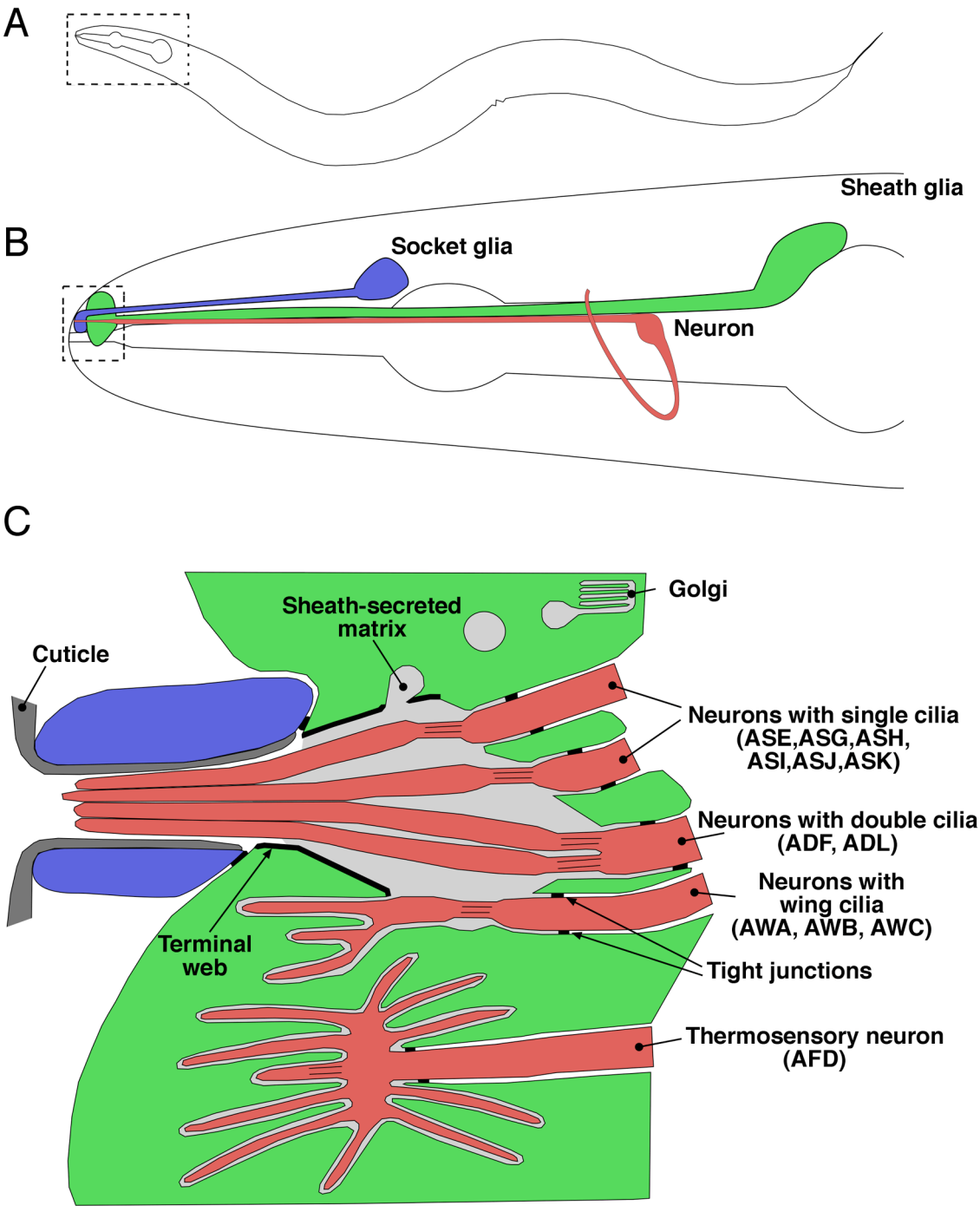
A
B
Sheath glia
Socket glia
Neuron
C
Golgi
Sheath-secreted matrix
Cuticle
Neurons with single cilia (ASE,ASG,ASH, ASI,ASJ,ASK)
Neurons with double cilia (ADF, ADL)
Neurons with wing cilia (AWA, AWB, AWC)
Terminal web
Tight junctions
Thermosensory neuron (AFD)

In addition to the amphids, six more classes of glia-containing sensory organs are found in *C. elegans*: the cephalic sensilla, the inner and outer labia, the anterior and posterior deirids and the phasmid. All of these organs have an architecture resembling that of the amphid, with neurons extending sensory dendrites through compartments formed by glial cells. *C. elegans* also has sensory neurons that are not associated with any glial cells.

C. elegans males possess four more classes of sensilla, located in the tail, that facilitate mating with hermaphrodites (Sulston et al., 1980): the hook, the spicules, the post-cloacal sensilla and the sensory rays. Although all of these male-specific sensilla include glial cells, studies of glia in the male have focused on the ray sensilla. Each ray consists of two sensory neurons that extend dendrites through a channel formed by a single glial cell known as the structural cell.

Morphogenesis

The amphid channel allows sensory neurons to communicate with the outside environment. A number of studies have provided insights into the morphogenesis of this compartment. These studies were initially enabled by the identification of *daf-6* (Riddle et al., 1981), a gene encoding a Patched-related transmembrane protein that acts within glia to regulate amphid morphogenesis (Herman, 1987; Perens and Shaham, 2005). In animals carrying mutations in the *daf-6* gene, the sheath glia compartment is bloated and malformed. Furthermore, sensory cilia appear trapped within the channel and are unable to reach the outside environment. *daf*-6 mutants are defective in behaviors that depend

on the direct contact of sensory neurons with the animal's surroundings (Albert et al., 1981; Perkins et al., 1986), suggesting that channel integrity is required for amphid functionality (Perens and Shaham, 2005).

DAF-6 lines the amphid channel and also localizes to apical surfaces of other luminal structures in *C. elegans*. Furthermore, animals mutant for both *daf-6* and *che-14*, a Dispatched homolog that is also important for amphid morphogenesis (Michaux et al., 2000), display defects in many tubular systems. These results suggest that the machinery for amphid compartment formation overlaps, at least to some extent, with that controlling tube formation, raising the possibility that glial ensheathment of neurons in other animals or contexts may also be related to tubulogenesis.

The amphid channel wraps snugly around the neuronal cilia it ensheaths, suggesting the possibility that a neuronal signal may be involved in controlling compartment diameter and shape. Interestingly, localization of DAF-6 along the length of this channel depends on the presence of neuronal sensory cilia. In animals carrying mutations that stunt or block cilia development, DAF-6 protein is no longer localized to the channel surface and accumulates instead in a punctate structure, which may localize to the sheath/socket junction (Perens and Shaham, 2005). Additionally, the compartment is slightly defective, with small branches forming laterally (Perens and Shaham, 2005).

Socket glia have been less intensively explored than their sheath glia counterparts. However, studies of the *C. elegans alr-1* gene support an important role for these cells in amphid structure. *alr-1* (Tucker et al., 2005) encodes the *C. elegans* homolog of the Paired class homeobox transcription factor Aristaless (Galliot et al., 1999), first

characterized in *Drosophila* (Schneitz et al., 1993). In humans, mutations of the Aristaless homolog ARX cause a range of neurological defects (Strømme et al., 2002). In *C. elegans*, *alr-1* animals hatch with no detectable abnormalities, but progressively lose amphid functionality as the animal grows. Ultrastructural studies revealed that in older *alr-1* mutants, the tight junctions between sheath and socket glia cannot be detected, while matrix material and sensory cilia can now be found throughout the tip of the head (Tucker et al., 2005).

The *alr-1* mutant defects reflect the importance of a precise and stable connection between the sheath and socket glial channels for sensory organ function. Embryonic ablation studies of socket glia progenitor cells reveal that long-range signaling may be involved in directing this connection. Specifically, Sulston et al. (Sulston et al., 1980) used a laser microbeam to ablate progenitor cells of specific sensory organ socket glia and found that the cognate neuron and sheath glia would associate with the socket glia of a different sensory organ. This observation suggests an active attraction between socket glia and neurons/sheath glia. The molecular basis of this attractive signal has not yet been determined.

Although the sensory compartment can form in the absence of cilia with only minor defects, glial and neuronal morphogenesis within the amphid sensory organ are intricately linked. The sensory neurons of the amphid extend dendrites over a length of about 100 microns towards the tip of the nose. These dendrites fasciculate into stereotyped bundles that run in parallel and in close proximity to the process of the amphid sheath glial cell. Recently, aspects of the mechanism underlying amphid process

extension and the coordination of glia and neuron process lengths have been described (Heiman and Shaham, 2009).

During embryogenesis, amphid sensory neurons are born near the tip of the developing head (Sulston et al., 1983). There they extrude a short projection that is attached to the tip of the nose. Posterior migration of the neuronal cell bodies then results in dendrite extension; a mechanism that has been coined retrograde extension (Heiman and Shaham, 2009). The tip anchor is composed of at least two proteins (Heiman and Shaham, 2009): the zona pellucida (ZP) domain protein DYF-7, which is secreted by the neurons, and DEX-1, a zonadhesin domain containing protein secreted by non-neuronal neighboring cells. DEX-1 and DYF-7 are similar to α and β tectorins, proteins that compose the tectorial membrane, an extracellular matrix that anchors hair cell cilia in the inner ear (Legan et al., 1997). Like the tectorins and other ZP domain proteins, DYF-7 can multimerize, and its multimeric state seems to be required for proper dendrite anchoring. These parallels suggest a common, evolutionarily conserved module utilized in sensory organ development.

dyf-7 and *dex-1* mutants are defective not only in the lengths of their amphid sensory dendrites, but also in the length of the sheath glia process, suggesting that the morphogenesis of neurons and glia in this sensory organ are tightly linked (Heiman and Shaham, 2009). Although it is not yet clear whether DEX-1 is expressed in the amphid sheath glia, other observations suggest a direct role for glia in amphid dendrite extension. First, ablation of the amphid sheath glia during embryogenesis results in short dendrites (Figure 1.4A), similar to the ones seen in *dyf-7* and *dex-1* animals (Taulant Bacaj and Shai Shaham, unpublished observations). A similar result is obtained in the cephalic

sensory organ where ablation of the CEPsh glia results in dendrite extension defects of the CEP neurons (Figure 1.4B) (Yoshimura et al., 2008). Second, expression of either *dex-1* or *dyf-7* cDNA by the amphid glia can rescue the dendrite extension defect of each respective mutant, suggesting that glia are positioned to establish or modify the extracellular matrix required for dendritic tip anchoring (Heiman and Shaham, 2009). Third, a study of amphid sheath glia gene expression using gene microarrays revealed that of the 298 glia-enriched gene transcripts, 159 encoded secreted/transmembrane proteins, including a number of proteins predicted to contain ZP domains that could, perhaps, interact with DYF-7 and DEX-1 (Bacaj et al., 2008).

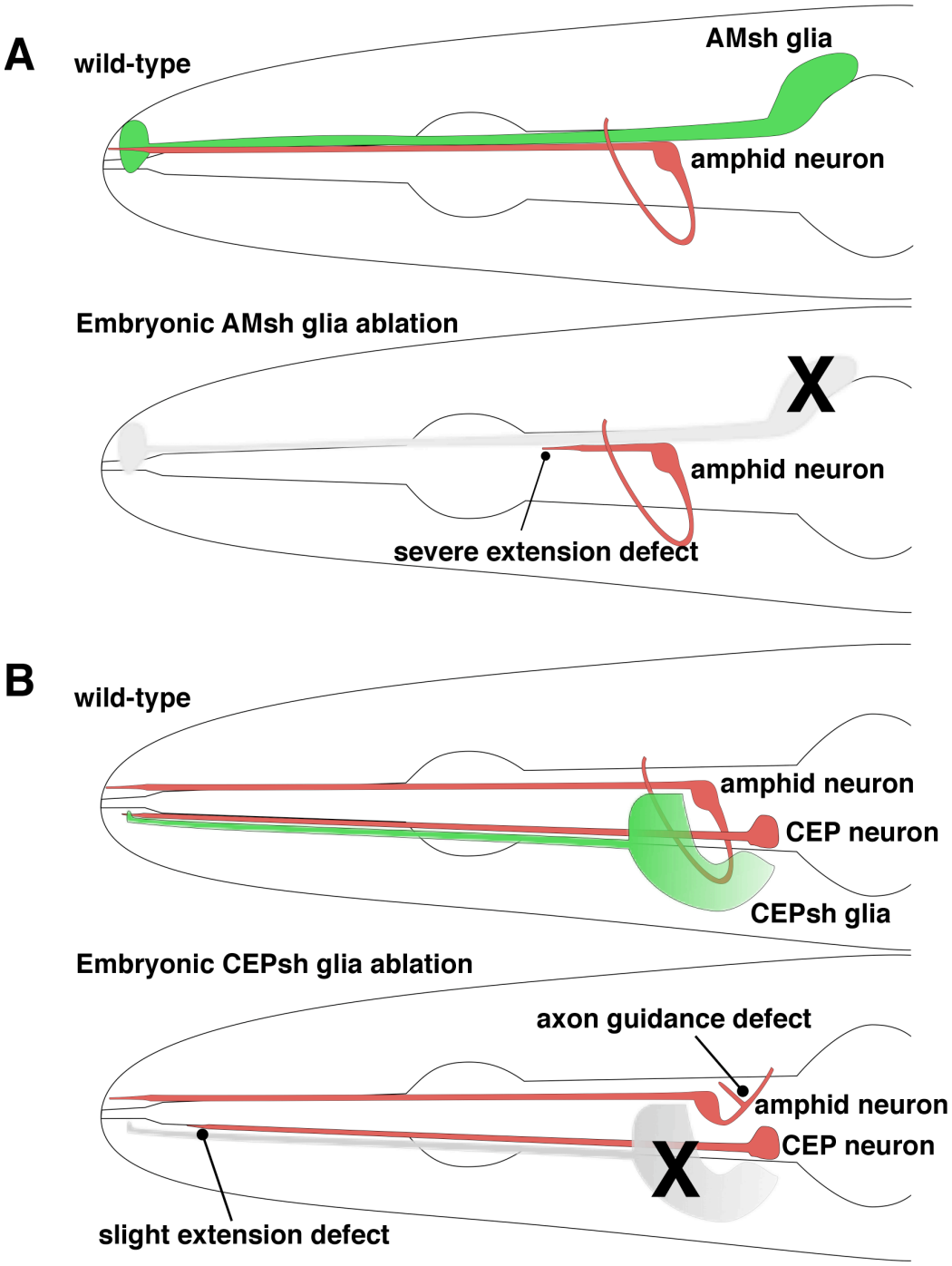

Figure 1.4. Embryonic ablation of the glia of sensory organs results in defects in neuronal morphogenesis. (A) Ablation of the amphid sheath glia during embryogenesis results in amphid neurons with dendrites that are much shorter than normal, reminiscent of *dex-1* and *dyf-7* mutants (see text). (B) Ablation of the CEPsh glia results in slightly shorter CEP dendrites, as well as axon guidance defects.

The gene *ram-5* also encodes a ZP domain protein and is expressed in many glial cells, including the structural cell of the ray sensilla in the male tail. Interestingly, in *ram-5* mutants, the overall architecture of the ray sensillum is grossly malformed due to defects in the shape of the glial structural cell (Yu et al., 2000), supporting the notion that ZP domain proteins secreted by both neurons and glia play important roles in shaping sensory organs.

Morphogenesis in dauer

The studies described so far refer to the processes that take pace during the standard development of *C. elegans*. However, an alternative developmental pathway is available to worms. Under stress (e.g. lack of food or increased temperature), *C. elegans* larvae can enter a developmental stage called dauer. Dauer animals are resistant to treatments that kill non-dauer animals and can survive up to a year without feeding. Upon establishment of more favorable conditions, animals exit the dauer state and resume development to become fertile adults. The integrity and normal morphogenesis of amphid sheath glia is required for dauer entry, as demonstrated by amphid sheath glia ablation studies (Vowels and Thomas, 1994), and by analysis of *daf-6* mutants, which were originally isolated as defective in dauer formation (Riddle et al., 1981).

The goal of dauer animals is to escape or outlast harsh environmental conditions and to steer towards better pastures. At least two adaptations in the sensory machinery of dauers may promote such behavior. First, upon dauer entry, the repertoire of odorant receptors expressed by individual sensory neurons in the amphid sensory organ is altered

(Peckol et al., 2001), perhaps sensitizing the animal to hints of improvement in the environment. Second, some amphid neurons undergo extensive morphological remodeling upon dauer entry (Albert and Riddle, 1983; Mukhopadhyay et al., 2008), none more striking than the AWC neuron, whose glia-embedded wing-like receptive ending greatly expands in dauer animals. This expansion results in extensive overlap of the receptive endings of the left and right AWC neurons. Although the precise significance of this remodeling is unknown (one hypothesis is that it may increase detection sensitivity toward attractive food cues), it is clear that glia play an important role in reshaping AWC (Figure 1.5A and 1.5B).

Accompanying the remodeling of the AWC neuron is a concomitant remodeling of the amphid sheath glia, which accommodates the large expansion in AWC neuron receptive ending surface area (Figure 1.5B). Glial remodeling consists of expansion of the glial processes around the AWC neurons, as well as fusion of the two sheath cells to create a continuous glial torus in the animal's nose. Mutations in the Otx/Otd transcription factor gene *ttx-1* prevent glial expansion and fusion, and rescue studies suggest that *ttx-1* normally functions within amphid sheath glia, presumably through the fusogen AFF-1 (Figure 1.5C) (Procko et al., 2011). Although *ttx-1* acts within glia, in *ttx-1* mutants remodeling of the AWC neurons is defective as well, with AWC receptive endings failing to overlap in the head of the animal, suggesting the possibility that glia guide AWC remodeling (Figure 1.5C). This hypothesis is supported by the observation that the glial processes will expand and fuse in animals in which the AWC neurons have been ablated (Figure 1.5D) (Procko et al., 2011).

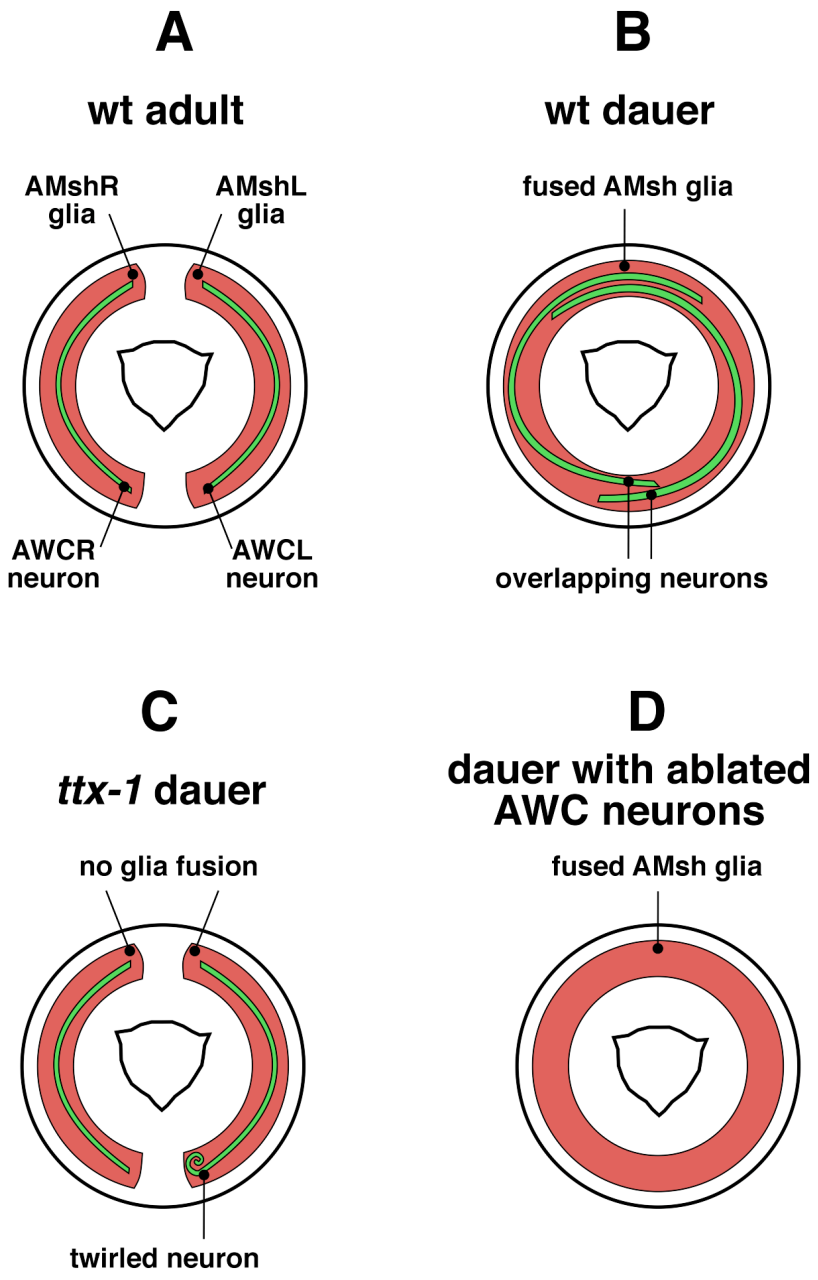

Figure 1.5. Sensory organ remodeling in dauer larvae. (A) Diagram of a cross-section at the tip of the head. The wing-like processes of the bilateral AWC neurons are ensheathed by the bilateral amphid sheath glia (L and R for left and right respectively). (B) In dauer animals the glia expand and fuse to accommodate the expansion of the neuronal wing processes. (C) If glia lack *ttx-1* they fail to expand and fuse, resulting in a lack of neuronal remodeling as well. (D) Conversely, glial remodeling takes place independently of neurons.

1.2.2. Glia in the sensory organs of *Drosophila melanogaster*

Compared to *C. elegans*, the sensory organs of *Drosophila* are many and varied; in broad terms, they consist of neurons, glia, and specialized epithelial cells. Among them, the morphogenesis of the mechanosensory organs found in the thorax, the microchaetes and the larger macrochaetes, has been extensively described (Hartenstein and Posakony, 1989). They provide an excellent example of the tight association between neurons and glia in sensory organs, as well as a fascinating parallel to the amphid sensory organ of *C. elegans*.

The ontogenesis of a mechanosensory organ begins in a field of homogeneous epidermal cells. Within this field, groups of neighboring cells form proneural clusters, distinguished by the expression of genes of the *achaete-scute* complex. Through lateral inhibition mediated by the Notch signaling pathway, neuronal fate is subsequently restricted to only one of the cells of this equivalence group, which will, through several rounds of asymmetric division, give rise to the four cells that constitute the mechanosensory organ.

The cell body of the bipolar sensory neuron resides subepidermally and projects an apical dendrite towards the epidermis. A sheath cell (a glial cell, also referred to as thecogen) that is the sister cell of the neuron, wraps around the dendrite. At the very tip of the neuronal process, the sheath secretes an electron-dense extracellular material that covers the tip of the dendrite. The dendrite-sheath bundle is surrounded by the shaft cell (or trichogen), which also forms the bristle of sensory organ, and is in turn surrounded by

the socket cell (or tormogen). Thus, the sensory dendrite is surrounded by three concentric cylinders formed by the sheath, the shaft and the socket (Figure 1.6)

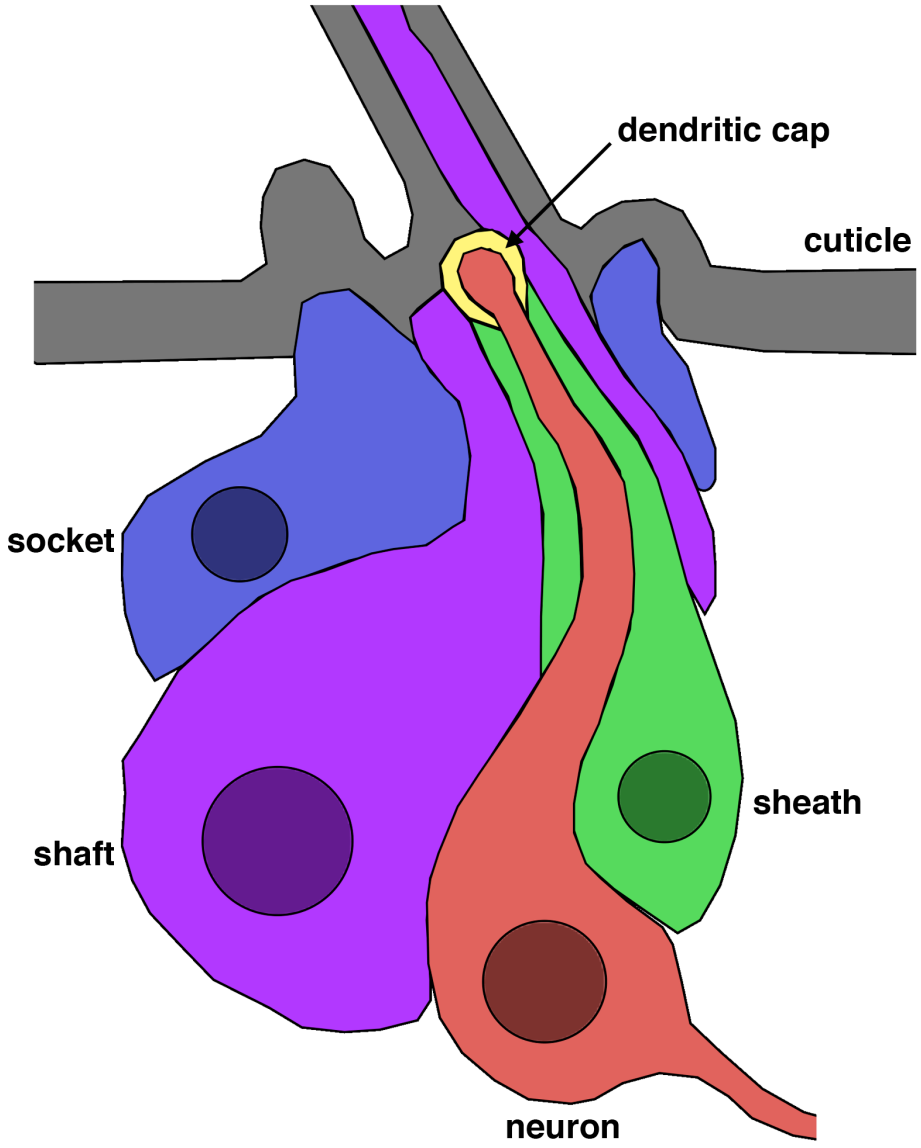

Figure 1.6. Schematic representation of a *Drosophila* sensory organ. The sensory neuron (red) extends a dendrite that is enveloped in a concentric fashion by the sheath, shaft and socket cells. The tip of the dendrite lies within the dendritic cap, extracellular material secreted by the sheath glia. Adapted from Hartenstein and Posakony, 1989.

The rearrangements that lead from four cells that reside upon the same plane to the elaborate structure of the mechanosensory organ have been described in great detail (Hartenstein and Posakony, 1989). First, the neuron shifts below the epidermis and begins to extend an axon basally, and a dendrite apically, through the overlying sheath cell. While the sheath is invaded by the neuron, the shaft and socket cells extend processes that wrap around the sheath. The cell bodies of all three non-neuronal cells also shift subepidermally, while their processes remain at the surface. The shaft cell proceeds to grow out the bristle, while cuticle is deposited on both shaft and socket. It is at this point that the sheath secretes the dendritic cap.

Despite the detailed descriptive studies of the cellular choreography that shapes mechanosensory organs in *Drosophila*, our understanding of the molecular mechanism is very limited. An interesting insight came from the observation (Hartenstein and Posakony, 1989) that the dendritic cap is specifically recognized by the antibody MAb21A6 (Zipursky et al., 1984). This antibody, which also stains the interrhabdomeral space in *Drosophila* ommatidia (Zipursky et al., 1984) in addition to mechanosensory organs, is specific to the agrin/perlecan-related glycoprotein encoded by the gene *eyes shut* or *spacemaker* (Husain et al., 2006; Zelhof et al., 2006). Eyes shut is a secreted protein required for formation of the interrhabdomeral lumen (Husain et al., 2006; Zelhof et al., 2006) and for preservation of cell shape in mechanosensory organs (Cook et al., 2008) upon increase of the ambient temperature.

The anatomy of the olfactory sensory organs of *Drosophila* has also been described in detail (Shanbhag et al., 2000; Shanbhag et al., 1999). The number of neurons differs, but the basic architecture is similar to the one described for the

mechanosensory organs, with a sheath cell that forms a sleeve around the inner dendrite of the sensory neuron(s) and is in turn surrounded by the socket and shaft cells. In this case, the dendrite extends an outer segment that resides within a lymph-filled cavity formed by the socket and shaft cells. The gustatory organs of Drosophila are also very similar (Pollack and Balakrishnan, 1997).

1.2.3. Glia in the sensory organs of vertebrates

In vertebrates, sensory organs can be as simple as the free nerve endings that detect noxious stimuli, or as complicated as the human eye (Burkitt et al., 1993; Ross et al., 1995). Throughout these levels of complexity, a tight association between neurons and glia, or glia-like cells, can be seen.

In the skin, the Pacinian corpuscles are mechanosensory organs that detect cross pressure changes and are particularly sensitive to vibrations (Figure 1.7A). These simple organs are oval shaped, 1 mm long (about the length of an adult *C. elegans*) and consist of an unmyelinated nerve ending that resides within a fluid-filled cavity which is surrounded by lamellae formed by a modified Schwann glial cell (Bell et al., 1994).

In the olfactory epithelium, sensory neurons are ensheathed by sustentacular cells (Figure 1.7B). These cells exhibit glia-like properties, beyond physical association with neurons, such as the ability to sustain high levels of phagocytotic activity following neuronal cell death after bulbectomy, as well as during normal early postnatal development (Suzuki et al., 1996). Additionally, sustentacular cells can promote

proliferation of postnatal neuronal precursor cells, a function typical of glial cells, through release of neuropeptide Y (Hansel et al., 2001).

In the inner ear, hair cells are surrounded by Deiters cells, which may act as a source of brain-derived neurotrophic factor (BDNF) (Montcouquiol et al., 1998), and express the glial marker glial fibrillary acidic protein (GFAP) (Rio et al., 2002) (Figure 1.7C).

In the vertebrate eye, retinal pigment epithelial cells contact photoreceptor cell cilia and phagocytose the membranous debris shed by the outer segment of the photoreceptor cells (Young and Bok, 1969). The retinal pigment epithelium also secretes a host of growth factors important for neuronal survival and is involved in nutrient transport and ion homeostasis in the subretinal space (Strauss, 2005). Also within the retina, the Müller glia are in tight association with photoreceptors and most other neuronal cells and are of critical importance to neuronal homeostasis and function (Newman and Reichenbach, 1996) (Figure 1.7D).

Despite these and other examples of intimate association between neurons and glia in sensory organs, the morphogenetic events that lead to these associations are virtually uncharacterized in vertebrates.

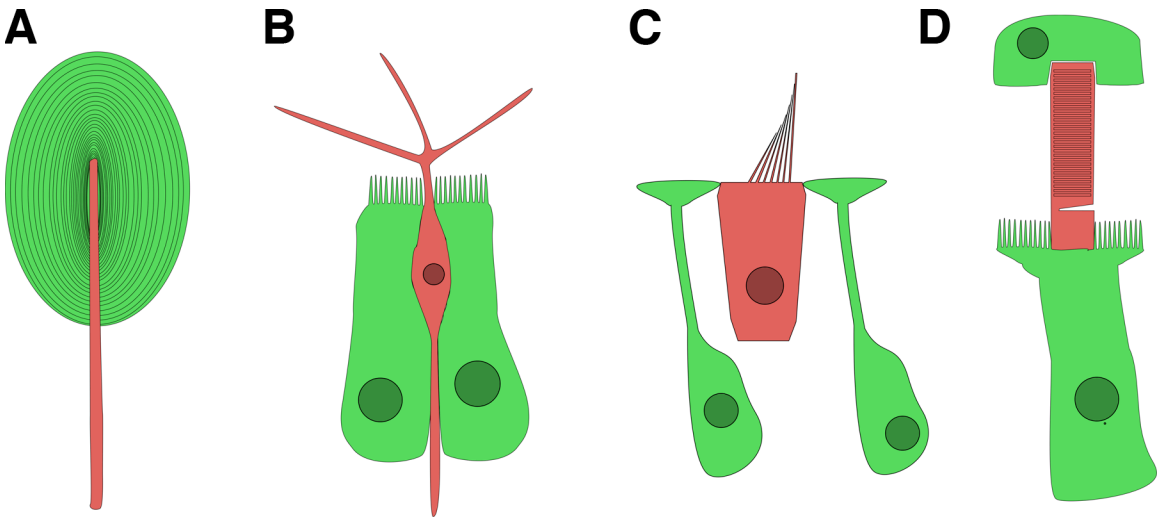

Figure 1.7. Schematic representation of neuron-glia association within vertebrate sensory organs. Glia in green, sensory cells in red. (A) Modified Schwann cells and unmyelinated nerve fiber in Pacinian corpuscles. (B) Olfactory neuron and sustentacular cells in the olfactory epithelium. (C) Hair cell and Deiter's cells in the inner ear. (D) Rod photoreceptor surrounded by retinal pigment epithelium cell (top) and Müller cell (bottom).

1.3. Glial compartments around other neuronal specializations: synapses, neuromuscular junctions, axons.

1.3.1. *Caenorhabditis elegans*

All glia in *C. elegans* are associated with sensory organs. However, the four CEPsh glia are unique as, in addition to associating with sensory neurons (Figure 1.8A and 1.8B), they also extend sheet-like processes that wrap around the nerve ring (Figure. 1.8A). Anatomically, these sheets may serve to isolate the nerve ring in the same way the blood-brain barrier isolates neurons in vertebrate brains. Consistent with this idea, the ancestral vertebrate has been postulated to have had a glial blood-brain barrier, with the endothelial barrier arising only later in evolution (Bundgaard and Abbott, 2008). However, no functional evidence supporting a barrier role for CEPsh glia has been described so far.

The CEP glial sheets that surround the nerve ring also send fine processes that penetrate deep within the nerve ring and contact a small number of synapses (Figure 1.8C), an architecture reminiscent of the fine processes of vertebrate astrocytes that surround synapses. As with vertebrate astrocytes (Bushong et al., 2002; Ogata and Kosaka, 2002; Halassa et al., 2007), CEPsh glial processes are organized in sharply defined, non-overlapping domains with respect to the neuronal processes they contact (Figure 1.8D), suggesting that tiling is a fundamental property of synapse-associated glial cells. The anatomy of CEPsh glia suggests the hypothesis that in evolution, glia may have first appeared in the periphery in association with sensory receptive endings, and

were then co-opted by the central nervous system to ensheath axons and neuron-neuron synapses (Heiman and Shaham, 2007).

Figure 1.8. The cephalic sheath glia. CEPsh glia physically interact with both the sensory receptive endings of the CEP neurons, and with neuronal synapses deep within the nerve ring. (A) The CEP sensillum displays the same basic architecture as the amphid. A thin anterior process from the CEPsh glia runs parallel to the CEP neuron, while a sheet-like posterior process wraps around the "brain" of the animal. (B) The anterior process establishes a channel similar to, but smaller than, the amphid channel. (C) Thin projections from the posterior process enter the nerve ring and can ensheath synapses, similar to astrocytes of vertebrate systems. (D) Schematic of a cross-section through the nerve ring. Each animal has four CEPsh glia that wrap around the nerve ring without overlapping with each other. Thus, CEPsh glia establish independent domains, in a fashion reminiscent of astrocytic domains. (B) and (C) are pseudo-colored EM pictures adapted from White et al., 1986.

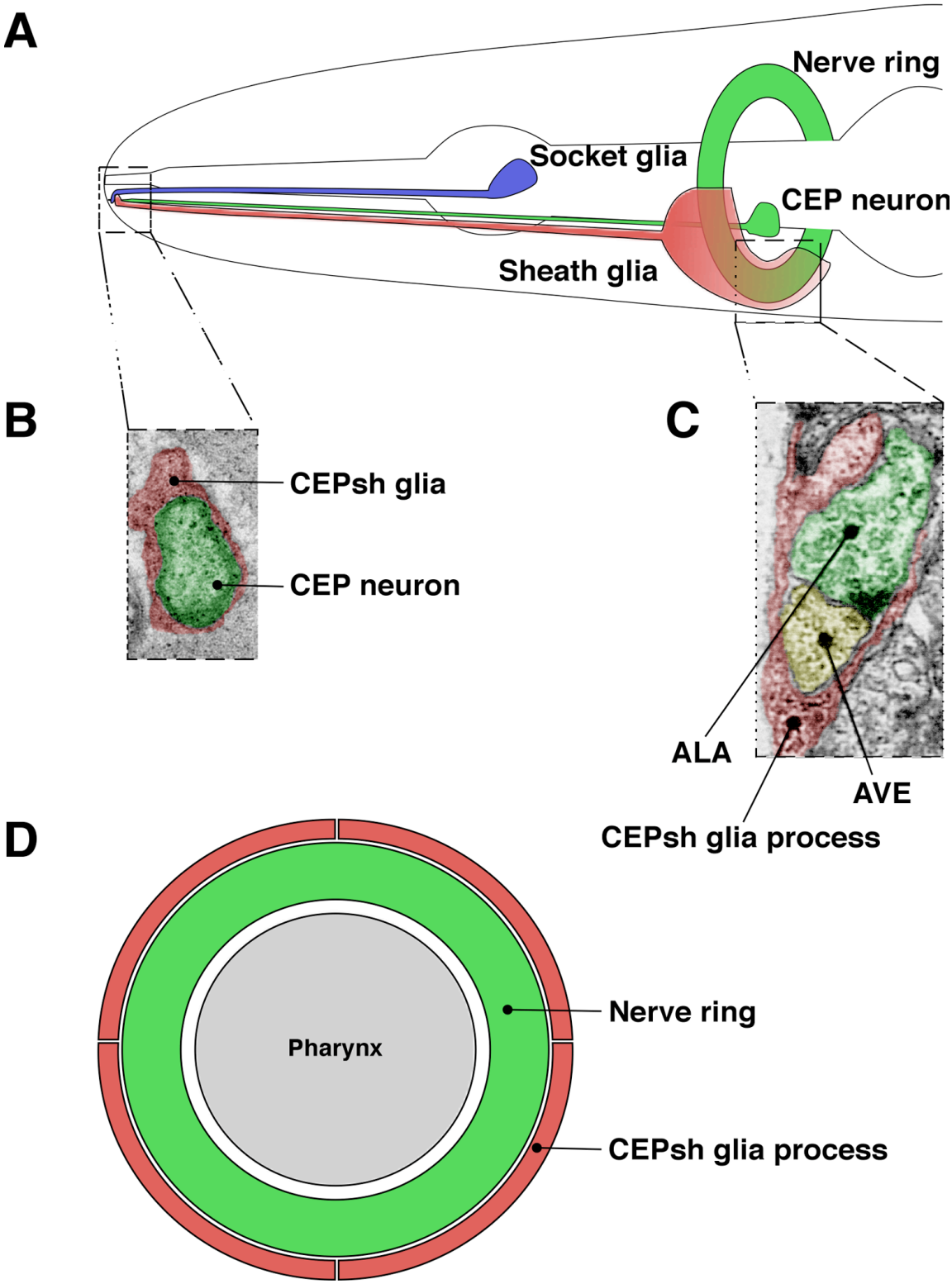
A
Nerve ring
Socket glia
CEP neuron
Sheath glia
B
CEPsh glia
CEP neuron
C
ALA
AVE
CEPsh glia process
D
Pharynx
Nerve ring
CEPsh glia process

Although most neuromuscular junctions in *C. elegans* are devoid of glial cells, GLR glia in worms are associated with muscles and the neurons that innervate them. *C. elegans* possesses three pairs of GLR cells (dorsal, ventral and lateral) that are arranged in a six-fold symmetrical fashion around the pharynx, just posterior to the nerve ring (White et al., 1986). From each GLR cell body emanates an anteriorly-directed, sheet-like process that wraps around the inside aspect of the nerve ring (Figure 1.9A). Here, GLR cells make gap junctions to head muscle cells, as well as to the RME motor neurons that innervate these muscles (Figure 1.9B). More anteriorly, the sheet-like processes narrow into thin extensions (Figure. 1.9A). Unlike other glial cells, GLR cells express the *C. elegans* homolog of myoD (Krause et al., 1994) and are of mesodermal origin. Although GLR glia could represent a fascinating analog to the Schwann glia of neuromuscular junctions, their morphogenesis and functions have not been studied. It is striking that, in *C. elegans*, only head muscles form partnerships with glia. These muscles mediate fine motor behaviors that are less stereotypical than the undulations produced by body wall muscles, perhaps explaining the need for glial companionship.

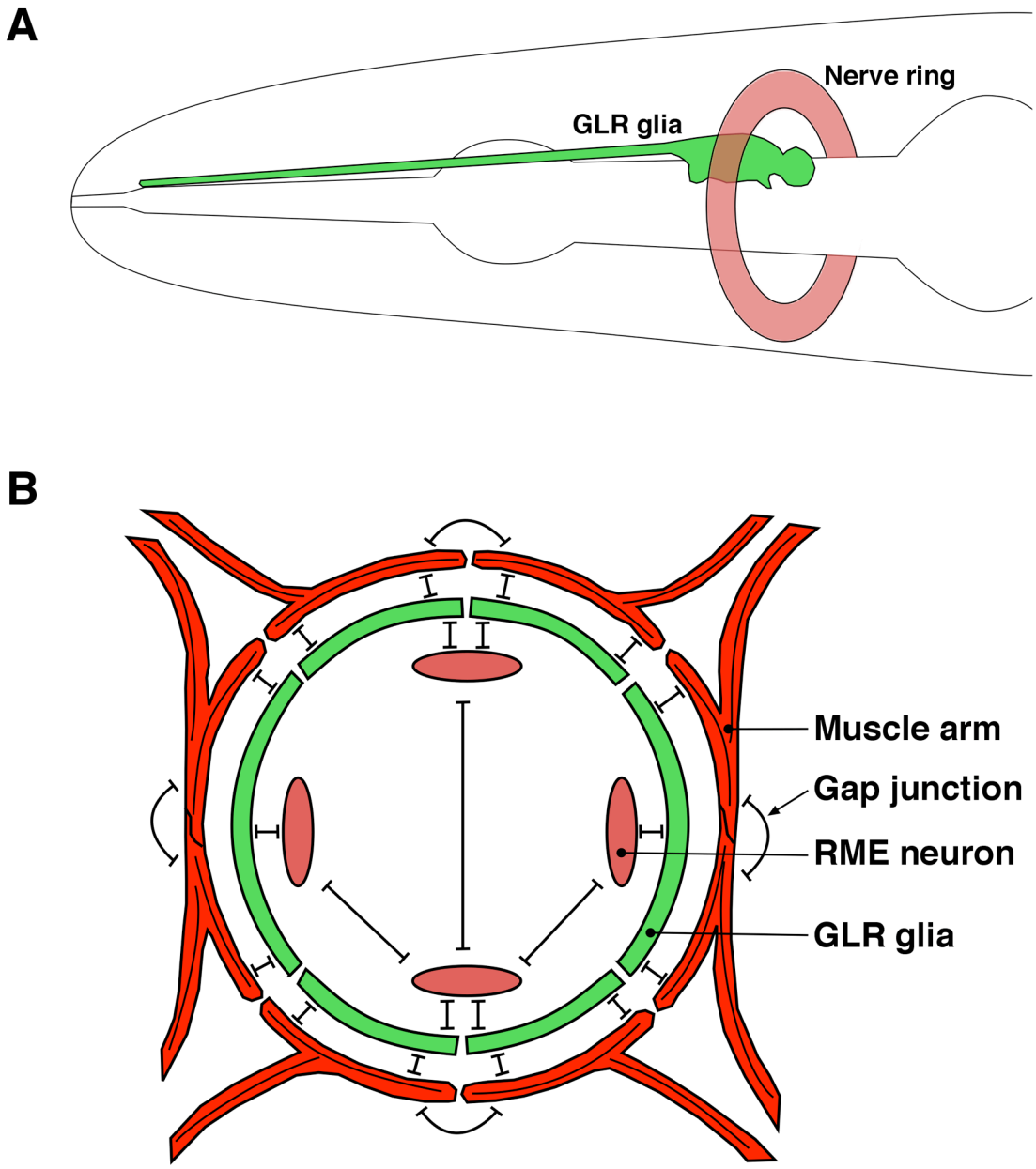

Figure 1.9. The GLR glia establish gap junctions that bridge neurons and muscles. (A) Each animal has six GLR glia. Only one is depicted here. The cell body lies posterior to the nerve ring. An anterior, sheet-like process lines the inside of the nerve ring and then tapers to a thinner process. (B) The sheet-like processes of the GLR glia form gap junctions with head muscle cells and the RME motor neurons that innervate them. Adapted from White et al., 1986.

Although, as previously mentioned, glial and neuronal process often run parallel to each other in sensory organs, axons are not ensheathed by glia and myelin-like structures are not observed in *C. elegans*. Axonal myelination by glia has arisen independently several times during animal evolution, in response to the need for either higher speeds or longer distances of electrical conduction (Hartline and Colman, 2007). The short length of neuronal processes in worms (less than 1 mm) results in negligible current loss, thus potentially negating the need for myelin ensheathment.

1.3.2. *Drosophila melanogaster*

There are three main classes of glia in the *Drosophila* CNS, all of which tightly ensheath neuronal cells: surface glia that surround and isolate the CNS, cortex glia that surround neuronal cell bodies, and neuropil glia that, as their name denotes, are associated with neuropils, dense networks of axonal, dendritic and glial processes (Freeman and Doherty, 2006). Recently, neuropil glia were found to consist of at least two distinct populations: ensheathing glia that line the borders of neuropils, and astrocytes that send processes deep within neuropils and extend fine process that invade synapse-rich regions (Doherty et al., 2009). This latter type of glia also expresses a variety of vertebrate astrocytic markers and is thus considered morphologically and functionally analogous to vertebrate astrocytes. At this point, we know very little about the morphogenesis or function of fly astrocytes.

The surface glia of *Drosophila* set up a structure homologous to the brain-blood barrier of vertebrates. This protects the *Drosophila* CNS from the high levels of

potassium ions present in the hemolymph, a fluid equivalent to the blood of vertebrates. The flattened, unbranched surface glia establish a continuous sheet that surrounds and isolates the CNS by forming glia-to-glia pleated septate junctions among each other as well as with some cortex glia (Pereanu et al., 2005). The establishment of this sheet is a fascinating developmental process: glia migrate from their place of birth to the surface of the developing nerve cord, where they expand until they touch their neighbors; as a network of cortical actin accumulates, spotted junctions start to appear. These junctions will eventually expand to form an epithelial seal by 20 hours of development (Schwabe et al., 2005). Surface glia morphogenesis, actin accumulation and septate junction formation depend on G protein-coupled receptor (GPCR) signaling in glial cells through the orphan GPCR Moody and the regulator of G protein signaling Loco. The primary defect in *moody* mutants is thought to be the formation of the cortical actin network, as this process precedes septate junction formation and is not perturbed in mutants of septate junction components (Schwabe et al., 2005). More than a few of these components have been characterized, including gliotactin, neurexin and contactin (Auld et al., 1995; Baumgartner et al., 1996; Faivre-Sarrailh et al., 2004). Interestingly, at least some of the building blocks of such glia-to-glia *Drosophila* junctions appear to be the same as the ones employed in the paranodal junctions between glia and neurons at the nodes of Ranvier in vertebrates (Bhat, 2003).

Peripheral nerves in *Drosophila* contain axons that are either individually ensheathed, or part of a bundle that is collectively ensheathed by inner glia, with an additional layer of outer glia surrounding the whole nerve (Leiserson et al., 2000). No true myelin sheath forms in *Drosophila* (similar to other invertebrates), and the genome

does not appear to have homologs of the vertebrate myelin genes. How do peripheral glia ensheath axons? Some of the mutants identified for their role in ensheathment, such as *loco* and *gliotactin* (Auld et al., 1995; Granderath et al., 1999), have more recently been shown to be required for formation of the septate junctions that hold together the sheet of peripheral glia (Schulte et al., 2003; Schwabe et al., 2005). Another gene, *wrapper* seems to be more directly involved in ensheathment. Wrapper is a member of the Ig superfamily that localizes to the surface of midline glia; in *wrapper* mutants, glia proliferation and migration are normal, but the cells fail to extend ensheathing processes around the axons of the midline (Noordermeer et al., 1998). Wrapper is though to mediate glial ensheathment of axons by directly binding to neurexin that is expressed on the surface of axons (Wheeler et al., 2009). Interestingly, neurexin is also a component of the glia-to-glia junctions, as mentioned earlier, another similarity between the machinery that links glia to glia and the one that links glia to neurons.

Although glia surround peripheral nerves in *Drosophila*, they were originally reported to stop at the axon branch point, before reaching the neuromuscular junction itself (Sepp et al., 2000). More recent studies (Fuentes-Medel et al., 2009) suggest that glia do invade neuromuscular junctions in *Drosophila*, but they are believed to do so only transiently. This hypothesis is based on the observation that glial process are not stereotypic, with great variation observed among identified muscles from different individuals (Fuentes-Medel et al., 2009). One of the functions of these invading processes appears to the clearance of presynaptic membrane debris originating from remodeling of presynaptic terminals during animal growth (Fuentes-Medel et al., 2009). Thus, in *Drosophila*, glia are associated with neuromuscular junctions and are important

for their development and function, but do not form stable, isolating compartments around them.

1.3.3. Vertebrates

In the vertebrate brain, astrocytes send out thousands of processes that ensheath synapses by wrapping around the presynaptic and postsynaptic terminals neurons (Spacek, 1985; Ventura and Harris, 1999; Oberheim et al., 2009). In humans, a single astrocyte is estimated to associate with up to two million synapses (Oberheim et al., 2006). A host of studies has sought to address the contributions of astrocytes to synapses, including their roles in establishment and maintenance of ionic balance, synaptogenesis and neurotransmission, but many mysteries remain (Barres, 2008; Halassa and Haydon, 2010).

If our understanding of the functions of astrocytic synaptic compartments is limited, we know almost nothing about their morphogenesis. In the first week of postnatal development, astrocytes sprout processes that by the third and fourth week of development begin to ramify profusely, becoming thinner and more spongiform and surrounding neuronal cells (Bushong et al., 2004). The elaboration of these processes could be directed by neuronal activity, as glial ensheathment in adult animals has been reported to increase following neuronal stimulation both in slice preparations and in vivo (Lushnikova et al., 2009; Wenzel et al., 1991; Genoud et al., 2006; Lushnikova et al., 2009). Activation of the EphA4 receptor tyrosine kinase, present on dendritic spines, by its ligand ephrin-A3, which localizes to the perisynaptic processes of astrocytes, has been

proposed to regulate dendritic spine morphology in the adult hippocampus (Murai et al., 2003). Given the bidirectional nature of Eph/ephrin signaling, it is intriguing to speculate that dendritic spines could in turn regulate astrocytic ensheathment. Interestingly, it has also been reported that activation of astrocytic EphA receptors by ephrins (either applied exogenously, or released by cleavage of their glycosylphosphatidylinositol anchors) leads to rapid sprouting of filopodial processes (Nestor et al., 2007). Whether any of these observations, made in adult animals or preparations from adult brains, is relevant to early development remains to be determined.

In the peripheral nervous system (PNS) of vertebrates, non-myelinating Schwann cells, or Remak cells, wrap around single or multiple axons, forming Remak bundles (Griffin and Thompson, 2008). Such bundles, however, are relatively rare, with the majority of glial ensheathment of axonal processes being accomplished through the formation of myelin sheaths by Schwann cells in the PNS and by oligodendrocytes in the CNS. Schwann cell bodies are located next to the axonal segment they myelinate, while oligodendrocytes extend multiple processes, each of which forms a myelin sheath around a different axonal segment (Figure 1.2). In both cases, myelin sheaths are formed by the spiral wrapping of glial plasma membrane around the axons. The unmyelinated sections of an axon that are found between Schwann- or oligodendrocyte-derived myelin segments are referred to as the nodes of Ranvier. The myelin sheath greatly increases the conduction velocity of axons as action potentials are propagated in a saltatory fashion from one node of Ranvier to the next. Additionally, restoration of the ion gradients necessary for action potential generation is limited to the node regions, greatly reducing the energy cost of propagation.

How do glia form myelin sheaths? Despite advances in our understanding of the specification of myelinating glia (Woodhoo and Sommer, 2008; Emery, 2010), the lipids and proteins that comprise the myelin sheath (Saher et al., 2005; Werner and Jahn, 2010), and the contributions of myelin in axonal integrity (Nave, 2010), the process of ensheathment is poorly understood. In the PNS, neuregulin 1, a transmembrane protein that localizes to axons, interacts with the epidermal growth factor receptors ErbB2/B3 on the surface of Schwann cells to activate the PI-3 kinase and induce myelination; the strength of neuregulin 1 – ErbB2/B3 signaling determines the thickness of the myelin sheath (Michailov et al., 2004; Taveggia et al., 2005). Signaling by BDNF through the p75 neurotrophin receptor has also been implicated in induction of myelination (Cosgaya et al., 2002) and regulation of the thickness of the myelin sheath (Tolwani et al., 2004). Interestingly, the p75 neurotrophin receptor is recruited by the Par-3 polarity protein, the first molecular link between establishment of cell polarity and myelination (Chan et al., 2006).

Not surprisingly, given its major roles in cellular morphogenesis, the actin cytoskeleton has been implicated in the ensheathment process itself. In co-cultures of myelinating Schwann cells and neurons, disruption of actin polymerization with cytochalasin D inhibits myelination in a dose-dependent and reversible fashion (Fernandez-Valle et al., 1997). Moreover, cytochalasin D treatment inhibits the expression of genes encoding myelin-specific proteins such as the myelin-associated glycoprotein (MAG) and P0.

The Rho family of GTPases, which includes Rho, Rac and Cdc42, are important regulators of the actin cytoskeleton (Etienne-Manneville and Hall, 2002). Similar to

other small GTP binding proteins, Rho family GTPases act as molecular switches that cycle between a GDP-bound (off) state and a GTP-bound (on) state. Rho kinase (ROCK) is an effector of the Rho GTPase that phosphorylates myosin II light chain (MLC) to activate actomyosin. Pharmacological inhibition of ROCK in co-cultures of Schwann cells and neurons does not affect Schwann cell proliferation and differentiation, but results in aberrant branching of Schwann cells and formation of multiple, independent myelin segments along the length of the axons (Melendez-Vasquez et al., 2004). This aberrant myelination pattern in Schwann cells is particularly striking, as it closely resembles the normal myelinating pattern of oligodendrocytes (Melendez-Vasquez et al., 2004). Indeed, in oligodendrocytes the Fyn tyrosine kinase (a member of the Src family of protein tyrosine kinases) is activated by integrin engagement and in turn activates the p190 RhoAGAP that downregulates Rho activity (Osterhout et al., 1999; Liang et al., 2004). Additionally, in an oligodendrocyte and neuron co-culture system, dominant negative versions of Rho induce outgrowth of oligodendrocytic processes while constitutively active versions inhibit outgrowth. The reverse is true for the Cdc42 and Rac GTPases, suggesting opposing effects of these actin regulators in oligodendrocytic branching (Liang et al., 2004). Finally, Lingo-1, a negative regulator of myelination by oligodendrocytes, has been shown to activate Rho (Mi et al., 2005). These studies suggest that downregulation of Rho activity is important for the branched pattern of myelination seen in oligodendrocytes.

Why is Rho inhibition so important for myelination by oligondendrocytes? Even in the absence of neurons, oligodendrocytes activate genes encoding for major myelin components (Dugas et al., 2006), including the transmembrane proteolipid protein (PLP).

Without neurons, however, PLP is produced and delivered to the plasma membrane, only to be retrieved through a cholesterol-dependent and clathrin-independent endocytosis pathway and targeted to late endosomes/lysosomes (Trajkovic et al., 2006). Neurons trigger the transfer of PLP from late endosomes/lysosomes back to the plasma membrane through a so far uncharacterized, diffusible, cAMP dependent signal that inhibits Rho GTPase activity within oligodendrocytes (Kippert et al., 2007; Trajkovic et al., 2006). Thus, inhibition of Rho activity promotes the delivery of myelin proteins and cholesterol to the plasma membrane of oligodendrocytes.

Two other major regulators of the actin cytoskeleton, and effectors of Rho family GTPases, the neural Wiskott-Aldrich syndrome protein (N-WASP) and the Wiskott-Aldrich syndrome protein family verprolin homologous protein (WAVE) are also required for myelination. Pharmacological inhibition of N-WASP in cell cultures results in reduced process extension by Schwann cells and oligodendrocytes (Bacon et al., 2007), while mice lacking N-WASP in Schwann cells show defects in myelination (Novak et al., 2011). Inhibition of WAVE1 also impairs process extension by oligodendrocytes, and WAVE1 knockout mice displayed hypomyelination in regions of the CNS (Kim et al., 2006).

Although astrocytes are associated with the blood-brain barrier of vertebrates (Banerjee and Bhat, 2007), the barrier itself is established not by glial cells, but by tight junctions among vascular endothelial cells. The exception is the blood-brain barrier of elasmobranch fish (fish whose skeleton is made from cartilage), which is established by perivascular astrocytes, and recent work suggests that the transition to an endothelial

barrier has arisen independently several times throughout the evolution of vertebrates (Bundgaard and Abbott, 2008).

1.4. Lumen formation

A salient feature of sensory organs such as the *C. elegans* amphid, the *Drosophila* mechanosensory organs, and the vertebrate Pacinian corpuscles is that the receptive endings of the sensory neurons reside within lumens formed by glial cells. Indeed, molecules such as DAF-16 and CHE-14 are involved not only in the morphogenesis of the amphid sensory organ, but in lumen formation in general. *che-14* mutants, in addition to being dye-filling defective (an assay for amphid morphogenesis), are also defective in excretory cell function (Michaux et al., 2000), and these defects are exacerbated in *che-14*; *daf-6* double mutants (Perens and Shaham, 2005). Thus, insight into lumen formation can inform us about sensory organ morphogenesis and vice versa.

Tubes are an integral component of many organs and systems such as the kidneys, the lungs, the reproductive system and the vasculature. These tubes can be as topologically simple as the tear duct, or as branched and convoluted as the circulatory system. Their size can vary from capillaries tight enough that red blood cells can barely squeeze through, to a uterus that can accommodate an embryo throughout its development. A cross section through a tube can reveal multiple cells tightly attached to each other through specialized junctions, a single cell forming a junction onto itself (as in the case of the socket glia), or a hollowed-out, junctionless tube (as in the case of the sheath glia). Despite the great variety in shape, size and cellular arrangement, the study of lumen formation in a variety of systems has allowed some common themes to emerge.

The morphological processes that lead up to tube formation are the most diverse step in tubulogenesis (Lubarsky and Krasnow, 2003). A common mechanism is the wrapping of epithelial tubes, as in the case of neural tube formation. Alternatively, cells organized in a cylindrical mass can form a tube by the elimination of cells at the center of the mass, in a process called cavitation. In cord hollowing, there is no cell loss as a lumen is formed between adjacent cells. In cell hollowing, a unicellular tube is formed. Tubes can also form by the wrapping of cellular processes around a substrate, or through budding from a pre-existing tube.

Whether a tube is formed by one or by many cells, these cells are typically polarized with the apical surface facing towards the center, to the luminal space, while the basolateral surface contacts adjacent cells and the underlying extracellular matrix (ECM). The apical and basolateral surfaces are separated by cellular junctions that keep the cells attached to each other and prevent the diffusion of lipids and proteins between the two surfaces, as well as the leakage of lumen material. Thus, establishment of apical-basal polarity is a critical step leading up to lumen formation (Bryant and Mostov, 2008). Three conserved polarity complexes mediate apical-basal polarization: the Par complex (consisting of Par3, Par6 and aPKC) and the Crumbs complex (consisting of Crumbs, Stardust, PATJ and others) are associated with the apical membrane, while the Scribble complex (consisting of Scribble, Discs large and Lethal giant larvae) is associated with the basolateral surface. These three complexes interact with each other and, by a system of mutual exclusion, define the apical and basolateral surfaces of polarized cells (Bilder et al., 2003; Tanentzapf and Tepass, 2003) and regulate cellular architecture by interacting with the Rho family of GTPases (Iden and Collard, 2008). Asymmetric

distribution of phosphoinositides is also important for polarity establishment, with phosphatidylinositol 4,5-bisphosphate playing a critical role in apical membrane determination, and phosphatidylinositol 3,4,5-trisphosphate being an important determinant of the basolateral membrane (Martin-Belmonte et al., 2007; Gassama-Diagne et al., 2006). Binding of integrin molecules on the basal surface to laminin in the extracellular matrix is also a key step in the establishment of cell polarity (Datta et al., 2011).

In the case of cord or cell hollowing, concomitant with the establishment of apical-basal polarity, lumen formation is achieved through coalescence of vesicles (Figure 1.10). Apical secretion of vesicles is also important in the regulation of lumen size, a critical aspect of tubulogenesis. In the following pages I will highlight the role of directed apical secretion in lumen formation and size regulation in selected systems.

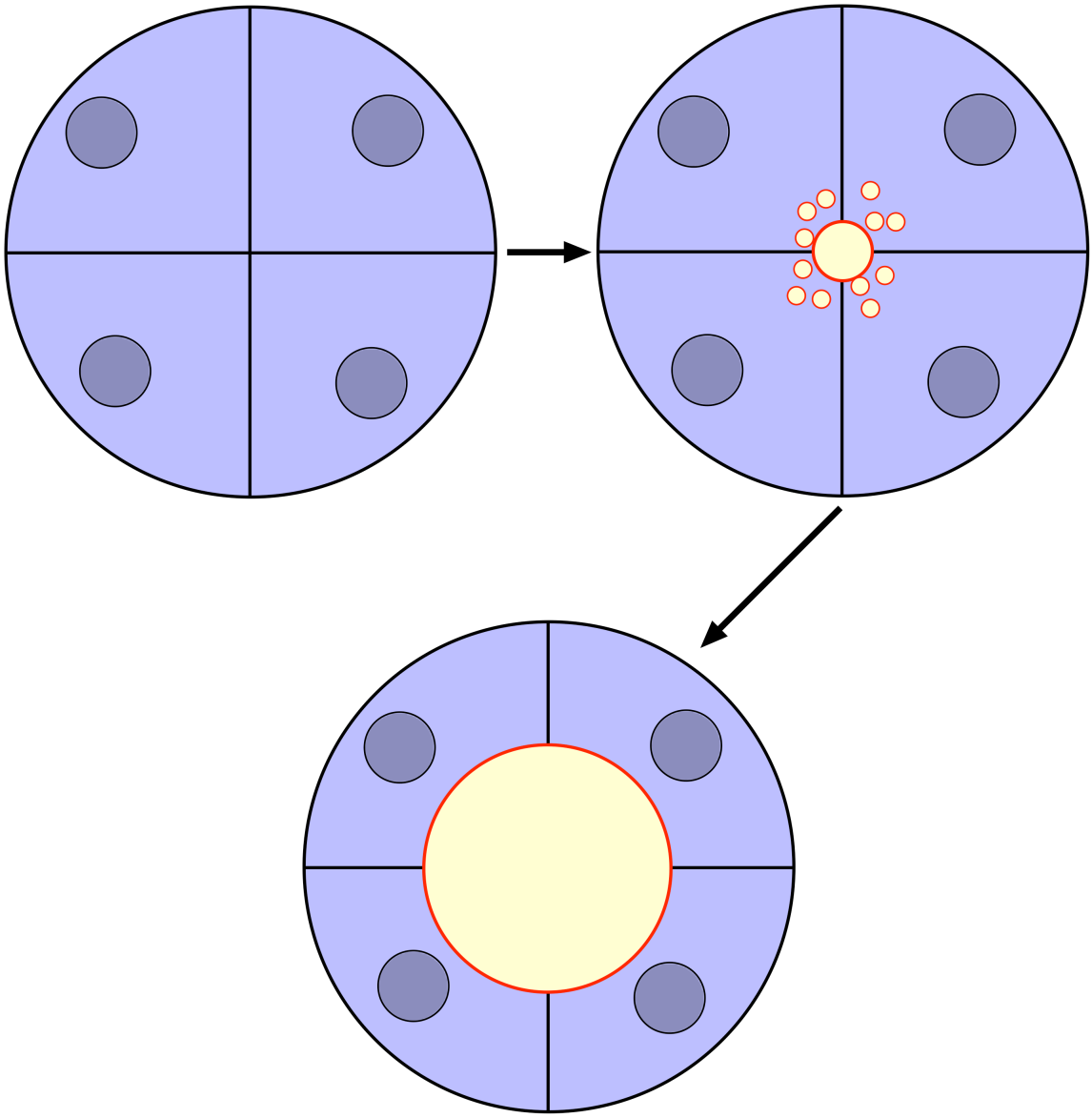

Figure 1.10. Directed apical secretion of vesicles drives lumen formation and expansion. Apical membrane in red, lumen in yellow.

1.4.1. Lumen formation in the MDCK cell culture system

Madin-Darby canine kidney (MDCK) cells, derived from the kidney distal tubule and collecting duct, have been an extremely useful system for the study of lumen formation in vitro. When these cells are grown in a three dimensional gel of extra-cellular matrix (ECM) they organize into hollow spheres formed by a monolayer of polarized epithelium, with the apical surface facing the inside of the cyst (Montesano et al., 1991b). Within these cysts, cell division occurs within the plane of the monolayer. Treatment with hepatocyte growth factor (HGF) induces the formation of epithelial tubes extending from the cysts (Montesano et al., 1991a). Following treatment, some cyst cells extend basal processes, migrate out of the monolayer, lose their apicobasal polarity and divide to form a chain of cells extending in a radial fashion (Yu et al., 2003). Further divisions give rise to a cord a few cells thick; within this cord the cells regain polarity and form a lumen that will eventually fuse with the central lumen of the cyst to form mature tubules.

When MDCK cells are grown as a monolayer, large intracellular vacuoles, referred to as the vacuolar apical compartment (VAC), are observed (Vega-Salas et al., 1987). It has been suggested that exocytosis of VACs is the driving force behind MDCK lumen formation (Vega-Salas et al., 1988). However, during MDCK cyst formation, VACs are only detected if Cdc42 activity is depleted (Martin-Belmonte et al., 2007). This observation suggests that during normal MDCK cyst formation smaller, apical-surface-targeted, vesicles are exocytosed in a Cdc42 dependent fashion to give rise to the lumen (Martin-Belmonte et al., 2007). Indeed, Cdc42 has recently been shown to interact with the exocyst complex and the Par polarity complex to direct Rab8/Rab11 positive

vesicles to the site of apical membrane initiation (Martin-Belmonte et al., 2007). These interactions link, at the molecular level, the establishment of the apical domain and vesicle coalescence for lumen formation.

1.4.2. Lumen formation in the excretory cell of *C. elegans*

The excretory system of *C. elegans* consists of four cells and has been reconstructed by electron microscopy in fine detail (Nelson et al., 1983). A large, H-shaped excretory cell extends bilateral canals that transverse nearly the full length of the body (the vertical lines of the "H") and are connected to each other (through the horizontal line of the "H") at the ventral side of the second bulb of the pharynx, at the head of the animal. A duct (formed by the duct cell) connects the excretory cell to the excretory pore (formed by the pore cell) that opens to the environment. The last component of the excretory system is the excretory gland cell, which arises from the fusion of two symmetrically positioned cells. It connects to the duct, similarly to the excretory cell, where it secretes material by exocytosis of large vesicles; the nature of this material is unknown. The function of the excretory system of *C. elegans* appears to be similar to that of the renal system of vertebrates: the excretory cell that extends throughout the body collects fluids that travel through the duct to the pore, from which they are released to the environment. Consistent with this, ablation of the excretory, duct, or pore cell results in death of the animal due to fluid accumulation (referred to as the "Rod" phenotype) (Nelson and Riddle, 1984). The function of the gland cell is not understood, as ablation does not result in an obvious phenotype.

The excretory cell has been a popular system for the study of lumen formation due to the distinct phenotype that arises from defects in its development and function, as well as its relatively large size (Buechner, 2002). During development, vacuoles (probably of pinocytic origin) form within the cell body and fuse to form the apical/luminal surface (Buechner, 2002; Berry et al., 2003). A thick material accumulates within the lumen, but it will have disappeared by the time the animal hatches (Buechner, 2002). After the lumen has formed, the excretory cell extends the long bilateral canals seen in the adult. Many genes that are involved in this process have been identified (Buechner, 2002). One group of genes encodes components of the extracellular matrix and integrins, the transmembrane proteins that bind to it, suggesting that the ability of the excretory cell to interact with the ECM is important for canal extension. Another group of genes important for canal extension encodes for cues used by neurons during axon extension, such as UNC-6/netrin (Hedgecock et al., 1990), suggesting that the excretory cell uses the same cues.

Genes important for excretory cell lumen formation (as opposed to canal extension) were isolated in a screen for mutations that result in the formation of cysts instead of a normal lumen ("Exc" phenotype) (Buechner et al., 1999). Many of these genes encode components and regulators of the cytoskeleton. For example, in *sma-1* mutants the excretory canal develops normally throughout embryogenesis, but, as the animal progresses through the larval stages, it becomes more and more bloated in diameter, until it forms a single cyst in adults. In these animals, the terminal web (a dense, subapical, actin-based cytoskeletal network) is separated from the apical membrane. *sma-1* encodes β_H-spectrin, a component of the actin cytoskeleton that is

presumably required for the attachment of the terminal web to the apical membrane (McKeown et al., 1998). Similar defects arise in mutations of *exc-7*, which encodes an mRNA binding protein that is required for *sma-1* translation. Cysts arise in mutants for *exc-5*, a gene encoding a guanine-nucleotide exchange factor (GEF) that is homologous to FGD1, an activator of Cdc42 (Suzuki et al., 2001; Gao et al., 2001), providing another link between regulation of the actin cytoskeleton and lumen morphogenesis. *erm-1* encodes a member of the Ezrin, Radixin and Moesin family of membrane-cytoskeleton linkers. Mutation of *erm-1* results in cystic phenotypes in tubular organs that are not stabilized by cuticle, including the canals of the excretory cell, without affecting the apical-basal polarity, junction assembly or integrity of these tubes (Göbel et al., 2004). *erm-1* was shown to functionally interact with *act-5*/Actin and *sma-1*/ β_H-spectrin, suggesting that the cystic phenotypes arise from defects in the attachment of the subcortical terminal web to the apical membrane. *exc-4* encodes a chloride intracellular channel (CLIC) that can translocate from the cytosol to the cell membrane and is required for normal lumen formation, with cysts arising in *exc-4* mutants (Buechner et al., 1999; Berry et al., 2003).

1.4.3. Lumen formation in the *Drosophila* trachea

Drosophila, like many terrestrial arthropods, relies on an elaborate tracheal system to facilitate gas exchange. The trachea of *Drosophila* embryos has a metameric structure as it originates from 20 independent units with similar branching patterns. These units, each consisting of about 80 cells, connect to each other to give rise to a single-layered epithelium that is lined with cuticle. The branching and fusion events that generate this network are under genetic control and provide a fascinating system for the study of organ morphogenesis (Ghabrial et al., 2003; Uv et al., 2003). As the animal enters the larval stages of development, the trachea ramifies greatly, this time by responding to the specific oxygen demands of the various tissues.

Recent studies have expanded our understanding of the lumen formation and expansion processes, which follow the cell fate specification, migration, branching and fusion events that establish tracheal architecture. These studies have demonstrated a central role for a transient intraluminal chitin scaffold that fills the tracheal space during early development. First, a series of chitin biosynthesis mutants were shown to have a cystic (bloated) tracheal lumen (Moussian et al., 2005; Devine et al., 2005; Araújo et al., 2005; Tonning et al., 2005). Importantly, the chitin scaffold is required primarily for limiting the expansion of the lumen, as well as the expansion of specific sections of the lumen, suggesting that it does not simply act by pushing out the tubular epithelium (Tonning et al., 2005). Furthermore, two genes encoding chitin modifying enzymes, *serpentine* and *vermiform* were also shown to be required for the normal morphogenesis of the tracheal lumen (Luschnig et al., 2006; Wang et al., 2006). Whereas in the absence of chitin the lumen is mostly bloated, mutation of these chitin deacetylases results in

convolution and lengthening of the tracheal lumen, without affecting its diameter. Interestingly, the texture of the intraluminal chitin is affected: instead of being fibrillar it is now homogeneous, suggesting that the physical properties of the scaffold are important for regulating the form and length of the tube. Exactly how chitin regulates the size and shape of the tracheal lumen remains to be determined.

Another set of genes that was initially isolated as required for normal size of the tracheal lumen turned out to consist of components of septate junctions such as *sinuous*/claudin (Wu et al., 2004), Na+/K+ ATPase (Paul et al., 2003), *megatrachea*/claudin-like (Behr et al., 2003), *lachesin* (Llimargas et al., 2004), and others (Wu and Beitel, 2004). As discussed in the section concerning the establishment of the blood-brain barrier in *Drosophila*, the main function of septate junctions is to enable epithelia to create a diffusion barrier. Flies with weak mutations in *coracle*, a gene encoding another component of septate junctions (Ward et al., 2001), have permeable epithelia, but normal trachea (Paul et al., 2003), suggesting that the diffusion barrier established by septate junctions is not relevant to their role in regulating the size of the tracheal lumen. In addition, double mutants for genes encoding both septate junction components and chitin biosynthesis display the same tracheal defects as the chitin biosynthesis mutants alone, i.e. chitin mutations are epistatic to septate junction mutations (Tonning et al., 2005). Indeed, septate junctions are required for the secretion of Vermiform into the luminal space, while septate junctions themselves develop normally in *vermiform* mutants (Wang et al., 2006). These intriguing results suggest that the luminal defects seen in septate junction mutants arise through their effects on the

transient intraluminal chitin scaffold. It remains to be determined how the laterally located septate junctions regulate apical secretion of Vermiform.

A recent study provided more insights into the pattern of apical membrane activity that guides the expansion of the tracheal lumen (Tsarouhas et al., 2007). The initial expansion of the lumen is driven by a pulse of exocytosis that drives the deposition of secreted proteins into the lumen, resulting in expansion of the luminal diameter. This process requires the small GTPase Sar1 that regulates budding of COPII vesicles from the endoplasmic reticulum towards the Golgi apparatus, and mutation of COPII subunits phenocopies *sar1* mutants. Although chitin is secreted in *sar1* mutants, the resulting scaffold is more narrow and dense than normal, suggesting that chitin-binding or -modifying proteins might not be normally secreted; indeed Vermiform secretion is defective in the *sar1* background. After this wave of apical secretion follows the clearance of solid material from the lumen. This event depends on a pulse of endocytic activity that requires the small GTPase Rab5, a master regulator of endocytosis. Clearance of the liquid that has accumulated in the lumen occurs at a later point by mechanisms that remain to be elucidated.

1.4.4. Lumen formation in capillaries

The capillaries of the circulatory system provide a fascinating system for the study of single-cell tubulogenesis through cell hollowing. Capillaries consist of endothelial cells, each forming a tube without autocellular junctions. These cells are arranged in a linear fashion with cellular junctions linking them together, much like a

long pipe made by the serial connection of smaller ones.

During in vitro capillary formation, integrin-ECM interactions stimulate the formation of vacuoles within the endothelial cells through endocytosis (Folkman and Haudenschild, 1980; Davis and Camarillo, 1996; Bayless et al., 2000). The vacuoles that arise from endocytosis appear to be "consumed" in the process of lumen formation, suggesting that their coalescence is the driving force behind tubulogenesis (Dyson et al., 1976; Wolff and Bär, 1972). It has been postulated that endocytosis following integrin activation is mediated by Cdc42 and its effector N-WASP, established regulators of actin cytoskeleton dynamics (Bayless and Davis, 2002). This was based on the observation that dominant negative versions of Cdc42 or N-WASP block capillary formation in vitro (Bayless and Davis, 2002). Although this remains a valid possibility, another interpretation, given the role of Cdc42 in apical exocytosis in MDCK cells (discussed above), is that Cdc42 and N-WASP are required for capillary formation because of their role in vesicle secretion.

Despite these and other studies supporting the idea that coalescence of vesicles drives capillary lumen formation, strong in vivo evidence came only recently. Taking advantage of the accessibility of the vasculature in developing zebrafish embryos, Kamei et al. were able to make high resolution recordings (Kamei et al., 2006). They demonstrated that vesicle fusion within the center of the endothelial cells results in the formation of "hollow" cells that are linearly arranged with cellular junctions. As these central vacuoles fuse to each other, a continuous capillary forms.

Interlude: A note on prescient introductions

My studies of sensory organ morphogenesis in *C. elegans* implicated the worm homolog of Nemo-like kinase, *lit-1*, the regulator of actin polymerization WASP, as well as the retromer complex in the regulation of the morphogenesis of the amphid sensory compartment. It is a testament to the power of genetics that the involvement of these molecules could not have been anticipated at the beginning of this project. However, in order to better prepare the reader for what lies ahead, I have included in the introduction a few brief sections that touch upon these subjects.

1.5. Nemo/LIT-1/Nemo-like kinase in development

1.5.1. *nemo* in *Drosophila* development

The *Drosophila* eye consists of approximately 800 individual ommatidia. Each ommatidium consists of about twenty cells, among which are eight photoreceptor cells referred to as R1 to R8. These cells arrange themselves to form a trapezoid (a four-sided figure with only one pair of parallel sides), with R3 forming the apex of the trapezoid. The compound eye established by these ommatidia is a polarized epithelium with a horizontal plane across the middle, referred to as the equator, separating the eye into dorsal and ventral sides. The ommatidia on either side have a chiral arrangement, pointing in opposite directions (away from the equator), resulting in mirror symmetry across the equator. This symmetry is established first by the assignment of the R3 and R4 fates through the planar cell polarity (PCP) that breaks the initial symmetry of the developing ommatidium (Simons and Mlodzik, 2008). Following this event, the

ommatidia rotate 90° clockwise on the dorsal side and 90° counterclockwise on the ventral side. Mutations in PCP components, such as *frizzled*, show defects in chilarity: R3 and R4 are not correctly specified, rotation is initiated in the wrong direction and the degree of rotation is disrupted (Zheng et al., 1995). However, rotation does take place in PCP mutants, suggesting that the molecular machinery that effects rotation is, at least partially, independent from PCP. In accordance with this hypothesis, a few genes that affect rotation but have no role in PCP have been isolated.

nemo, a gene encoding a serine/threonine kinase homologous to the family of mitogen-activated (MAP) kinases, was initially identified in *Drosophila* as required for the last 45° of the 90° ommatidial rotation (Choi and Benzer, 1994). Over-expression of *nemo* results in over-rotation of the ommatidia, (Chou and Chien, 2002), suggesting that *nemo* is part of the driving force behind rotation. More recently, *nemo* has also been implicated in regulating the speed at which the first 45° rotation takes place (Fiehler and Wolff, 2008). Importantly, no defects in PCP are seen in the eyes of *nemo* mutants (Choi and Benzer, 1994).

Mutations in *scabrous*, a gene encoding a fibrinogen-related secreted protein (Baker et al., 1990; Mlodzik et al., 1990), result in ommatidia over-rotation, while over-expression of *scabrous* results in under-rotation. This under-rotation phenotype is enhanced by deletion of one copy of *nemo*, and suppressed by over-expression of *nemo*, giving rise to the hypothesis that *scabrous* acts by antagonizing *nemo* activity (Chou and Chien, 2002). This hypothesis is complicated by the observation that the *scabrous* over-rotation does not persist in the adult animals, in contrast to the under-rotation seen in *nemo* mutants (Brown and Freeman, 2003).

Finally, signaling through the epidermal-growth factor receptor (EGFR) regulates ommatidial rotation (Gaengel and Mlodzik, 2003; Strutt and Strutt, 2003; Brown and Freeman, 2003), with mutants for EGFR and EGF ligands having both over-rotated and under-rotated ommatidia. Interestingly, although EGF signaling is required shortly after the 90° rotation brought about by *nemo* activity, defects in ommatidia orientation in EGFR mutants arise significantly later, suggesting a mechanism independent of *nemo* (Brown and Freeman, 2003). In accordance with this hypothesis, there is no synergy between *nemo* and EGF signaling mutations (Brown and Freeman, 2003).

nemo has been shown to regulate many other processes in *Drosophila*. Indeed, *nemo* mutants display many phenotypes beyond defective ommatidial rotation, such as rounder and shorter wings with extra vein material, defective polarity of wing hairs and abdominal bristles, as well as reduced viability and infertility among the escapers (Choi and Benzer, 1994; Verheyen et al., 2001). Genetic interaction studies suggest that *nemo* inhibits vein formation by antagonizing *Wingless*/Wnt signaling (Verheyen et al., 2001; Zeng and Verheyen, 2004); as discussed later, this appears to be a conserved role of the Nemo kinase. In *Drosophila*, *nemo* is maternally provided and injection of *nemo* dsRNA into embryos greatly reduces viability (Verheyen et al., 2001). *nemo* is expressed during early development throughout the embryo where it affects segmentation and promotes the activity of the homeodomain transcription factor Even-skipped (Braid et al., 2010). Later in embryonic development it is enriched in the central nervous system (Verheyen et al., 2001). In the nervous system, Nemo promotes synapse growth in larval neuromuscular junctions by enhancing bone morphogenetic factor (BMP) signaling (Merino et al., 2009). More specifically, within motors neurons, Nemo is reported to phosphorylate the

R-Smad Mad (which is also activated by BMP signaling) and promote its translocation from the neuromuscular junction to the cell nucleus. There, Mad activates transcriptional networks that lead to formation of synaptic butons. Interestingly, genetic studies have led the same group to propose the opposite role for Nemo, in antagonizing BMP signaling, during *Drosophila* wing formation (Zeng et al., 2007). In vitro studies suggest that Nemo antagonizes BMP signaling by phosphorylating Mad and inhibiting its nuclear accumulation (Zeng et al., 2007). These observations suggest that the interactions between Nemo and TGF-β signaling must be modulated by other, so far uncharacterized factors.

1.5.2. *lit-1*/Nlk in *C. elegans* development

The *C. elegans* homolog of *nemo* was identified as *lit-1* (loss of intestine) for its role in endoderm induction (Kaletta et al., 1997). During the four cell stage of embryonic development, Wnt signaling from the P2 cell to the EMS cell results in the polarization of EMS and its asymmetric division to MS, in which Wnt signaling is inactive and which will give rise to mesoderm, and E, in which Wnt signaling is active and which will give rise to endoderm (Rocheleau et al., 1997; Thorpe et al., 1997; Eisenmann, 2005). In *lit-1* mutants, this Wnt-dependent polarization event does not take place and the EMS cell produces two MS cells, resulting in embryonic lethality due to lack of endodermal tissues.

How does *lit-1* regulate this Wnt pathway? LIT-1 can phosphorylate and form a stable complex with the β-catenin WRM-1, and this complex is able to phosphorylate the

TCF/LEF homolog of *C. elegans* POP-1 (Rocheleau et al., 1999). β-catenin/WRM-1 is absolutely required for POP-1 phosphorylation, and the MAP Kinase kinase kinase (MAP3K) MOM-4 enhances the activity of the LIT-1/WRM-1 complex (Shin et al., 1999). Phosphorylation of POP-1/ TCF/LEF results in its export from the nucleus (Rocheleau et al., 1999; Shin et al., 1999; Lo et al., 2004). Therefore, two cells are produced following the division of EMS: an anterior MS cell with high nuclear levels of POP-1/ TCF/LEF and a posterior E cell with low nuclear levels of POP-1/ TCF/LEF (Lin et al., 1995; Rocheleau et al., 1997; Meneghini et al., 1999) (Figure 1.11).

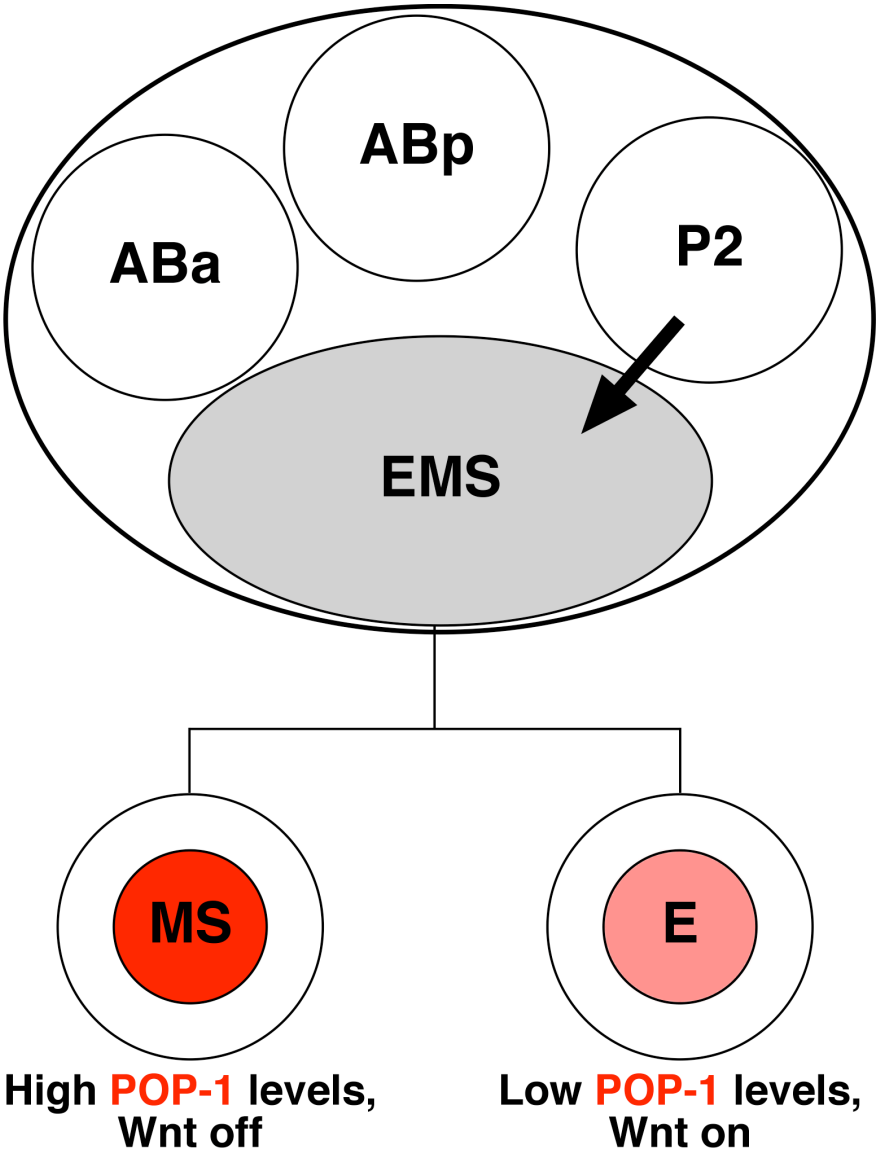

Figure 1.11. P2 to EMS induction during the four-cell stage of *C. elegans* embryogenesis. A Wnt signal from the P2 cells induces the polarization of EMS. Division of EMS results in an anterior MS cell with high POP-1/ TCF/LEF nuclear levels, in which expression of Wnt targets is off, and a posterior E cell with low POP-1/ TCF/LEF nuclear levels, in which expression of Wnt targets is turned on.

Interestingly, as mentioned before, Wnt signaling is activated in the E cell, the one characterized by low levels of nuclear POP-1/ TCF/LEF. How can this discrepancy be explained? One early hypothesis suggested that POP-1/ TCF/LEF acts as a repressor of Wnt signaling and its export from the nucleus leads to derepression. However, the currently accepted model is significantly more nuanced. It is now believed that activation of Wnt signaling in the E blastomere is driven by an interaction between molecules of POP-1/ TCF/LEF that remain in the nucleus and another β-catenin found in *C. elegans*, SYS-1 (Kidd et al., 2005). Thus, the current consensus is that high levels of nuclear POP-1/ TCF/LEF shut down Wnt signaling because β-catenin/SYS-1 is present at low levels. Wnt signaling leads to stabilization of β-catenin/SYS-1 in the E cell (Huang et al., 2007), but this is not enough for activation of Wnt targets; the levels of nuclear POP-1/ TCF/LEF must be reduced in order for the few SYS-1/POP-1 complexes to be able to bind to the promoters of target genes and activate their transcription (Kidd et al., 2005; Huang et al., 2007) (for a detailed discussion of this intriguing model, see Phillips and Kimble, 2009).

This non-canonical realization of the Wnt signaling pathway (dubbed the "Wnt/β-catenin asymmetry pathway" to differentiate it from the planar cell polarity pathway (Mizumoto and Sawa, 2007b)) is involved in many other cell fate decisions in *C. elegans*, under the control of *lit-1*. These include the asymmetric divisions of the T cell in the tail of the animal (Herman, 2001), the B cell division in the male tail (Wu and Herman, 2006), the Z1 and Z4 cells in the gonad (Siegfried and Kimble, 2002), the seam cells along the length of the body (Takeshita and Sawa, 2005), and the ABprpapaaa neuronal progenitor (SMDD/AIY mother) cell (Bertrand and Hobert, 2009).

1.5.3. Nemo-like kinase (Nlk) in vertebrate development

In vertebrates, Nlk was first identified in mice based on its homology to the *Drosophila nemo* (Brott et al., 1998). It is highly expressed in the brain of adult animals, acts as a serine/threonine kinase that can be auto-phosphorylatated, and, based on subcellular fractionation studies, localizes primarily to the nucleus (Brott et al., 1998). Depending on their genetic background, Nlk deficient mice can survive embryogenesis, but display a series of neurological defects, as well as defects in bone marrow formation (Kortenjann et al., 2001).

In zebrafish, Nlk has been shown to promote Wnt signaling (Thorpe and Moon, 2004), while in *Xenopus* it has been shown to antagonize Wnt signaling (Ishitani et al., 1999). These conflicting results could potentially be reconciled by the new model for Wnt regulation by Nlk that has emerged from work in *C. elegans* (Kidd et al., 2005; Phillips and Kimble, 2009).

Nlk has been shown to promote neurogenesis in zebrafish embryos by inhibiting the Notch signaling pathway (Ishitani et al., 2010). More specifically, Nlk was shown to phosphorylate the intracellular domain of Notch (NotchICD) that is proteolytically released after activation of Notch by Delta. This phosphorylation inhibits the formation of the Notch transcriptional activation complex that normally leads to the expression of suppressors of neuronal fate.

Finally, in *Xenopus*, Nlk, activated by TAK-1 (the vertebrate homolog of the MAP3K MOM-4 of *C. elegans*), has been shown to bind to and phosphorylate the

transcription factor STAT3, during activation of the JAK-STAT signaling pathway in mesoderm induction (Ohkawara et al., 2004).

1.6. WASP and the actin cytoskeleton

At the very heart of the myriad contributions of the actin cytoskeleton to cell shape, cell motility, and membrane dynamics lies the ability of globular actin (G-actin) monomers to assemble into filamentous actin (F-actin). These filaments can be either unbranched or branched, but in either case, their formation depends on actin nucleation factors, since spontaneous filament assembly is inefficient. This is because the actin dimer, a necessary intermediate for the formation of a filament, is very unstable (Pollard and Borisy, 2003).

The nucleation of branched filaments is achieved by the Arp2/3 complex (Goley and Welch, 2006). The Arp2/3 complex can attach to a pre-existing actin filament and mimic an actin dimer or trimer. Thus, it acts as a base for the initiation of a new filament that sprouts off the pre-existing one, at a 70° angle, forming y-branched actin networks. For efficient filament formation, the Arp2/3 complex requires, besides a pre-existing filament, the help of nucleation-promoting factors, a variety of which have been characterized (Campellone and Welch, 2010).

Probably the best-characterized nucleation-promoting factor is the Wiskott-Aldrich syndrome protein (WASP). The gene encoding WASP was shown to be mutated in WAS patients (Derry et al., 1994), and shortly afterward, WASP was identified as an effector of the Rho family GTPase Cdc42 and a promoter of actin polymerization

(Symons et al., 1996) (WASP is expressed specifically in haematopoietic cells; in other tissues the more broadly expressed neural-WASP (N-WASP) serves the same purpose). As previously discussed, Rho family GTPases are important regulators of the actin cytoskeleton (Etienne-Manneville and Hall, 2002). Similar to other small GTP binding proteins, these GTPases act as molecular switches that cycle between a GDP-bound (off) state and a GTP-bound (on) state. Under resting conditions, N-WASP is autoinhibited and thus unable to stimulate actin polymerization; a variety of mechanisms lead to the release of this autoinhibition (Higgs and Pollard, 2001). These include interaction of N-WASP with Cdc42-GTP through its GTPase binding domain (GBD), interaction of the smaller basic-rich domain with membrane bound phosphatidyl inositol 4,5-bisphosphate and binding of other regulators to the proline-rich region of N-WASP. The C-terminal region of N-WASP is the business end of the molecule. This region is characterized by the WCA domain: W for WASP homology 2 domain, C for connector region, and A for acidic region. This domain is responsible for binding to the Arp2/3 complex and promoting the addition of actin molecules to the growing branch (Rohatgi et al., 1999) (Figure 1.12).

Figure 1.12. The molecular architecture of N-WASP. The depicted domains are: WH1 for WASP homology 1, B for basic region, GDB for GTPase binding domain, PolyP for proline rich domain, W for WASP homology 2 domain, C for connector domain, and A for acidic domain.

1.7. The retromer complex

The retromer is a protein complex that facilitates retrograde transport of transmembrane proteins from early endosomes to the Golgi; initially identified in yeast (Seaman et al., 1998), this complex has since been found to be molecularly and functionally conserved in metazoans as well as plants (Seaman, 2005; Bonifacino and Hurley, 2008). To achieve retrograde transport, the retromer associates with the cytoplasmic surface of the endosomal membrane, recognizes the intracellular domain of the target transmembrane protein (the cargo), and induces bending of the membrane, thus facilitating the scission of a vesicle enriched for the cargo, which can then be targeted to the Golgi. Two subunits make up a functional retromer comlex: the cargo-recognition subunit, and the membrane-bending subunit (Figure 1.13). The cargo recognition subunit is a heterotrimer consisting of Vps35, Vps29 and Vps26, with the larger Vps35 protein being the one that interacts with the intracellular tail of the transmembrane cargo protein. The membrane-bending subunit is a heterodimer of two sorting nexin (SNX) proteins (van Weering et al., 2010). More than 30 sorting nexins (not all of them associated with the retromer) have been identified in mammals (Cullen, 2008), and the exact combination that forms the dimer can vary, with SNX1, SNX2, SNX5, SNX6 and SNX32 being the ones most commonly reported. Two distinct domains account for the activity of sorting nexins. One is an N-terminal Phox-homology (PH) domain that recognizes phosphoinositides (the exact species varies between nexins) and thus targets sorting nexins to the endosomal membrane. The other is a C-terminal BAR domain (Bin/Amphiphysin/Rvs) that consists of three α-helices. Interaction between the BAR domains of two SNX molecules leads to the formation of a rigid, banana-shaped dimer,

which can induce membrane bending (Peter et al., 2004). Thus, the Vps subunit binds to the cargo, while the SNX subunit binds and bends the mebrane; the accumulation of a large number of retromer complexes on the cytoplasmic surface of the endosome results in the formation of long tubules, enriched for the cargo protein, that can bud off and coalesce with the Golgi network. In this way, the retromer can be used to recycle transmembrane proteins that are internalized during endocytosis, before they are destroyed as the endosome matures into a lysosome.

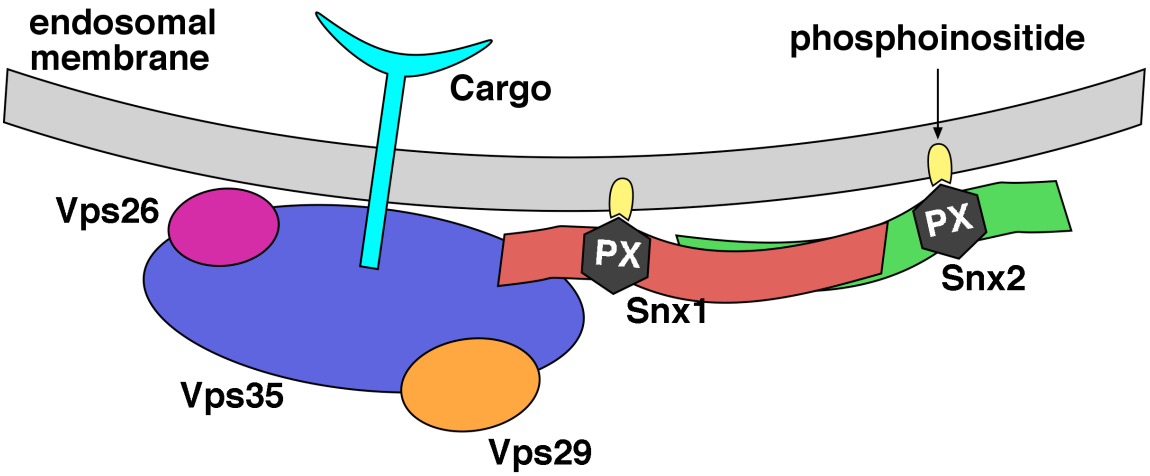

Figure 1.13. Schematic of the retromer complex (Hierro et al., 2007). The cargo-recognition domain consists of Vps35, Vps26 and Vps29. The membrane-bending domain is a heterodimer of sorting nexins (Snx1 and Snx2 are depicted here, but other combinations can occur). The sorting nexins bind to phosphoinositides through their PX domains, while the banana shaped BAR domain induces membrane curvature. The concentrated action of many retromer complexes induces the sprouting of tubules, enriched for the cargo, off the endosomal membrane.

A fascinating example of the importance of the retromer in development concerns Wnt signaling in *C. elegans* and *Drosophila*. In *C. elegans*, initial studies identified a role for Wnt signaling in the anterior/posterior polarity of the mechanosensory neurons ALM and PLM (Prasad et al., 1998). These studies also demonstrated that VPS-35 is required within Wnt secreting cells for polarity establishment, suggesting a role for the retromer in efficient Wnt signaling. Another study showed that *vps-35*, *vps-26* and *vps-29* (the genes encoding the cargo-selecting subunit of the retromer) are required within Wnt-producing cells of the tail for the establishment of the EGL-20/Wnt posterior-to-anterior gradient, which regulates migration of the Q neuroblasts (Coudreuse et al., 2006). Importantly, the same study showed that the retromer is also required for the induction of Wnt target genes during *Xenopus* embryogenesis. Interestingly, mutation of *snx-1* had no effect on Wnt signaling on its own, and only slightly increased the penetrance of the *vps* mutants, suggesting a potential redundancy between *snx* genes.

What is the mechanistic basis behind the requirement for the retromer in Wnt signaling? If the retromer acts in retrieving transmembrane proteins from the endosomal compartment and sending them to the Golgi, what is the protein that is retrieved here? The answer to these questions came from five independent studies, two in *C. elegans* (Pan et al., 2008; Yang et al., 2008), and three in *Drosophila* (Franch-Marro et al., 2008; Belenkaya et al., 2008; Port et al., 2008). Wnt is synthesized in the endoplasmic reticulum and, after the addition of two lipid moieties (Takada et al., 2006; Willert et al., 2003) it progresses to the Golgi network, where it binds to Wntless (MIG-14 in *C. elegans*) (Bänziger et al., 2006; Bartscherer et al., 2006). Wntless is a transmembrane protein that facilitates release of the Wnt ligand into the extracellular space, as vesicles

carrying Wntless-Wnt complexes fuse with the plasma membrane. After release of Wnt, Wntless is absorbed through endocytosis into early endosomes. It is at this point that the retromer comes in. As the *C. elegans* and *Drosophila* studies showed, the retromer mediates the retrograde transport of Wntless, recognized by Vps35, from the endosome to the Golgi. There, it can be re-used for the secretion of Wnt. In accordance with this model, Wntless levels are reduced in a *vps35* background, and secretion of Wnt in a *vps35* background can be rescued by overexpression of Wntless. Again, it is interesting that none of these studies address the role of the membrane-bending subunit of the retromer in Wnt signaling.

Chapter 2

Reconstruction of amphid pocket morphogenesis in wild-type and *daf-6* embryos

Summary

In this chapter I describe my efforts to understand the developmental basis of the defects observed in *daf-6* mutants. To achieve this, Yun Lu performed electron microscopy on serial sections of wild-type and *daf-6* embryos. By reconstructing these sections, I was able to show that the components of the amphid (the sensory dendrites, the sheath glia and the socket glia) come together normally in *daf-6* mutants, and that the sensory compartment opens to the environment. These results argue that *daf-6* is not required for either of these morphogenetic steps. However, soon after the amphid primordium has formed, it expands abnormally in *daf-6* embryos, suggesting that *daf-6* is involved in restricting the size of the sensory compartment.

2.1. *daf-6*/Patched-related inhibits amphid sensory compartment growth

As discussed in the introduction, the amphid sheath glial cell forms a compartment that surrounds the ciliated endings of amphid sensory neurons, constraining them into a tight bundle (Figure 2.1A,B). Within this bundle, ten sensory cilia are stereotypically arranged in three successive columns containing 3, 4, and 3 cilia respectively (Figure 2.1B) (Ward et al., 1975). Work previously published by our lab reported the cloning and characterization of *daf-6*, a Patched-related gene required for amphid channel morphogenesis (Perens and Shaham, 2005). In adult *daf-6*(*e1377*) mutants, the amphid channel is grossly enlarged, the socket and sheath glia channels are not continuous, and distal portions of sensory cilia are neither bundled, nor exposed to the environment (Figure 2.1C,D).

It is interesting to note that *n1543*, another allele of *daf-6*, displays less bloating and the cilia appear to be exposed to the environment in at least some animals. Bent cilia, trapped within the animals are observed, and *daf*-6(*n1543*) mutants also fail to dye-fill; however, they can enter dauer more frequently than *e1377* animals (Elliot Perens, personal communication). These observations suggest that *n1543* is a weaker allele than *e1377*, and, more interestingly, that *daf-6* could have a broader role in the physiology of the amphid.

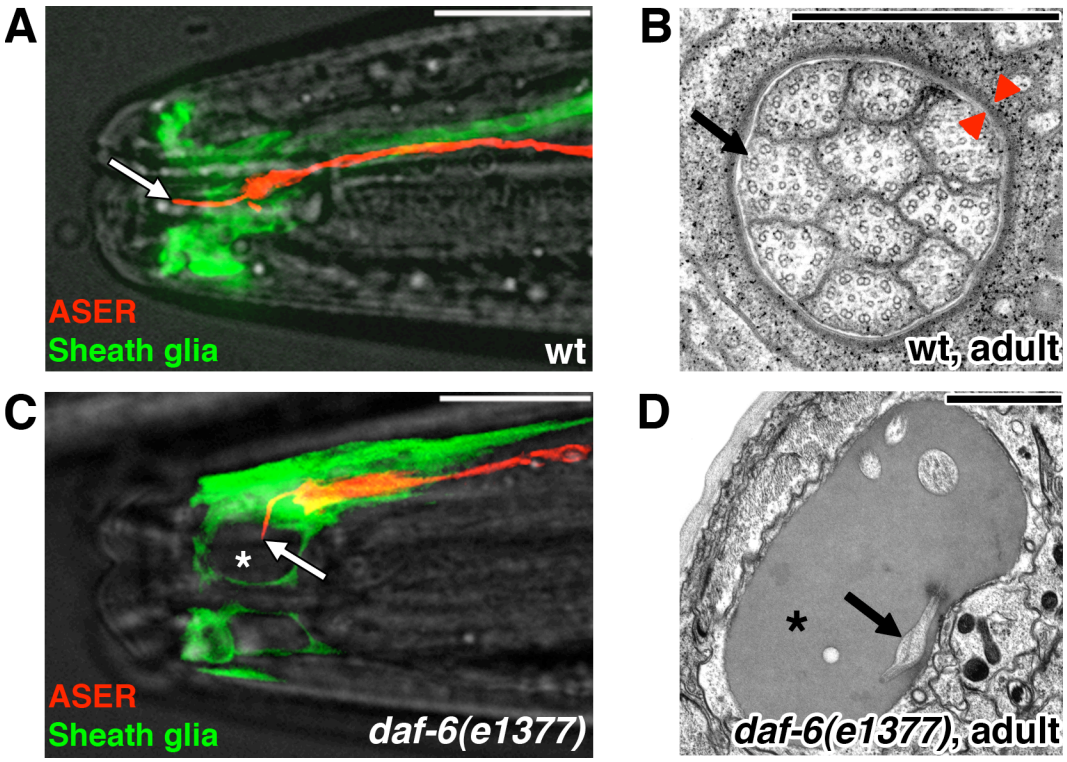

Figure 2.1. Amphid sensory compartment morphology of adult wild-type and *daf-6* animals. (A, C) The ASER neuron and the amphid sheath glia visualized, respectively, with mCherry (red; driven by the *gcy-5* promoter) and GFP (green; driven by the *T02B11.3* amphid sheath promoter (Wang et al., 2008)) in a wild-type (A) or *daf-6*(*e1377*) (C) animal. The ASER neuron extends a single cilium through the length of the amphid channel in the wild type (arrow). In the mutant, the cilium is bent and not exposed to the environment, and the amphid pocket is bloated (asterisk). (B, D) Electron micrographs of a cross-section through the anterior portion of the amphid sheath glia channel in an adult wild-type animal (B) or a *daf-6*(*e1377*) mutant (D). Arrow in (B), sensory cilium. Red arrowheads indicate subcortical electron dense material. Arrow in (D), bent cilium. Asterisk, bloated sheath glia channel. Note difference in magnification between (B) and (D). White scale bars, 10 μm. Black scale bars, 1 μm.

At least two interpretations of this phenotype are possible: first, *daf-6* might act to open the sheath glia channel at its anterior end. Thus in *daf-6* mutants, the channel would form but remain sealed, and would continuously enlarge as matrix material is deposited. Second, *daf-6* might act to constrain the luminal diameter of the sheath glia channel. Thus, in *daf-6* mutants, the sheath and socket glia would properly align and form an open compartment, yet without lateral constraints on its size, the sheath channel would expand circumferentially. In this latter model, loss of the sheath-socket junction would be a later, secondary defect.

To discriminate between these possibilities, Yun Lu used electron microscopy (EM) to follow the development of amphid sensory compartments in wild-type and *daf-6*(*e1377*) mutant embryos. She employed high-pressure freezing (see materials and methods) to fix embryos at several time points between 300 and 450 minutes post-fertilization, the time period during which the amphid is generated (Sulston et al., 1983), and collected serial sections. By analyzing these sections, I was able to reconstruct key aspects of amphid sensory compartment morphogenesis.

By 380 minutes, sensory dendrites that have not yet formed cilia are evident in wild-type embryos. These dendrites are laterally ensheathed by the sheath glial cell, but the sheath cell also forms a cap blocking the anterior portion of the compartment and preventing access of neuronal processes to the socket (Figure 2.2). Structures resembling basal bodies (the initial sites of cilia construction) are visible at dendrite endings (black arrowhead in Figure 2.2). Filamentous structures can be seen within the sensory compartment. Interestingly, neighboring dendrites form electron dense structures at points of contact, which could denote junctions. In the adult animal, the dendrites form

junctions with the sheath glia, but not among themselves, suggesting that dendrite-to-dendrite attachments could be transient and limited to the period of amphid morphogenesis.

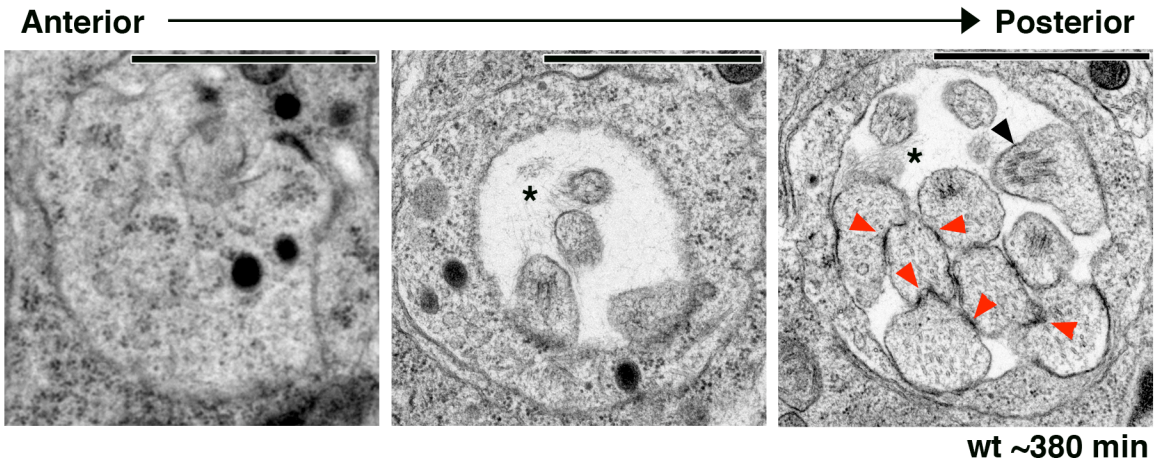

Figure 2.2. Electron micrographs of cross-sections through the amphid primordium of a wild-type embryo at 380 minutes of development. At this point in development, the amphid sensory compartment is blocked anteriorly by a cap formed by the sheath glia (left). More posteriorly (middle and right), the sheath wraps around the dendrites of the amphid neurons. Asterisks mark filaments. In right image, basal bodies can be discerned (black arrowhead), as well as junction-like electron dense structures between neighboring dendrites (red arrowheads). Scale bars, 1 μm.

By 400 minutes, a well-defined amphid primordium is formed in wild-type embryos (Figure 2.3). The sheath glia cap is gone and the open channel is continuous with the socket glia channel (Figure 2.3 left). At this stage, the socket channel is devoid of neuronal processes as dendritic tips have yet to extend cilia. Again, structures resembling basal bodies are visible at dendrite endings and fibrous densities can be seen within the amphid sensory compartment.

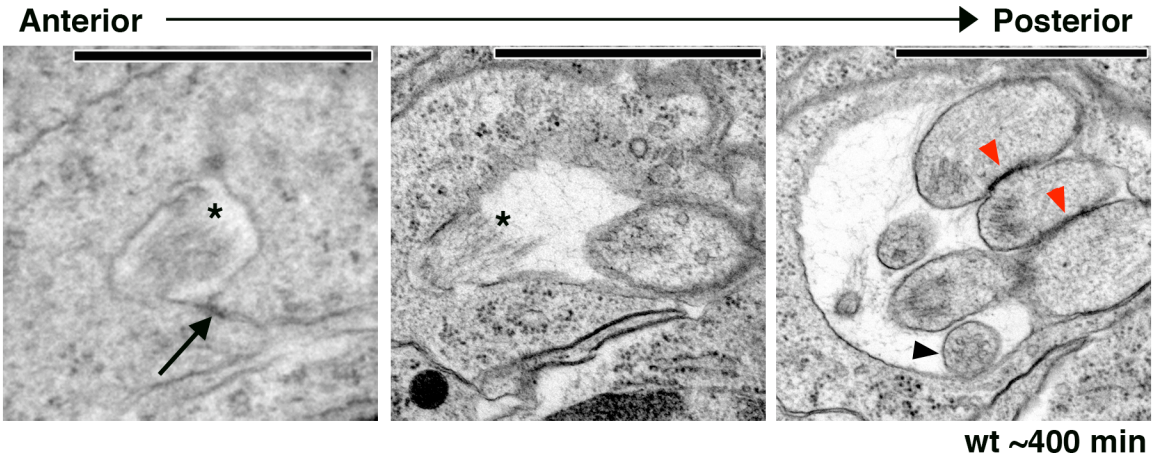

Figure 2.3. Electron micrographs of cross-sections through the amphid primordium of a wild-type embryo at 400 minutes of development. The amphid sensory compartment has now opened anteriorly and the self junction of the socket glia can be discerned (arrow in left image). More posteriorly (middle and right), the sheath wraps around the dendrites of the amphid neurons. Asterisks mark filaments. In right image, basal bodies can be discerned (black arrowhead), as well as junction-like electron dense structures between neighboring dendrites (red arrowheads). Scale bars, 1 μm.

These fibers are more prominent in longitudinal sections through the amphid primordium. In Figure 2.4, a dense arrangement of filaments can be seen to traverse the socket channel and form a link between the tips of the sensory dendrites and the outside of the embryo. Although the nature of these filaments is unclear, they are consistent with the extracellular matrix proposed to anchor dendrites during retrograde extension (Heiman and Shaham, 2009).

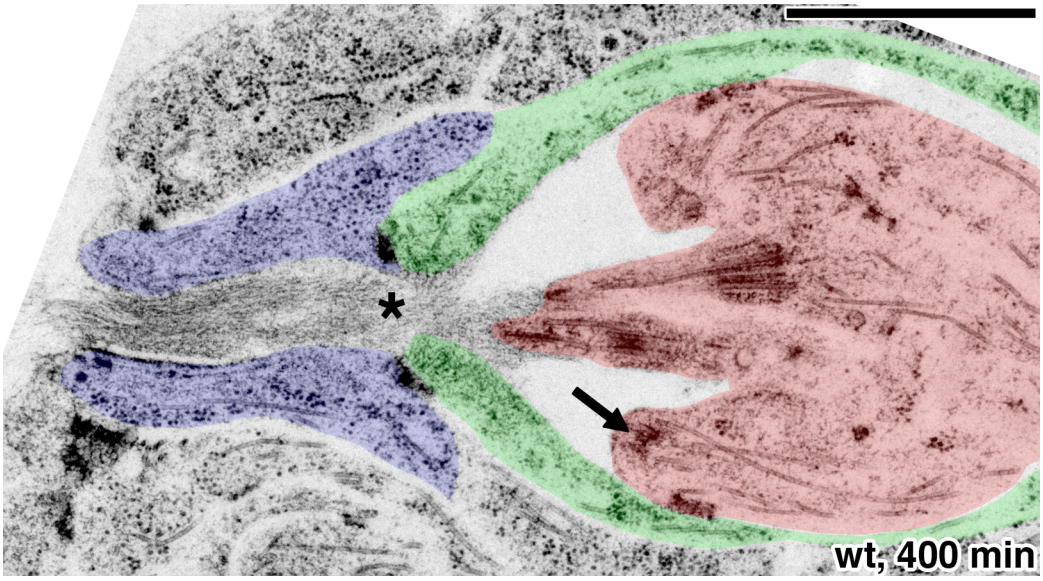

Figure 2.4. Electron micrograph of a longitudinal section through the amphid primordium of a wild-type embryo at 400 minutes of development. The socket is pseudo-colored in blue, the sheath in green and the dendrites in red. Asterisk marks filaments, arrow marks a basal body. Scale bar, 1 μm.

In *daf-6* mutant embryos, the initial stages of amphid development are unperturbed (n=3). By 400 minutes, the sheath and socket channels are aligned and open as seen in serial cross-sections (Figure 2.5)

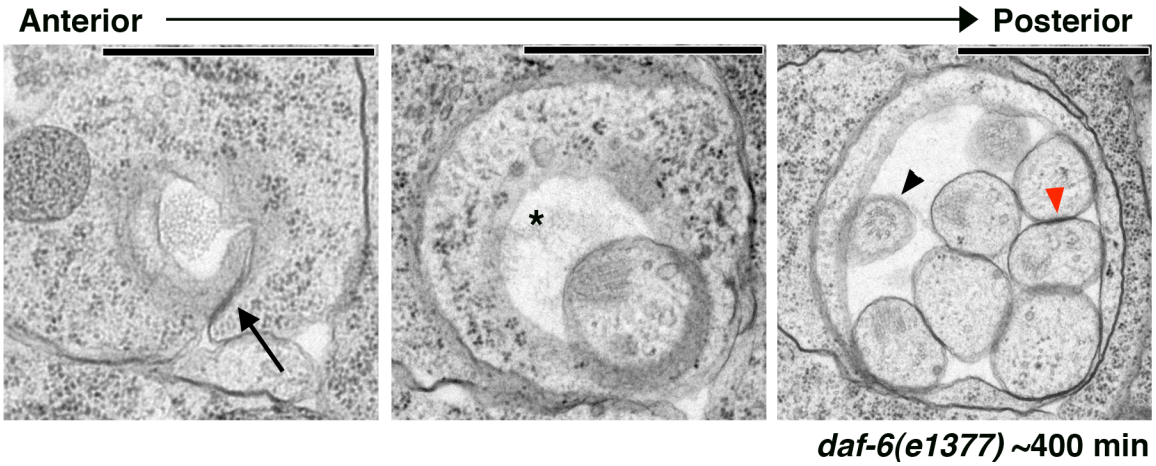

Figure 2.5. Electron micrographs of cross-sections through the amphid primordium of a *daf-6* embryo at 400 minutes of development. The amphid primordium appears to be normal (compare to Figure 2.3). The self junction of the socket glia is marked by an arrow in left image. Asterisk marks filaments. In right image, basal bodies can be discerned (black arrowhead), as well as junction-like electron dense structures between neighboring dendrites (red arrowhead). Scale bars, 1 μm.

In a longitudinal section (Figure 2.6), dendrites lacking cilia, but containing basal body-like structures, can be seen within the sheath channel, while filaments emanating from the dendrite tips and traversing the sheath and socket channels are also observed.

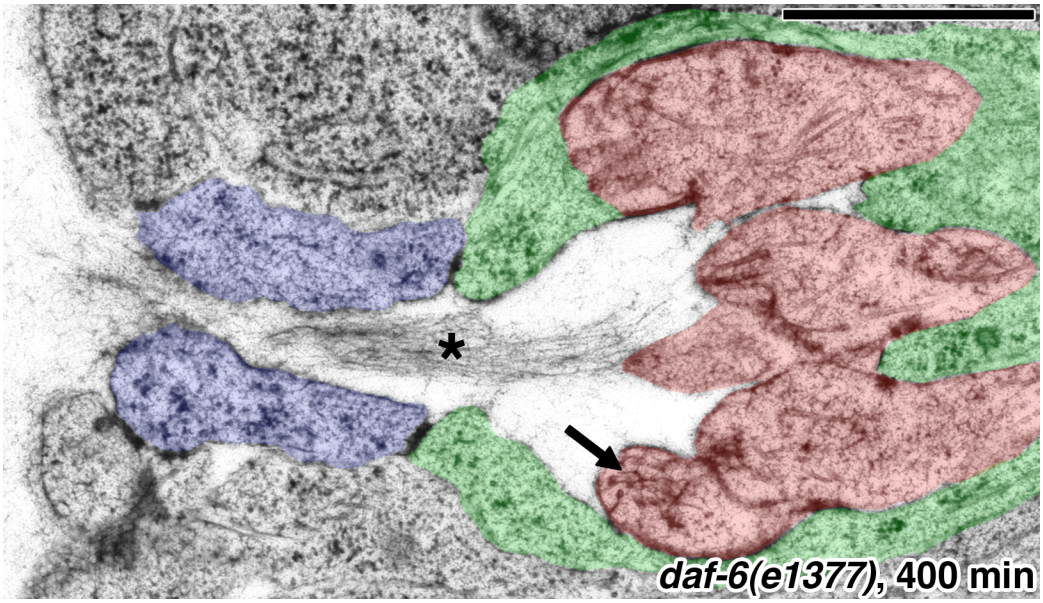

Figure 2.6. Electron micrograph of a longitudinal section through the amphid primordium of a *daf-6* embryo at 400 minutes of development. The socket is pseudo-colored in blue, the sheath in green and the dendrites in red. Asterisk marks filaments, arrow marks a basal body. Scale bar, 1 μm.

Despite the normal morphology of *daf-6* amphids at 400 minutes of development, only slightly later, at 420 minutes (before cilia have formed), bloating of the amphid sheath channel is apparent, and dendrites begin to unbundle (Figure 2.7B, compare to 2.7A).

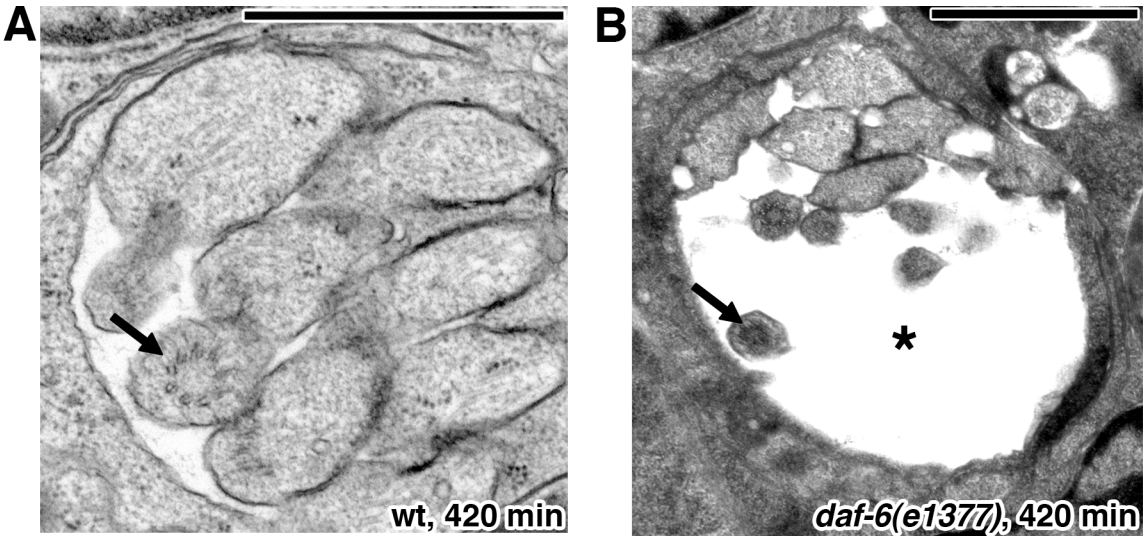

Figure 2.7. Electron micrographs of cross-sections through the amphid primordium at 420 minutes of development. (A) wild-type and (B) *daf-6*. Arrows mark basal bodies. Asterisk marks bloating of the sensory compartment. Note difference in scale between (A) and (B). Scale bars, 1 μm.

These studies indicate that *daf-6* is not required for aligning the sheath and socket channels, or for opening the amphid sensory compartment. Rather, *daf-6* seems to function in restricting compartment growth.

Chapter 3

Opposing activities of LIT-1/NLK and DAF-6/Patched-related direct sensory compartment morphogenesis in *C. elegans*

Summary

In this chapter I describe my studies concerning the role of *lit-1* in the morphogenesis of the amphid sensory compartment. I show that *daf-6* is suppressed by mutations of *lit-1*/Nemo-like kinase (NLK), a gene that acts within glia, in counterbalance to *daf-6*, to promote sensory compartment expansion. Although LIT-1 has been shown to regulate Wnt signaling, my studies demonstrate a novel, Wnt-independent role for LIT-1 in sensory compartment size control. I show that the LIT-1 activator MOM-4/TAK1 is also important for compartment morphogenesis and that both proteins line the glial sensory compartment. LIT-1 compartment localization is important for its function and requires neuronal signals. Furthermore, the conserved LIT-1 C-terminus is necessary and sufficient for this localization. I found that this domain binds both actin and the Wiskott-Aldrich syndrome protein (WASP), an actin regulator. I show that actin is highly enriched around the amphid sensory compartment, and that WASP is important for compartment expansion and functions in the same pathway as LIT-1. These studies uncover a novel, Wnt-independent role for the conserved Nemo-like kinase LIT-1 in controlling cell morphogenesis in conjunction with the actin cytoskeleton, and suggest that the *daf-6* and *lit-1* glial pathways constitute a rheostat used to control sensory compartment size.

3.1. A screen for suppressors of *daf-6*

The abnormal expansion of the amphid sensory compartment in *daf-6* mutants suggests that active processes promote compartment expansion and that these processes are balanced by *daf-6* activity during development. I surmised that mutations in genes promoting compartment expansion might, therefore, counteract the loss of *daf-6* and restore compartment size and function.

A screen for suppressors of *daf-6* had already been performed in our lab by Elliot A. Perens (Perens, 2006) in order to identify genes that regulate amphid morphogenesis, and will be succinctly described here. Elliot screened for mutants able to generate a normal compartment in the absence of *daf-6* function, taking advantage of an easily scored *daf-6* defect: the inability to form dauer larvae, a phenotype that is fully recessive and fully penetrant in the *e1377* allele of *daf-6*. Dauer is an alternative developmental state induced by starvation and perception of high concentration of dauer pheromone. Dauer animals are highly resistant to environmental insults and can survive in the presence of 1% sodium-dodecylsulfate (SDS) (Cassada and Russell, 1975). *daf-6* mutants fail to become dauer larvae, presumably due to their sensory deficits (Riddle et al., 1981), and are thus killed by exposure to SDS. Elliot therefore randomly mutagenized animals homozygous for the strong loss-of-function *daf-6*(*e1377*) allele (Perens and Shaham, 2005) using ethyl methanesulfonate (EMS), allowed F2 animals to starve, and treated them with SDS. Resistant animals could have suppressed the *daf*-6 amphid sensory compartment defects, or could have constitutively activated a more downstream step in dauer formation. To distinguish between these mutant classes, he examined the ability of amphid sensory neurons to fill with dye provided in the medium.

When exposed to a solution of the lipophilic dye DiI, wild-type animals readily take up the dye into exposed amphid neurons. *daf-6* animals fail to do so, presumably due to their defective amphid sensory compartments (Figure 3.1), a phenotype referred to as "Dyf" for "dye-filling defective" (Perkins et al., 1986; Starich et al., 1995).

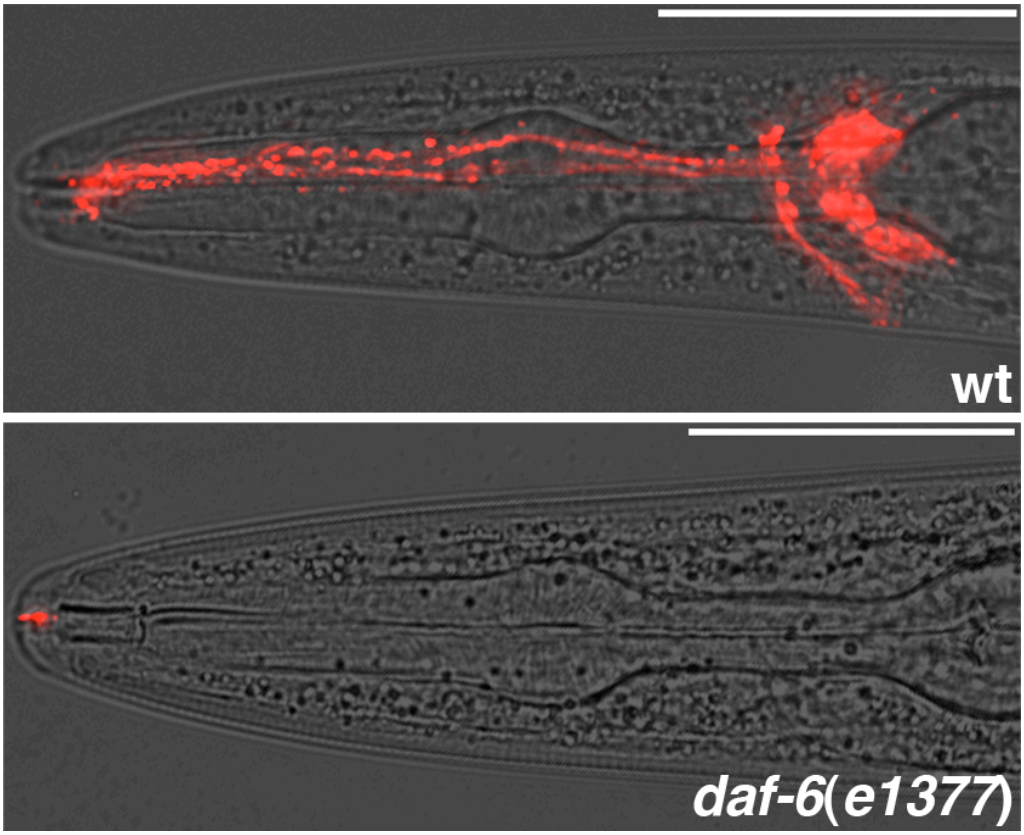

Figure 3.1. The dye-filling assay. Overlay of DIC and fluorescence microscopy images of the indicated genotypes after dye-filling with DiI (see Material and Methods). Scale bars, 10 μm.

From a screen of 60,000 mutagenized genomes, Elliot identified seven mutants that survived SDS treatment, dye-filled properly and had normal ultrastructure (Perens, 2006).

3.2. *ns132* suppresses the amphid sensory compartment defects of *daf-6* mutants

One of the *daf-6* suppressors isolated by Elliot Perens was given the allele designation *ns132* (Perens, 2006). As shown in Figure 3.2A, approximately 40% of *ns132; daf-6*(*e1377*) animals are able to take up dye in at least one amphid. Likewise, the *ns132* allele was able to suppress amphid channel defects in another *daf-6* mutant, *n1543*.

To further confirm the rescue of the *daf-6* amphid defects in *ns132*; *daf-6*(*e1377*) animals, I examined amphid sensory compartments using fluorescence microscopy. I found that cilia in these double mutants projected through a compartment of normal appearance (Figure 3.2B). In addition, *ns132*; *daf-6*(*e1377*) individuals that displayed normal dye-filling in one of the two amphids had one amphid channel that resembled a wild-type channel by EM serial reconstruction (Figure 3.2C; n=3). Interestingly, even in rescued amphids, cilia packing was more variable compared to the regular 3:4:3 packing observed in wild-type animals, and the amphid sensory compartment was somewhat wider than normal (Figure 3.2C, compare to Figure 2.1B), perhaps reflecting a partial suppression of the *daf-6* defects.

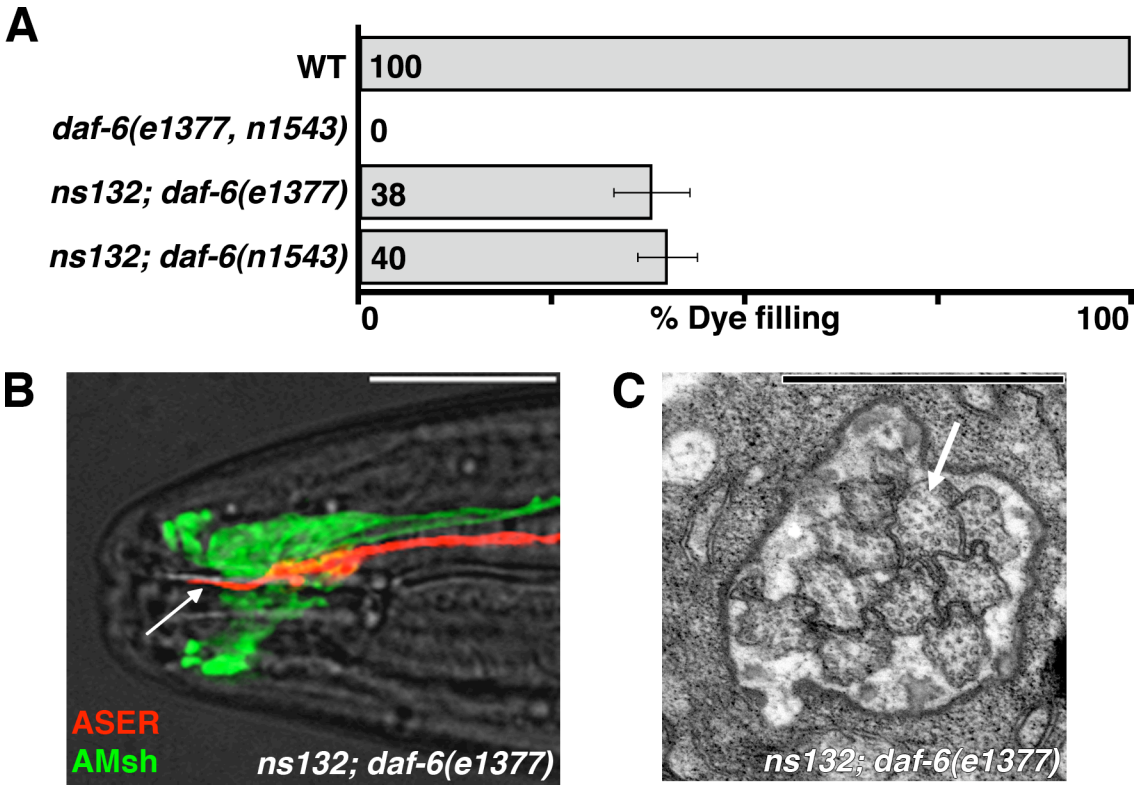

Figure 3.2. *ns132* is a suppressor of *daf-6*. (A) Dye-filling in animals of the indicated genotypes (n≥90). *daf-6*(*n1543*) was linked to *unc-3*(*e151*). Error bars denote standard error of the mean, s.e.m. (B) The ASER neuron and the amphid sheath glia, visualized with mCherry (red) and GFP (green), respectively, in an *ns132*; *daf-6*(*e1377*) animal. Arrow, ASER cilium. Left is anterior. Scale bar, 10 μm. (C) Electron micrograph of a cross-section through the amphid sheath channel of an *ns132*; *daf-6*(*e1377*) adult animal. Arrow, cilium. Scale bar, 1 μm.

3.3. *ns132* is an allele of *lit-1*/NLK

Previous work by Elliot Perens had shown that the mutation responsible for the suppression of *daf-6* in the strain *ns132*; *daf-6*(*e1377*) is located on chromosome III (Perens, 2006). I verified this result and proceeded to more finely map *ns132* using standard SNP mapping techniques (Wicks et al., 2001). The fundamental idea behind this approach is to cross the mutant, isolated in the N2 Bristol strain commonly used in the lab, to a strain isolated in Hawaii that carries a variety of single nucleotide polymorphisms (SNPs), many of which have been characterized. By recovering the mutant phenotype and determining the SNPs that co-segregate with the phenotype, the relevant locus can be determined. The specific strategy I used is depicted in Figure 3.3. Animals of the Hawaiian strain (HW, red) are crossed into *ns132*; *daf-6* animals that also carry *unc-3*(*e151*), a recessive mutation that results in uncoordinated animals and is closely linked to the *daf-6* locus. Thus, cross-progeny from this cross can be easily separated from the uncoordinated self-progeny, picked onto fresh plates, and allowed to lay eggs. The presence of *unc-3* allows, in the subsequent step, the isolation of animals that are most likely homozygous for *daf-6*, thus resolving the problem that arises from the fact that animals that have suppressed *daf-6* cannot be readily distinguished from animals that have a wild-type allele of *daf-6*. Unc animals that dye-fill normally are presumably homozygous for both *daf-6* and the suppressor, and are picked onto fresh plates and allowed to produce progeny. The Unc and non-Dyf phenotypes are verified in these progeny, which are subsequently used to provide DNA for SNP determination.

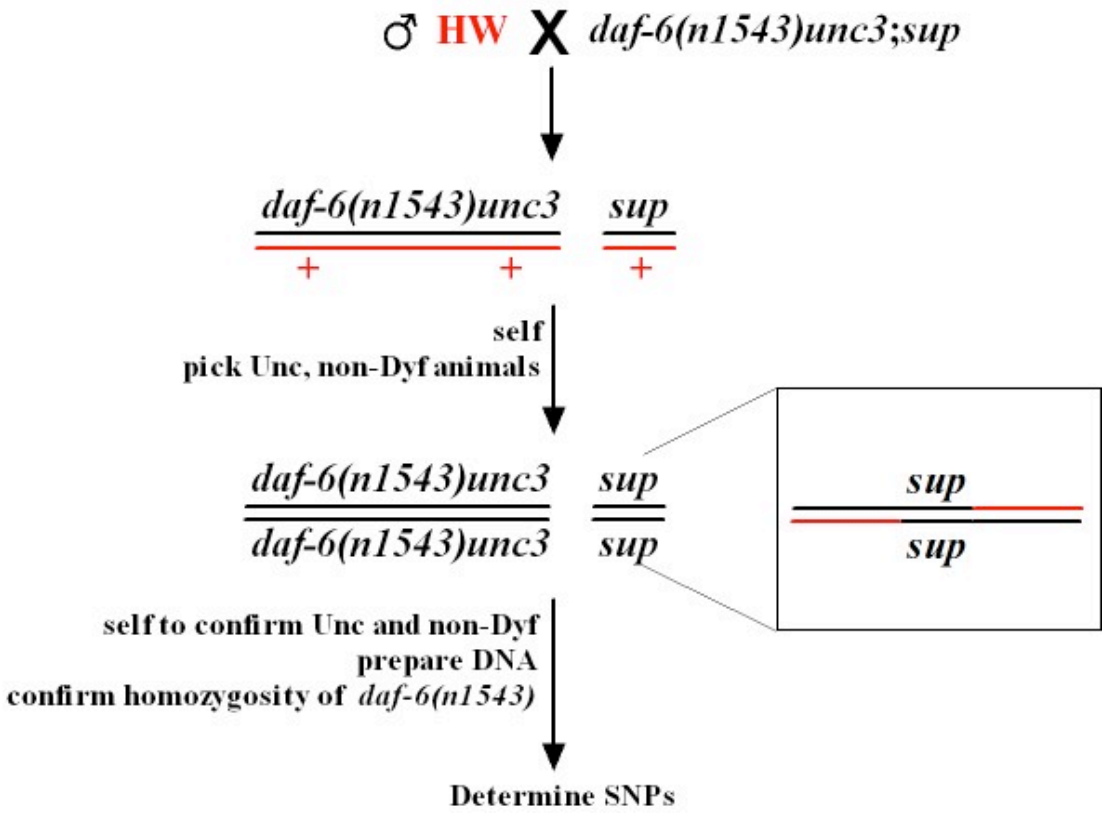

Figure 3.3. The strategy for SNP mapping of the *ns132* suppressor. Hawaiian is represented in red, N2 in black. For details, see text.

Using this strategy, I was able to map *ns132* to the far right arm of chromosome III, past the SNP F54F12:17329 at genetic position +20.72 (Figure 3.4A). Transgenic rescue experiments using cosmids from this region indicated that the relevant locus resided within the region covered by the cosmid W06F12 (Figure 3.4B). A construct containing the *lit-1* locus was able to rescue, that is, restore dye-filling defects to *ns132*; *daf-6*(*e1377*) animals (Figure3.4B), while the same locus amplified from the *ns132*; *daf-6*(*e1377*) strain failed to do so. A transgene in which the *lit-1* promoter region (2.5 kb upstream of the *lit-1* start codon) drives the *lit-1* cDNA also rescued. Furthermore, a temperature-sensitive mutation in *lit-1*, *t1512*, also suppressed the dye-filling defects of *daf-6*(*n1543*) mutants.

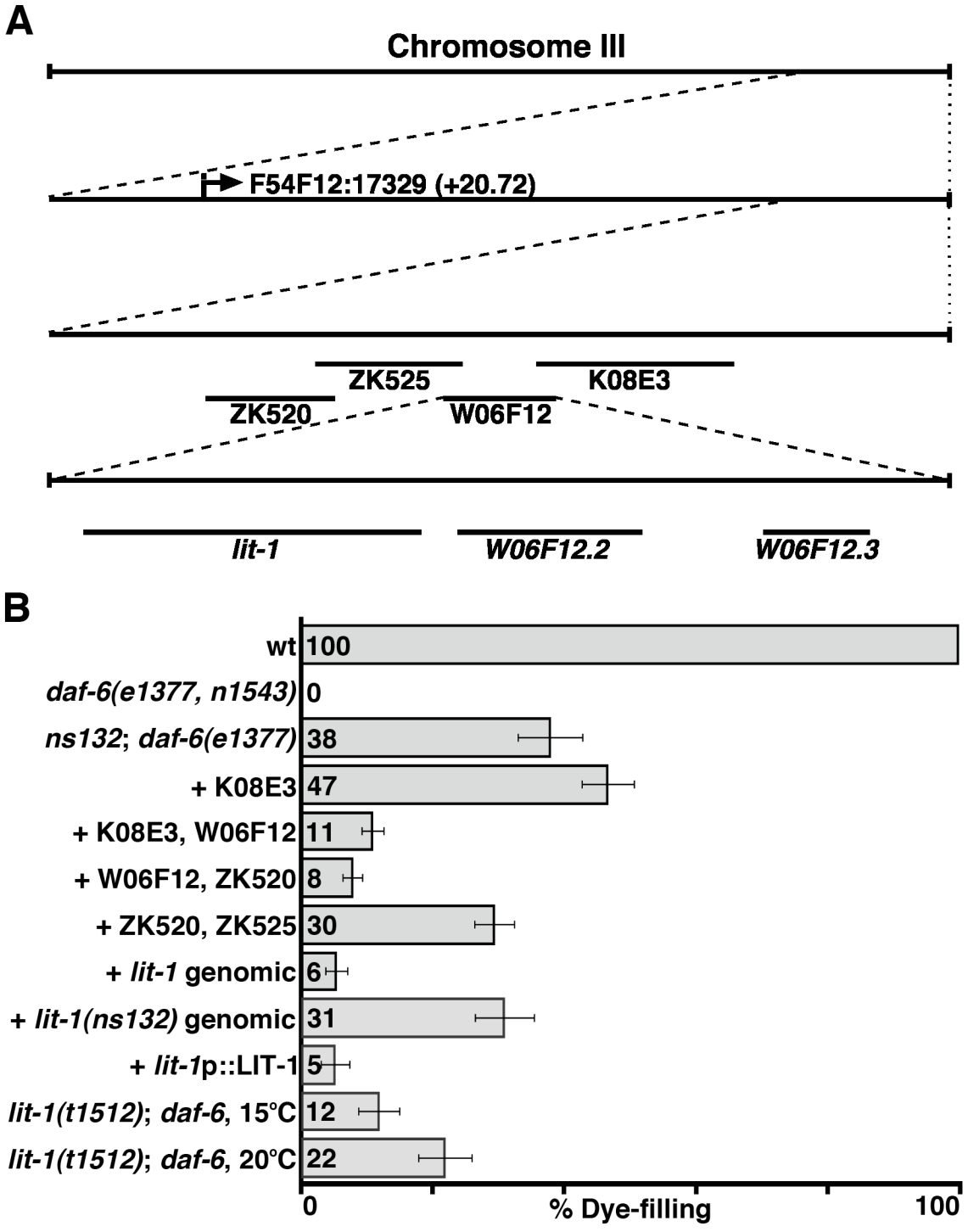

Figure 3.4. *ns132* is an allele of *lit-1*. (A) Schematic of the region defined by SNP mapping and cosmid rescues as the site of the *ns132* mutation. (B) Dye-filling in animals of the indicated genotypes (n≥90). Unless otherwise noted, *daf-6* refers to the *n1543* allele. *lit-1*(*t1512*) was linked to *unc-32*(*e189*). Error bars, s.e.m.

Finally, through sequencing, I found that animals containing the *ns132* allele have a C-to-T mutation in the coding region of *lit-1* that converts codon 437, encoding glutamine, to a stop codon. This mutation is predicted to result in a truncated LIT-1 protein (Figure 3.5), lacking the last 26 amino acids of the carboxy-terminal (C-terminal) domain. The truncated region has been highly conserved through evolution (Figure 3.5), similar to the rest of the C-terminal domain and the kinase domain.

Taken together, these results demonstrate that *ns132* is an allele of *lit-1*.

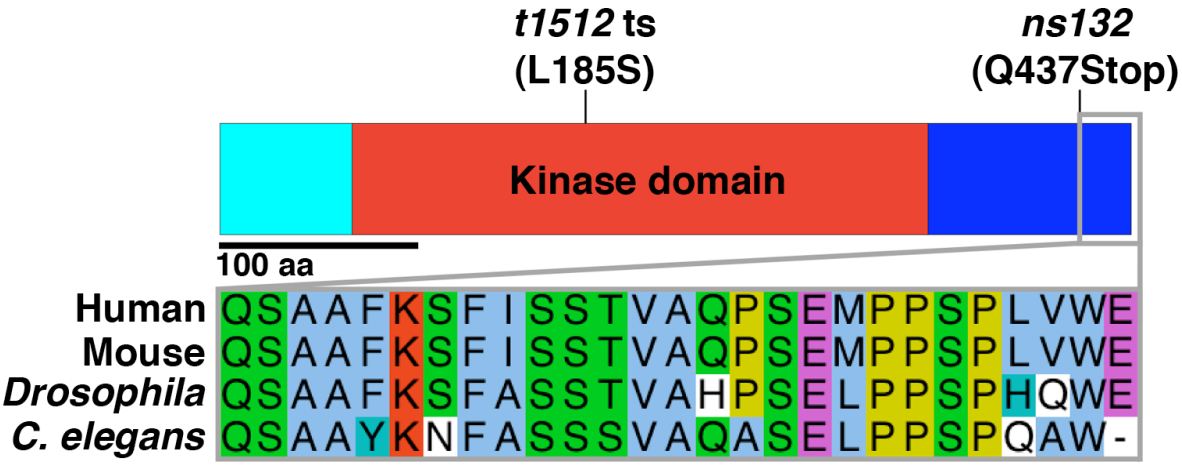

Figure 3.5. Schematic of LIT-1 and the lesions of the alleles used in this study. Top: Schematic of the LIT-1 protein. Light blue, non-conserved N-terminal domain. Red, conserved kinase domain. Dark blue, conserved C-terminal domain. Bottom: Alignment of the region truncated in *lit-1*(*ns132*) from different species.

3.4. A maternal rescue effect for *lit-1* in amphid morphogenesis

During the collection of recombinants for SNP mapping, I observed a high rate of false positives, that is, animals that were isolated as homozygous for *daf-6* and non-Dyf (hence presumably homozygous for *ns132*) produced a brood in which only a few animals could dye-fill. This observation could be explained by either a partial dominance by *ns132*, or a maternal rescue effect. Having identified the molecular lesion in *ns132*, I was now able to distinguish between these two possibilities. Thus, I performed two series of crosses, depicted in Figure 3.6. In both cases, animals homozygous for *daf-6* and heterozygous for *ns132* were produced. However, in cross (A) the *ns132* allele is provided by the mother, while in cross (B) it is provided by the father. In the first case only 2% of the progeny can dye-fill, while in the latter 10% do so. These results suggest that *ns132* is only slightly dominant, but there is a considerable maternal rescue effect as far as the ability of *ns132* to suppress *daf-6* is concerned.

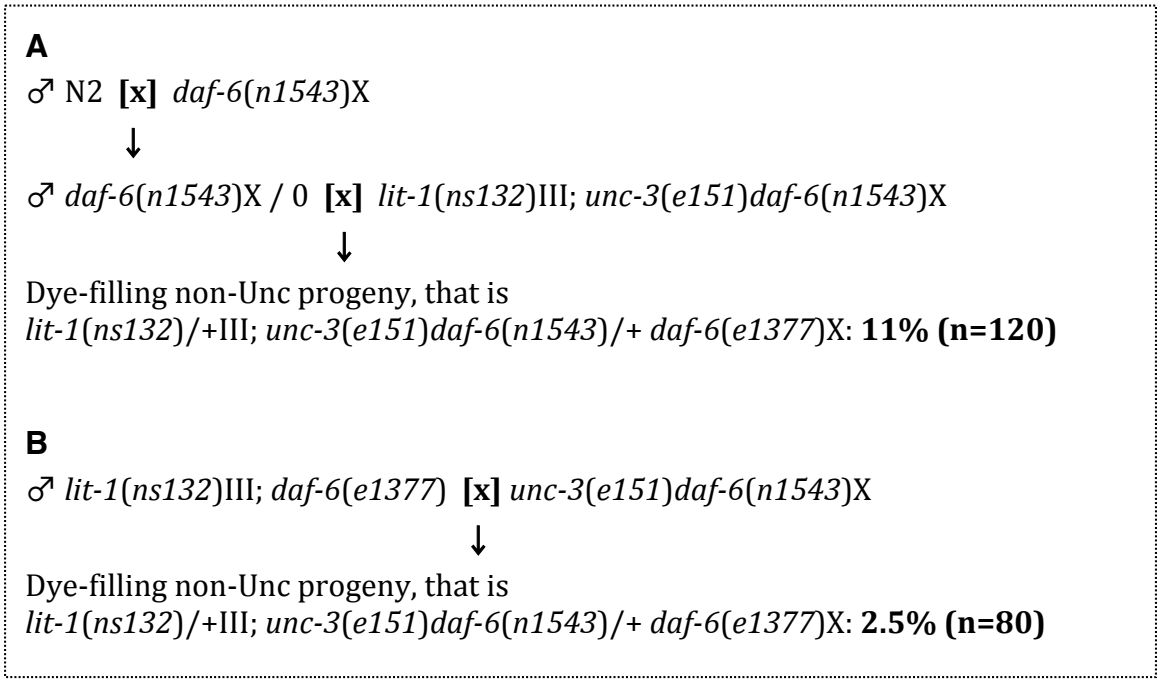

Figure 3.6. A maternal rescue effect for *lit-1* in amphid morphogenesis. For details see text.

3.5. LIT-1 functions in amphid glia during compartment formation

To determine in which cells *lit-1* functions to regulate compartment development, I first examined its expression pattern by generating animals that express a transgene in which the *lit-1* promoter drives a nuclearly-localized dsRed fluorescent protein (NLS-RFP). I found that *lit-1* is expressed in amphid sheath glia (Figure 3.7A), among other cells. In addition, the expression pattern of this reporter partially overlaps with that of *ptr-10* (Figure 3.7B), a gene expressed in ensheathing glia of other sensory organs (Yoshimura et al., 2008), suggesting that *lit-1* could act in compartment formation in other *C. elegans* sensory structures as well.

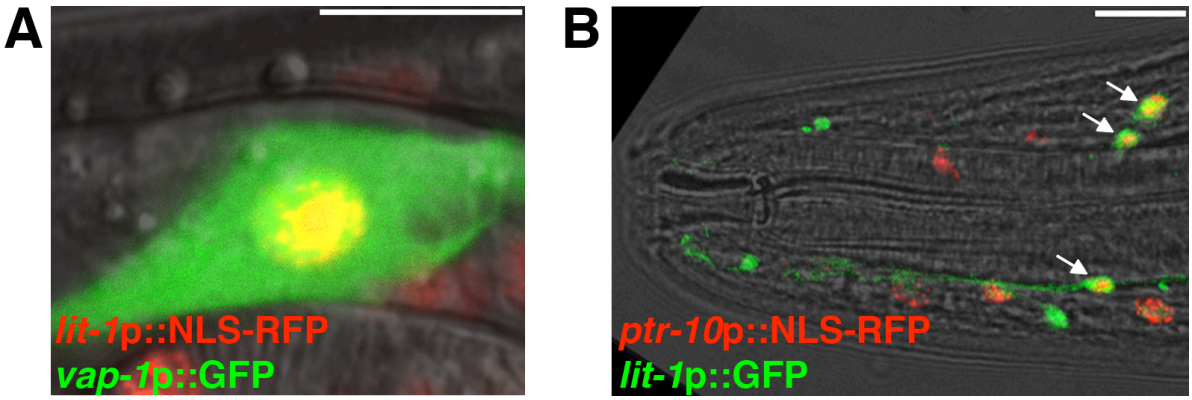

Figure 3.7. *lit-1* is expressed within glia. (A) Image of an amphid sheath glial cell body expressing *lit-1*p::NLS-RFP (red; in nucleus) and *vap-1*p::GFP (green). Yellow, overlapping expression. Left is anterior. Scale bar, 10 µm. (B) Image of an adult (head) expressing *lit-1*p::GFP (green) and *ptr-10*p::NLS-RFP (red). Arrows, cells with overlapping expression. Left is anterior. Scale bar, 10 µm.

Next, I pursued cell-specific rescue experiments to determine in which cells *lit-1* can act to regulate compartment morphogenesis. I generated *lit-1*(*ns132*); *daf-6*(*e1377*) animals containing a transgene in which a *lin-26* promoter fragment drives expression of the *lit-1* cDNA in glia, but not neurons, of embryos at the time of amphid sensory compartment formation (Landmann et al., 2004). I found that transgenic animals were rescued, i.e. failed to fill with dye (Figure 3.8), supporting the notion that *lit-1* can act in glia to regulate compartment morphology. Importantly, expression of the *lit-1* cDNA in amphid sensory neurons during the time of amphid morphogenesis (using the *dyf-7* promoter, (Heiman and Shaham, 2009)) failed to rescue *lit-1*(*ns132*); *daf-6*(*e1377*) animals (Figure 3.8).

To determine whether *lit-1* can control amphid sensory compartment structure after compartment formation is complete, I examined *lit-1*(*ns132*); *daf-6*(*e1377*) animals

expressing the *lit-1* cDNA under the control of the sheath glia-specific *vap-1* promoter. *vap-1* expression begins in late embryos (Perens and Shaham, 2005), after the compartment has formed. I found that these transgenic animals were not rescued (Figure 3.8), supporting the conclusion that *lit-1* is required within amphid sheath glia at the time of amphid morphogenesis to influence compartment formation.

Finally, to ascertain whether the kinase activity of LIT-1 is required, I generated a mutant *lit-1* cDNA that disrupts the ATP binding domain (VALKK to VALKG), and which has been shown to eliminate LIT-1 kinase activity in vitro (Rocheleau et al., 1999). *lit-1*(*ns132*); *daf-6*(*e1377*) animals carrying a *lin-26* promoter::LIT-1(K97G) cDNA transgene still displayed 30% dye-filling, similar to controls, suggesting that LIT-1 kinase activity is indeed required for glial compartment morphogenesis (Figure 3.8).

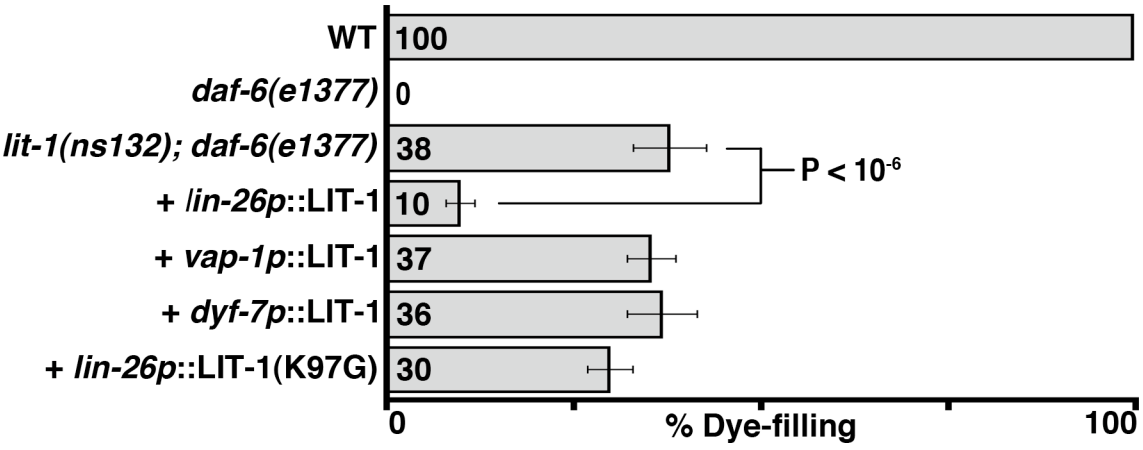

Figure 3.8. *lit-1* acts within glia, during the time of amphid morphogenesis, to regulate sensory compartment formation. Dye-filling in animals of the indicated genotypes (n≥90). Error bars, s.e.m. P-value calculated using Chi-squared test.

3.6. *lit-1* promotes amphid sensory compartment expansion

Since *daf-6* normally acts to restrict amphid sensory compartment expansion, the observation that *lit-1* mutations suppress *daf-6* suggests that *lit-1* may normally promote compartment growth. Consistent with this idea, the *lit-1*(*ns132*) allele enhances the dye-filling defects of *che-14*(*ok193*) mutants (Figure 3.9). CHE-14 is similar to the *Drosophila* and mammalian protein Dispatched, and is important for apical secretion and amphid sensory compartment morphogenesis (Michaux et al., 2000), suggesting a role in lumen expansion. The enhancement of *che-14* defects by *lit-1*(*ns132*) suggests that both genes may be involved in this process.

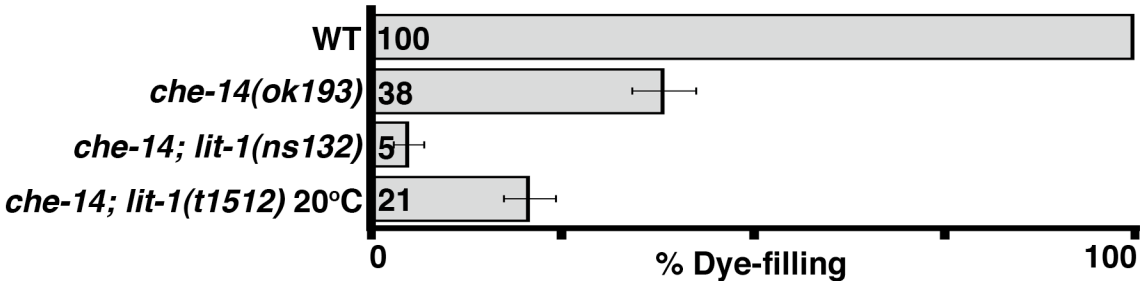

Figure 3.9. *lit-1* enhances the dye-filling defect of *che-14*. Dye-filling in animals of the indicated genotypes (n≥100).

To further test the idea that *lit-1* promotes compartment expansion, I examined *lit-1*(*ns132*) single mutants for dye-filling abnormalities; however, no defects were observed (Figure 3.10), suggesting that amphid morphology in these animals may be normal. However, two observations suggest that *ns132* is a weak allele of *lit-1*. First, the *ns132* lesion truncates only 26 amino acids from the C-terminus of the LIT-1 protein, and leaves

the kinase domain intact (Figure 3.5). Second, null alleles of *lit-1* are embryonic lethal (Kaletta et al., 1997; Rocheleau et al., 1999), whereas *ns132* mutants are fully viable.

To examine the consequences of more severe defects in *lit-1* function, I therefore turned to animals homozygous for the *lit-1*(*t1512*) temperature-sensitive allele. *lit-1*(*t1512*ts) animals grow nearly normally at 15°C, but exhibit early embryonic lethality at 25°C (Kaletta et al., 1997). At 20°C, some *lit-1*(*t1512*ts) embryos escape lethality and grow to adulthood. I reasoned that in some of these escapers, LIT-1 activity could be low enough to allow us to discern defects in amphid morphogenesis. Indeed, as shown in Figure 3.10, nearly 50% of *lit-1*(*t1512*ts) adults grown at 20°C exhibit defects in a sensitized amphid dye-filling assay, developed to detect weak defects in dye-filling (in this assay animals are incubated for 15 min in 1 μg/mL of dye, instead of 1.5 h at 10 μg/mL of dye as in the regular dye-filling assay; see also materials and methods). These results suggest that amphid structure, and perhaps compartment morphogenesis, has been perturbed in these mutants.

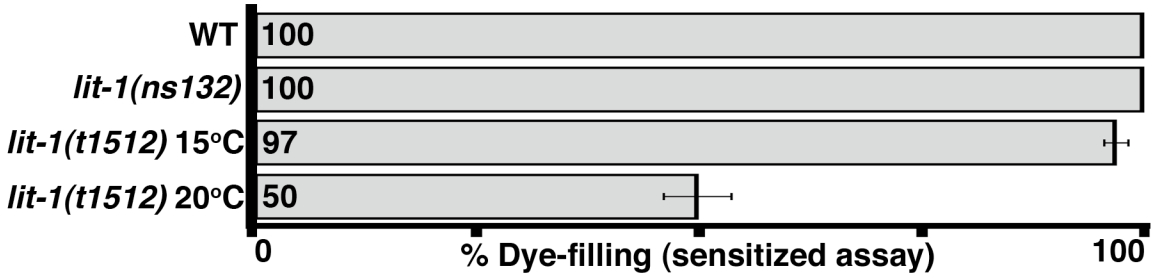

Figure 3.10. A sensitized dye-filling assay reveals the sensory compartment defects of *lit-1* mutants. Dye-filling in animals of the indicated genotypes (n≥100).

To assess whether compartment morphology is indeed perturbed, Yun Lu performed serial-section EM on dye-filling defective adult *lit-1*(*t1512*ts) animals raised at 20°C (n=3). Whereas in wild-type animals a cross-section through the sheath channel immediately posterior to the socket-sheath boundary (yellow line in Figure 3.11) reveals the stereotypical 3:4:3 arrangement of the ten channel cilia, in *lit-1*(*t1512*ts) mutants, the amphid sensory compartment has a smaller diameter, and contains fewer cilia (Figure 3.11). Fewer cilia are also found in the socket channel in *lit-1*(*t1512*ts) animals (data not shown). Furthermore, in wild-type animals, cross sections roughly 1 μm posterior to the sheath-socket junction (blue line in Figure 3.11) reveal a less packed arrangement of cilia that are loosely surrounded by the sheath glia membrane; by contrast, in *lit-1*(*t1512*ts) animals the sheath glia is tightly wrapped around individual cilia (arrowheads in Figure 3.11), consistent with the idea that compartment diameter is reduced. Importantly, despite the posterior displacement of some cilia in *lit-1*(*t1512*ts) animals, the total number of cilia is normal (blue section in Figure 3.11).

Taken together, the *che-14*, dye-filling, and EM studies suggest that *lit-1* opposes *daf-6* by promoting channel expansion during amphid morphogenesis.

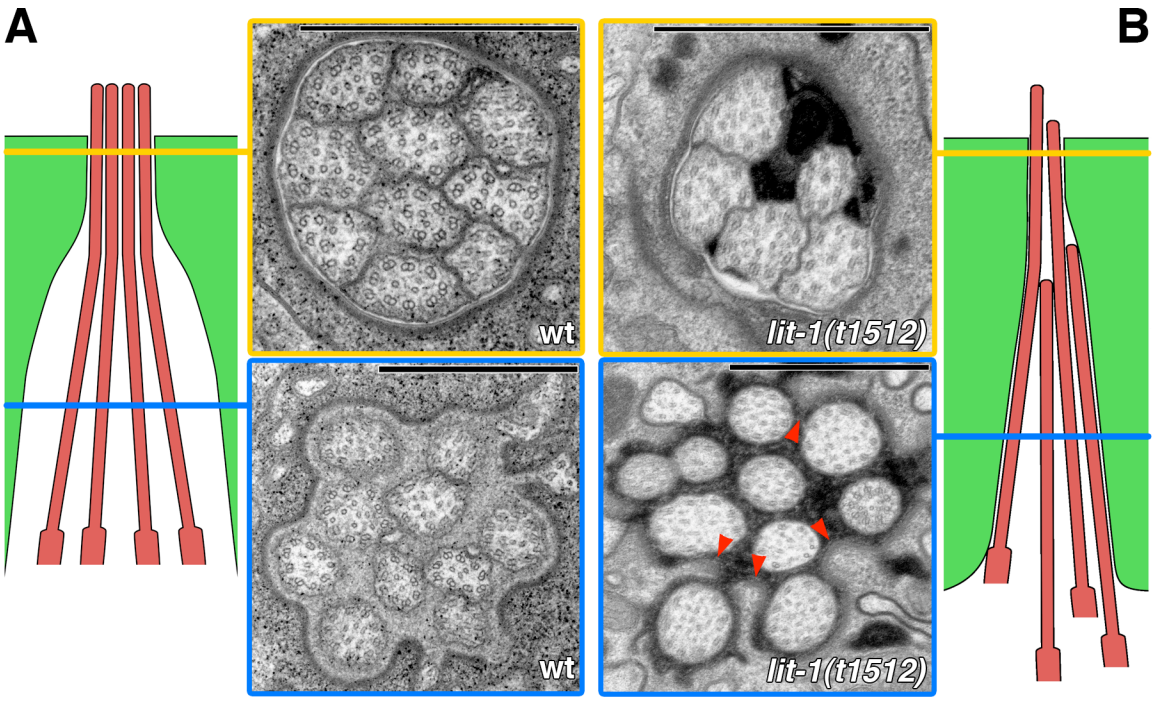

Figure 3.11. The diameter of the amphid sensory compartment is reduced in *lit-1*(*t1512*ts) mutants. (A) Left: Schematic of the arrangement of the cilia (red) and the sheath glial channel (green) in a wild-type adult animal. Not all cilia are depicted. Right: electron micrograph of cross-sections of the amphid channel. Section outlined in yellow is just below the socket-sheath junction; blue outlined section is approximately one micron posterior. Scale bars, 1 µm. (B) Same as in (A), but for a dye-filling defective *lit-1*(*t1512*ts) adult animal. The panel arrangement is a reflection of the one in (A). Red arrowheads, tight ensheathment of individual cilia by the sheath glia. Scale bars, 1 µm.

3.7. Mutation of the MAP kinase kinase kinase *mom-4*/TAK1 also suppresses the compartment defects of *daf-6* mutants

The kinase activity of LIT-1 was previously shown to depend on MOM-4/TAK1, a MAP kinase kinase kinase. MOM-4 increases LIT-1 kinase activity in vitro and mutations in *mom-4* interact genetically with mutations in *lit-1* during anterior/posterior polarity establishment in early embryos (Shin et al., 1999). I therefore tested whether mutations in *mom-4* could also suppress the dye-filling defects of *daf-6* mutants. While complete loss of *mom-4*, like loss of *lit-1*, leads to early embryonic lethality, some animals homozygous for a temperature-sensitive allele of *mom-4*, *ne1539*ts, can escape lethality. I found that whereas only 1% of *mom-4*(*ne1539*ts); *daf-6*(*e1377*) double-mutant escapers grown at 15°C exhibit suppression of the *daf-6* dye-filling defect, 18% of surviving animals grown at 20°C can take up dye (Figure 3.12). This observation suggests that *mom-4* acts similarly to *lit-1* in compartment expansion.

To assess whether *mom-4* and *lit-1* could function in the same pathway to promote channel expansion, I examined dye-filling in *daf-6* mutants that were also homozygous for both *lit-1*(*ns132*) and *mom-4*(*ne1539*ts) alleles. I found that the *mom-4*; *lit-1*; *daf-6* triple mutant is viable at both 15°C and 20°C and is not suppressed to a greater extent than *lit-1*; *daf-6* double mutants at either temperature (Figure 3.12). This result is consistent with the idea that *lit-1* and *mom-4* function in the same pathway to control channel expansion, similar to their established roles in embryonic cell polarity.

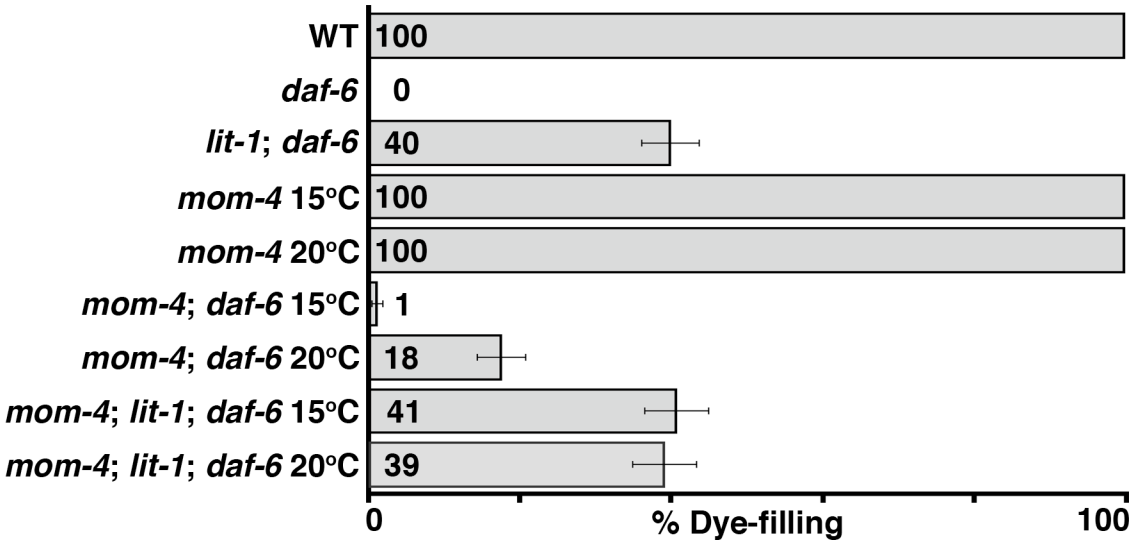

Figure 3.12. Mutation of *mom-4* /MAP3K suppresses the sensory compartment defects of *daf-6* mutants. Dye-filling in animals of the indicated genotypes (n≥100). The alleles used are: *daf-6*(*n1543*) linked to *unc-3*(*e151*), *lit-1*(*ns132*) and *mom-4*(*ne1539*ts).

The roles of *lit-1* and *mom-4* in Wnt signaling in *C. elegans* have been extensively studied (Mizumoto and Sawa, 2007b; Phillips and Kimble, 2009). In this context, MOM-4 activates LIT-1, which then phosphorylates and forms a complex with the β-catenin WRM-1. The LIT-1/WRM-1 complex phosphorylates the *C. elegans* TCF/LEF transcription factor POP-1, resulting in reduction (but not elimination) of POP-1 nuclear levels and activation of transcription (Figure 1.11, (Rocheleau et al., 1999; Shin et al., 1999; Lo et al., 2004; Kidd et al., 2005)). I therefore examined animals containing mutations in Wnt signaling components for defects in dye-filling, or for suppression of the *daf-6* dye-filling defects. Surprisingly, mutations in Wnt-encoding genes, the *C. elegans* Wntless homolog *mig-14*, required for Wnt protein secretion, Wnt receptors, β-

catenins, or *pop-1*/ TCF/LEF, the main LIT-1 target in the Wnt signaling pathway, have no effect on dye-filling, and show no, or minimal, suppression of *daf-6* (Table 3.1).

Although I cannot eliminate the possibility that multiple redundant Wnt pathways contribute to channel formation and that these operate through LIT-1 targets other than POP-1, the most parsimonious interpretation of these data is that the MOM-4/LIT-1 kinase module operates independently of Wnt signaling to promote expansion of the amphid glial compartment.

Table 3.1. Components of the Wnt signaling pathway do not affect amphid morphogenesis

Common name	*C. elegans* gene name	Allele	% Dye-filling[a]	% Dye-filling in *daf-6(n1543)*[b]
Porcupine	*mom-1*	RNAi	ND[c]	0
Wntless	*mig-14*	*mu71*	100	5
		ga62	100	2
Wnt	*lin-44*	*n1792*	100	0
	egl-20	*mu27*[d]	100	0
	cwn-1	*ok546*	100	3
	cwn-2	*ok895*	100	0
	mom-2	*ne834*	100	0
		or309	100	ND
Frizzled	*lin-17*	*n671*	100	4
		n698	100	ND
		n3091	100	ND
	mig-1	*e1787*	100	6
	mom-5	*or57, zu193*	100	ND
		RNAi	ND	0
	cfz-2	*ok1201*	100	5
	mig-1 lin-17; cfz-2	*e1787, n677, ok1201* respectively	100	0
Dishevelled	*mig-5*	*rh147*	100	0
	dsh-1	*ok1445*	100	0
		RNAi	ND	0
	dsh-2	*ok2162*	100	ND
		RNAi	ND	0
Ryk	*lin-18*	*e620*	100	0
β-catenin	*bar-1*	*ga80*	100	2
	wrm-1	*ne1982*	100	1
	hmp-2	RNAi	ND	0
	sys-1	*q544*	100	ND
		RNAi	ND	0
TCF/LEF	*pop-1*	*q624*	100	0
		RNAi	ND	0
ROR1	*cam-1*	*ks52*	100	8
Van Gogh/ Strabismus	*vang-1*	*ok1142*	100	0

[a] n≥100 for each genotype.

[b] Full genetic background was *unc-3*(*e151*) *daf-6*(*n1543*) except for RNAi experiments where background was *rrf-3*(*pk1426*); *unc-3*(*e151*)*daf-6*(*n1543*). *rrf-3* increases the

sensitivity to RNAi (Simmer et al., 2002), but does not affect dye-filling (data not shown); n≥100 for all experiments.

[c] ND, not determined.

[d] The reference *egl-20* allele *n585* harbors a background mutation that suppresses the dye-filling defects of *daf-6*(*n1543*). The *mu27* allele, shown here, has the same molecular lesion as *n585* (Maloof et al., 1999), but does not suppress *daf-6*.

3.8. LIT-1 and MOM-4 proteins localize to the amphid sensory compartment

Although the suppression of *daf-6* by *mom-4* was reproducible and statistically significant ($P<10^{-6}$, Chi-squared test), the weakness of the suppression made it difficult to interpret transgenic rescue studies aimed at determining in which cells *mom-4* functions. Previous work from our lab, however, has shown that *mom-4* is expressed within cultured embryonic amphid sheath glia (Bacaj et al., 2008), consistent with the idea that it can act together with *lit-1* in this cell.

To determine where within the amphid sheath glia LIT-1 and MOM-4 are localized, I generated animals expressing either GFP::MOM-4 or a rescuing GFP::LIT-1 fusion protein in amphid sheath glia using the *T02B11.3* amphid sheath promoter (Wang et al., 2008). Strikingly, I found that both fusion proteins were tightly associated with the amphid sensory compartment (Figure 3.13), a localization similar to that of the terminal web depicted in figure 1.3.

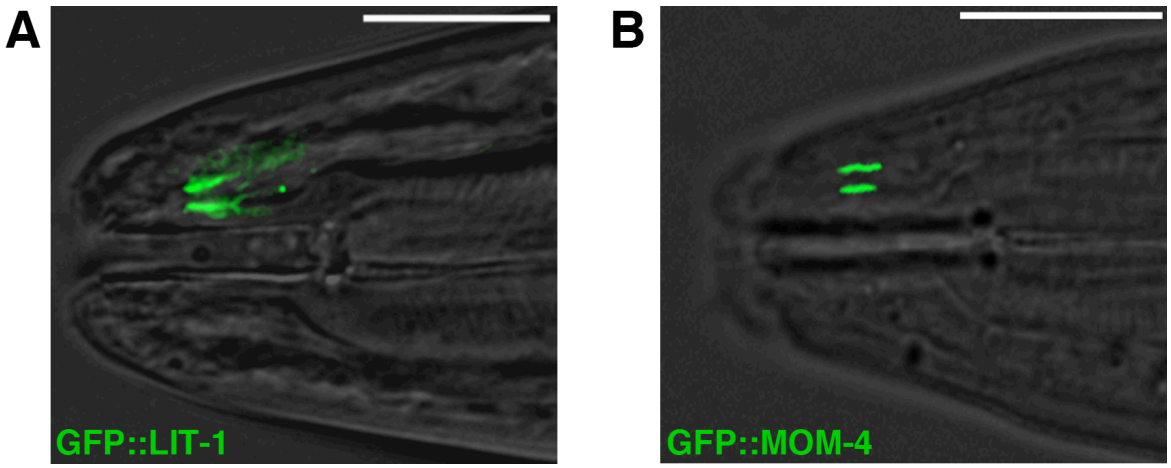

Figure 3.13. LIT-1 and MOM-4 line the amphid sensory compartment. The *T02B11.3* promoter (Wang et al., 2008) driving GFP::LIT-1 (A), and GFP::MOM-4 (B). Compare to terminal web lining depicted in figure 1.3. Anterior is to the left. Scale bars, 10 μm.

To determine whether LIT-1 localization requires functional *mom-4*, I examined localization of the GFP::LIT-1 fusion protein in *mom-4*(*ne1539*ts) single mutants at 20°C. GFP::LIT-1 was properly localized in all animals I observed (n=44), suggesting that LIT-1 localizes to the sheath channel independently of its regulator.

3.9. The localization of LIT-1 to the amphid sensory compartment depends on neuronal signals

The DAF-6 protein is mislocalized in animals lacking neuronal cilia, accumulating only at the sheath-socket junction rather than along the length of the sheath glia channel (Perens and Shaham, 2005). To examine whether LIT-1 also requires cilia to properly localize, I examined animals harboring a loss-of-function mutation in *daf-19*, which encodes a transcription factor required for ciliogenesis (Swoboda et al., 2000).

Previous EM studies demonstrated that, despite minor defects, a channel of normal length is generated in these mutants (Perens and Shaham, 2005). As shown in Figure 3.14, in *daf-19* mutants LIT-1 no longer lines the entire channel, but is restricted to its anterior aspect. Thus, neuronal signals regulate LIT-1 glial localization.

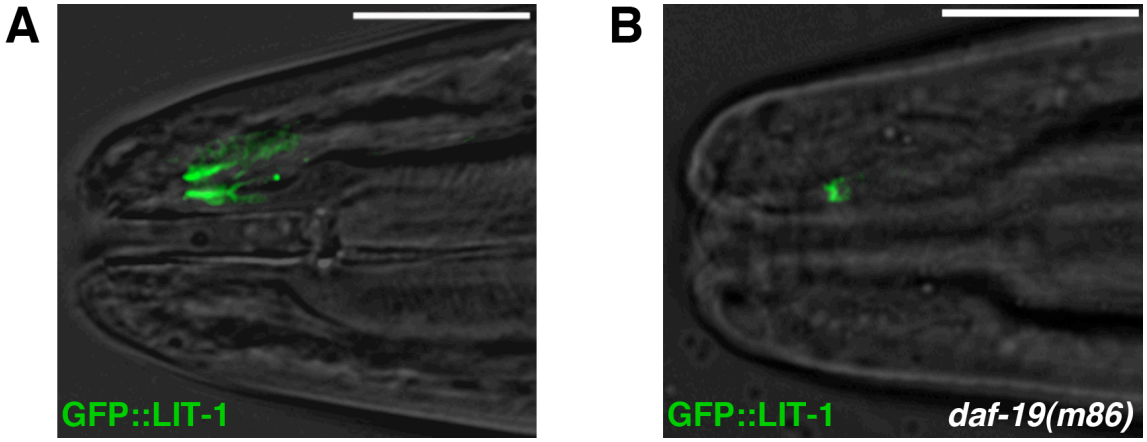

Figure 3.14. Neuronal signals are required for the localization of LIT-1 to the amphid sensory compartment. The *T02B11.3* promoter (Wang et al., 2008) driving GFP::LIT-1 in a wild-type (A) and *daf-19* (B) background. *daf-19*(*m86*) animals also carried the *daf-16*(*mu86*) allele to prevent dauer entry. Anterior is to the left. Scale bars, 10 μm.

3.10. The C-terminus of LIT-1 is necessary and sufficient for amphid sensory compartment localization

Because of the distinct localization of LIT-1, I wondered whether the *lit-1*(*ns132*) allele, predicted to encode a truncated version of LIT-1 that lacks the last 26 amino acids of the protein, disrupts LIT-1 localization. To address this, I expressed GFP-tagged LIT-1(Q437Stop) (the mutation corresponding to *ns132*) in wild-type animals, and examined

its localization. While GFP::LIT-1 reproducibly lines the amphid sensory compartment, GFP::LIT-1(Q437Stop) fails to localize in about one-third of transgenic animals, and is instead diffusely distributed throughout the cell (Figure 3.15B and 3.15E). This result suggests that the highly conserved C-terminal region of LIT-1 may be required for compartment localization. In addition, the fraction of animals in which GFP::LIT-1(Q437Stop) is mislocalized (31%, Figure 3.15E) mirrors the fraction of *daf-6* mutants suppressed by the *lit-1*(*ns132*) allele (Figure 3.2A), raising the possibility that mislocalization may account for the suppression we observed.

The observation that GFP::LIT-1(Q437Stop) still localizes to the amphid channel in some animals suggested that the C-terminal 26 amino acids may represent only a portion of the full targeting domain. To test this idea, I generated animals expressing a GFP::LIT-1ΔCt fusion protein in which all sequences downstream of the kinase domain are deleted. I found that in these animals, LIT-1 never accumulated at the amphid sensory compartment, and was diffusely distributed throughout the cell (Figure 3.15C and 3.15E), demonstrating that the C-terminal domain is necessary for LIT-1 compartment localization.

To determine whether the C-terminal domain of LIT-1 is sufficient for channel localization, I generated animals expressing a GFP::LIT-1Ct fusion protein in which GFP is fused to the C-terminal domain of LIT-1 alone. Remarkably, I found that this fusion protein invariably accumulated at the amphid sensory compartment in a pattern identical to that of full-length LIT-1 (Figure 3.15D and 3.15E).

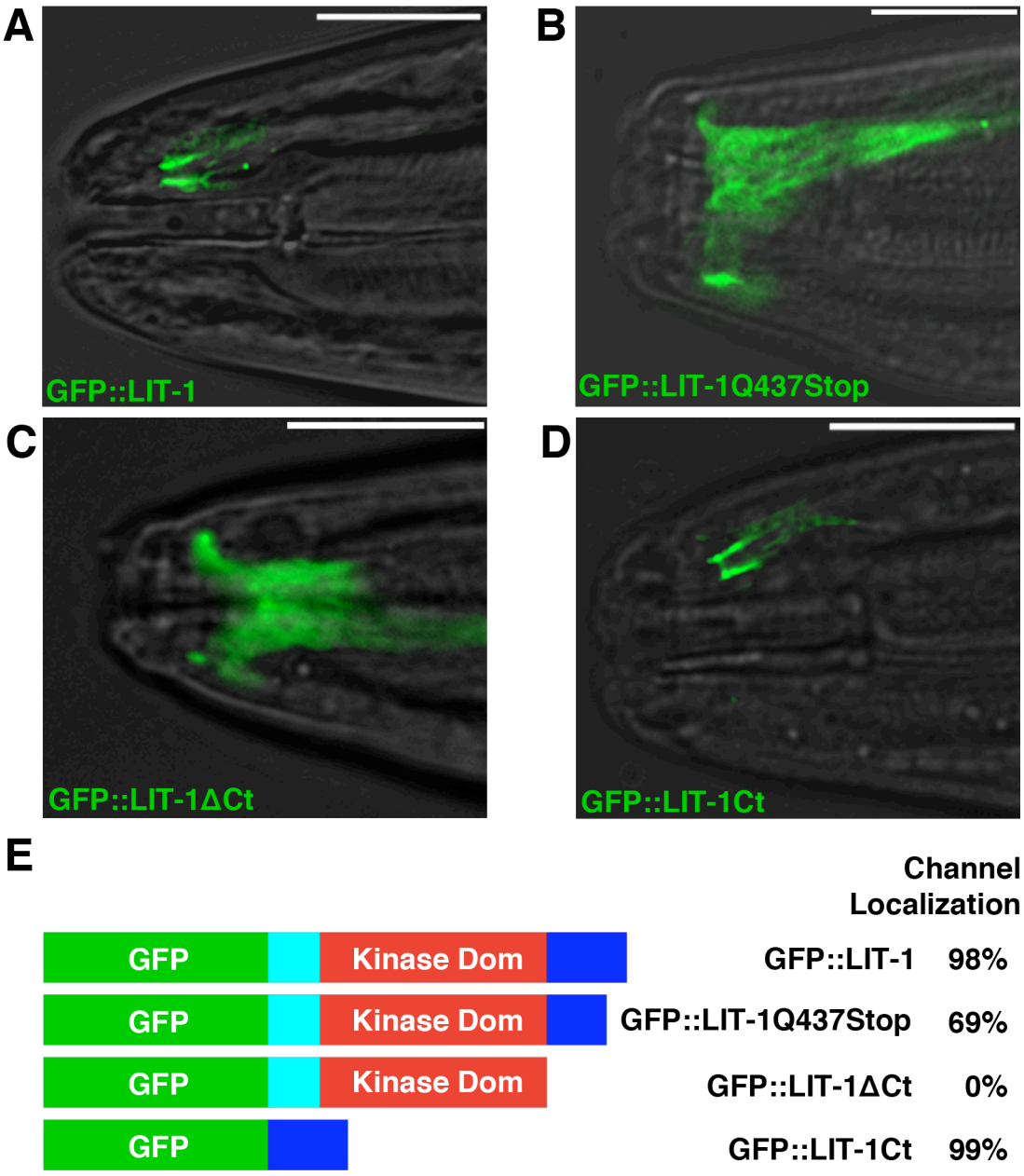

Figure 3.15. Sensory compartment localization of different versions of LIT-1. (A-D) Images of adult animals expressing the indicated GFP fusion proteins. Animals are otherwise wild-type. The *T02B11.3* amphid sheath promoter (Wang et al., 2008) was used to drive all constructs. Anterior is to the left. Scale bars, 10 μm. (E) Quantification of channel localization of indicated LIT-1 protein fusions (n≥100).

Previous work has shown that LIT-1 can also localize to the cell nucleus (Lo et al., 2004; Takeshita and Sawa, 2005; Mizumoto and Sawa, 2007a), and I found this to be the case for amphid sheath glia as well (Figure 3.16). However, disruption of the C-terminal domain of LIT-1 does not result in its exclusion from the nucleus (Figure 3.16), suggesting that nuclear functions of LIT-1 may not be abrogated in *lit-1*(*ns132*) mutants.

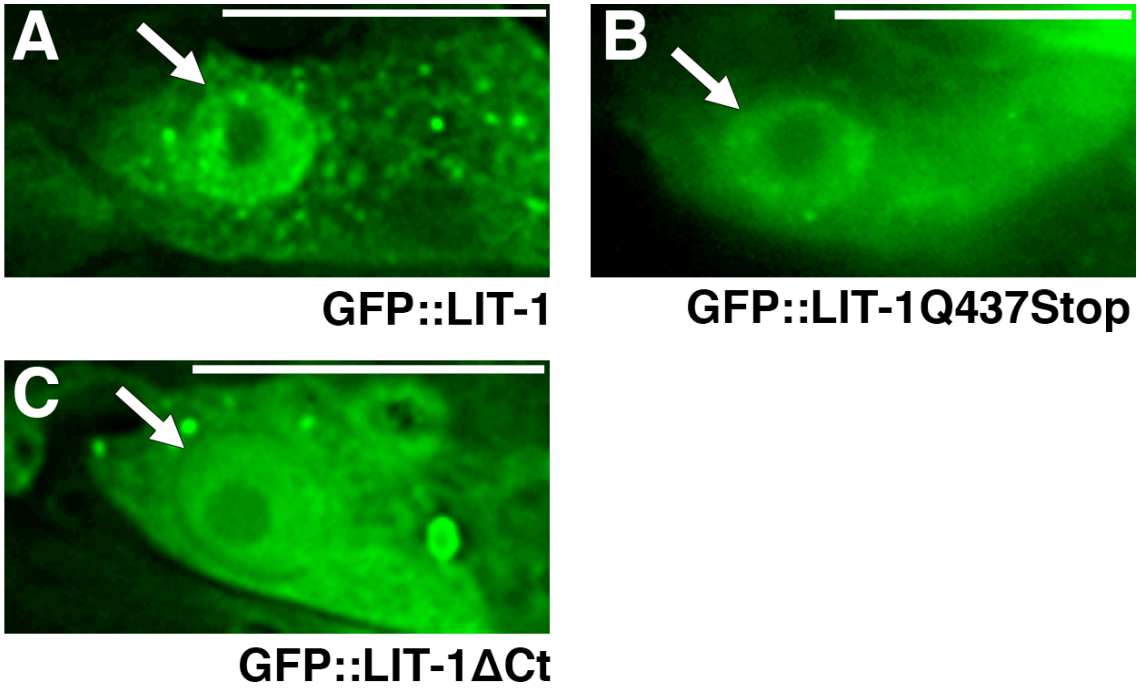

Figure 3.16. The nuclear localization of LIT-1 is not abrogated by disruption of the LIT-1 C-terminal domain. (A-C) Fluorescence images of sheath glia cell body and nucleus in animals transgenic for the indicated GFP::LIT-1 fusion protein. Arrow, cell nucleus. Scale bar, 10 μm. The *T02B11.3* promoter was used to drive all constructs.

Although the C-terminal domain of LIT-1 is highly conserved from *C. elegans* to mammals, its function is not well studied. The studies presented here demonstrate that this domain is both necessary and sufficient for LIT-1 localization to the amphid sensory compartment, and suggest that proper localization is important for LIT-1 function in compartment formation.

3.11. A yeast two-hybrid screen for proteins that interact with the C-terminal domain of LIT-1

Because of the importance of the LIT-1 C-terminal domain for compartment localization, I decided to use this domain as bait in a yeast two-hybrid screen with the aim of identifying candidate proteins that interact with LIT-1 during compartment expansion. From a screen of approximately 10^6 clones, I identified 26 positive clones (Table 3.2; see also materials and methods). While some clones were isolated multiple times, others were found only once, suggesting that the screen was not saturated.

Table 3.2. Clones identified from a yeast two-hybrid screen for proteins that interact with the carboxy-terminal domain of LIT-1

Gene	No. clones found	Description
mep-1	1	zinc-finger protein
T24E12.9	1	protein of unknown function
vit-3	2	vitellogenin
fbp-1	1	fructose 1,6-bisphosphatase
act-4	4	actin
Y87G2A.1	2	protein of unknown function
wsp-1	1	WASP
ztf-16	1	zinc-finger protein
C50F4.1	1	protein of unknown function
C44B12.5	6	protein of unknown function
nrde-3	1	argonaute protein
ost-1	1	osteonectin, ECM protein
unc-52	1	perlecan, ECM protein
tag-30	1	protein of unknown function
vit-4	1	vitellogenin
C34F11.3	1	adenosine monophosphate deaminase

Several of the yeast two-hybrid hits presented in Table 3.2 are intriguing. ZTF-16 is a transcription factor that unpublished work by Carl Procko in the lab has shown to be required for glial remodeling during dauer formation. Since LIT-1 has been shown to regulate the activity of other transcription factors (such as TCF/LEF), and given the role of LIT-1 in sensory compartment morphogenesis described here, it will be interesting to investigate the role of LIT-1 in glial remodeling in dauer animals. Also intriguing is the protein C44B12.5, a transmembrane protein of unknown function that is conserved in nematodes and was identified in 6 clones. The most intriguing among these hits, however, were the proteins ACT-4/Actin and WSP-1/WASP. I therefore proceeded to

verify the yeast two-hybrid screen results for these two hits by performing a growth assay and a β-galactosidase enzymatic activity assay (Figure 3.17), and to further investigate their roles in amphid sensory compartment morphogenesis.

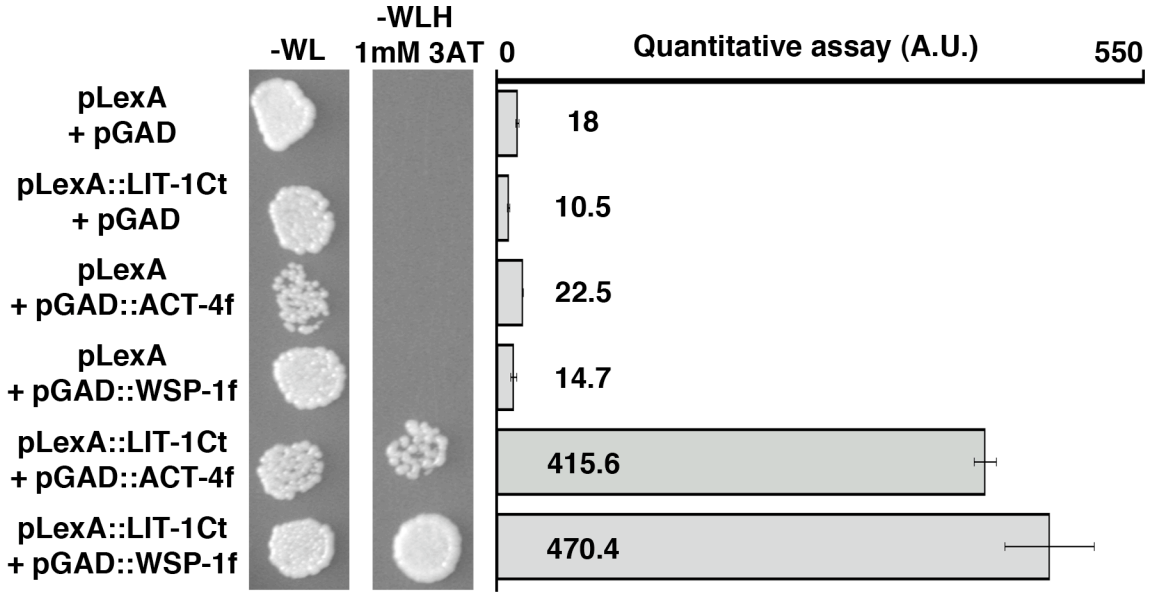

Figure 3.17. ACT-4 and WSP-1 interact with the C-terminal domain of LIT-1. Growth assay (left) and quantitative β-galactosidase enzymatic activity assay (right) demonstrating the interaction between LexA fused to the LIT-1 carboxy-terminal domain and GAD fused to fragments of ACT-4 or WSP-1. Error bars, standard deviation. f, fragment. –WL, medium without Tryptophan and Leucine. –WLH, medium without Tryptophan, Leucine and Histidine. 3AT, 3-amino-1,2,4-triazole. A.U., arbitrary units.

3.12. ACT-4 is enriched around the amphid sensory compartment

Among the 26 interacting clones identified, 4 encoded the *C. elegans* actin protein ACT-4. EM studies of the amphid sheath glia channel had previously shown that the channel is lined by an electron dense subcortical layer (red arrowheads in Figure 2.1B) (Perkins et al., 1986). A similar layer can be seen in other highly secreting cells such as pancreatic acinar cells and adrenal chromaffin cells. In these cells, this electron dense layer has been demonstrated to be enriched in actin (Drenckhahn and Mannherz, 1983; Lee and Trifaró, 1981). Other luminal structures, such as the excretory cell of *C. elegans* and the trachea of *Drosophila*, are also characterized by such terminal webs (see introduction).

To determine whether ACT-4 might be part of the electron-dense subcortical layer near the amphid sensory compartment, I examined animals expressing a GFP::ACT-4 fusion protein in amphid sheath glia. Strikingly, I found that although GFP::ACT-4 was seen throughout the cell, it was highly enriched at the amphid sensory compartment (Figure 3.18A). I wondered whether other actin proteins also accumulate at the channel and, therefore, generated animals expressing a protein fusion of GFP to ACT-1. Again, I found increased channel localization (Figure 3.18B), suggesting that actin filaments may be components of the subcortical density.

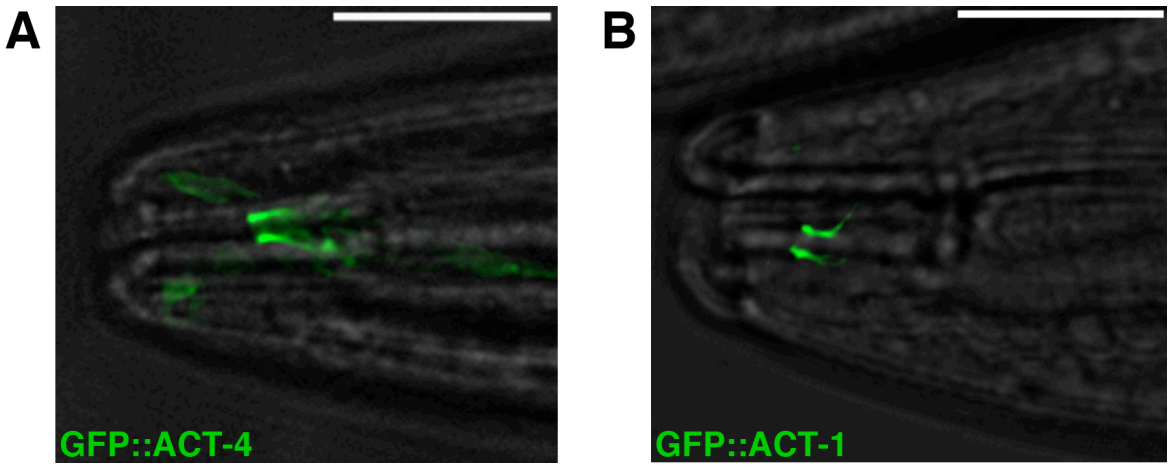

Figure 3.18. Actin is enriched around the amphid sensory compartment. The *T02B11.3* promoter (Wang et al., 2008) driving GFP::ACT-4 (A) and GFP::ACT-1 (B).). Compare to terminal web lining depicted in figure 1.3. Anterior is to the left. Scale bars, 10 μm.

To examine the localization pattern of ACT-4 at higher resolution, Shigeki Watanabe, in the lab of Erik Jorgensen, used scanning EM coupled with photo-activated localization microscopy (PALM). In this method, fluorescent electron microscopy (fEM), serial sections are imaged by scanning EM and using single-molecule fluorescence of mEos::ACT-4 (Watanabe et al., 2011). Images are then superimposed, using fiduciary markers (fluorescent gold beads), to reveal the subcellular localization of fluorescent proteins. As shown in Figure 3.19A, in the anterior portion of the amphid channel, where an electron dense subcortical region has been described, mEos::ACT-4 is localized near the sensory compartment membrane (blue trace). mEos::ACT-4 does not localize to the sensory compartment in more posterior sections (Figure 3.19B, 2 μm posterior to 3.19A), which should lack the subcortical electron density. These

observations support the notion that actin is intimately associated with the glial sensory compartment, and that the subcortical density is composed in part of actin.

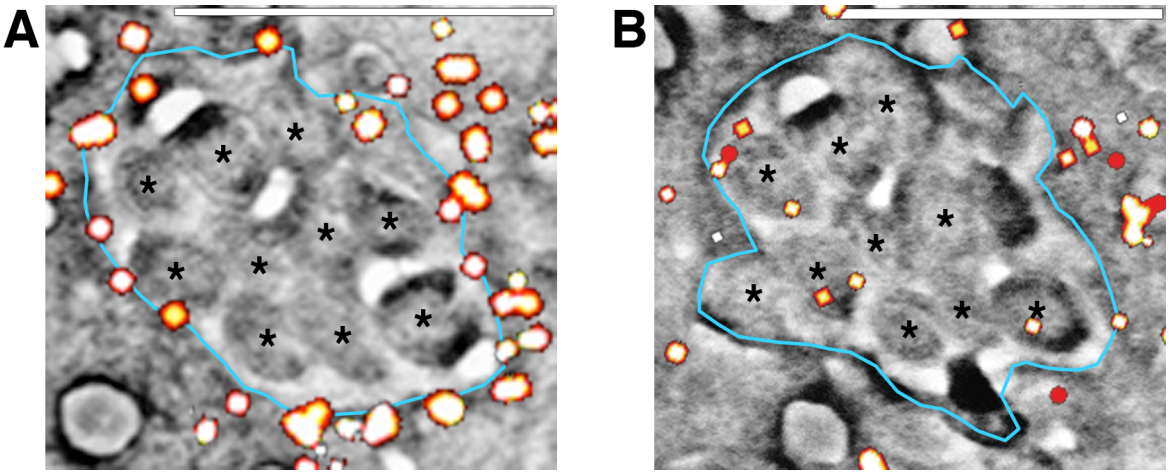

Figure 3.19. Actin is enriched at the anterior region of the amphid sensory compartment. fEM of a cross-section through the amphid channel (blue trace) just below the socket-sheath junction (A) or 2 μm posterior (B). White puncta indicate mEos::ACT-4 localization. Asterisks, cilia. Scale bars, 1 μm.

GFP::ACT-4 was also properly localized in *lit-1*(*ns132*) mutants (n=50), suggesting that actin accumulates around the sensory compartment independently of *lit-1*, and consistent with the possibility that actin may recruit LIT-1.

To test this possibility, I tried to disturb GFP::ACT-4 localization by treating the animals with an inhibitor of actin polymerization, cytochalasin D. After a 2 hour incubation with 1 mM of the drug, the cell bodies of the sheath glia assumed a rounded morphology, indicative of breakdown of the actin cytoskeleton. However, the sensory compartment localization of neither GFP::ACT-4 nor GFP::LIT-1 was disturbed. This

result suggests that the subcortical actin around the amphid channel could be part of a stable structure with a lower turnover rate than the rest of the actin cytoskeleton.

3.13. The actin regulator WASP binds LIT-1 and is required for sensory compartment expansion in *daf-6* mutants

In addition to actin, the yeast two-hybrid studies suggested that the LIT-1 C-terminal domain can also bind to the proline-rich region of WSP-1, the *C. elegans* homolog of the Wiskott-Aldrich Syndrome Protein (WASP) (Table 3.2, Figure 3.17). Furthermore, I was able to immunoprecipitate the LIT-1 C-terminal domain using WSP-1 from cultured *Drosophila* S2 cells co-expressing both proteins (Figure 3.20; see also materials and methods).

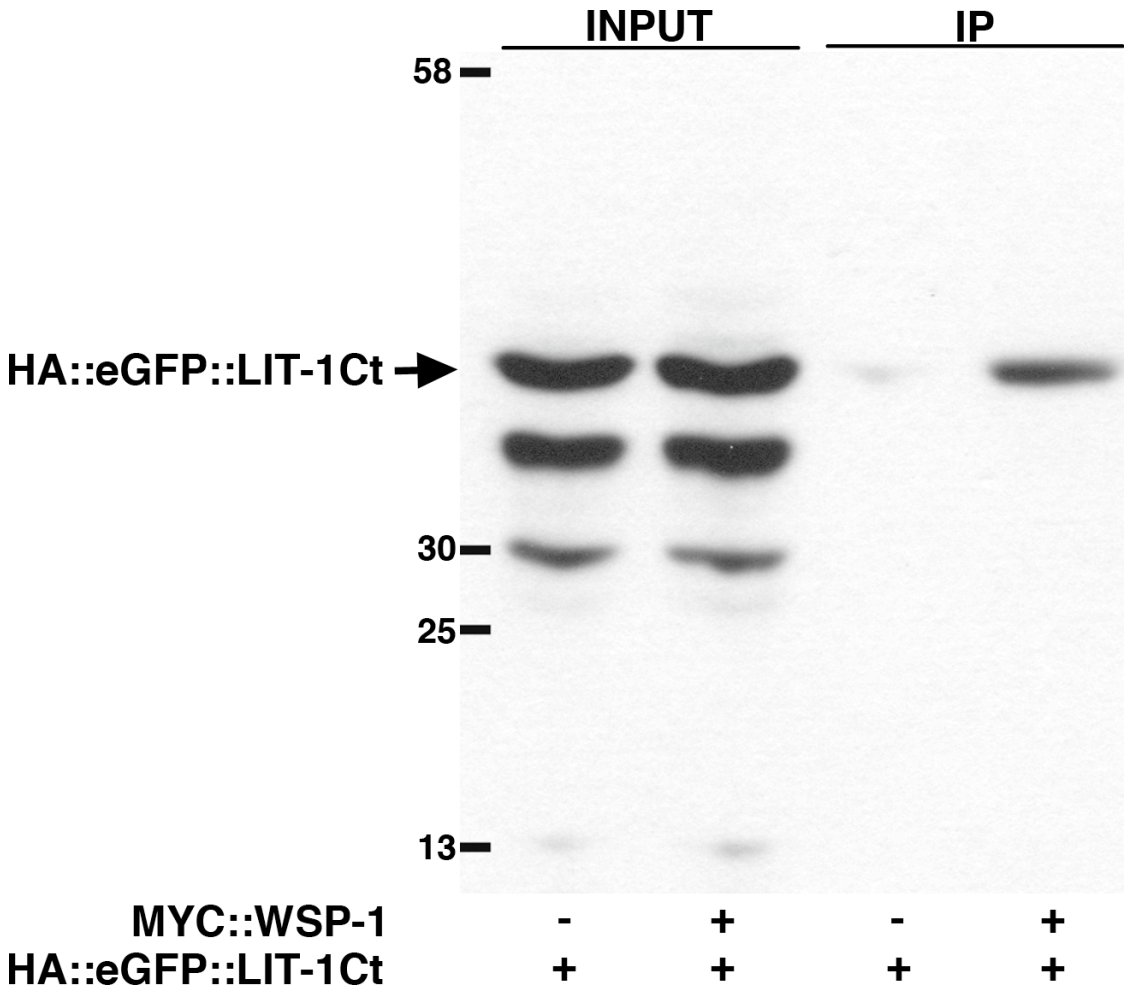

Figure 3.20. The carboxy-terminal domain of LIT-1 co-immunoprecipitates with WSP-1. *Drosophila* S2 cells were transfected with HA::eGFP::LIT-1Ct with or without MYC::WSP-1. Cell lysates were immunoprecipitated using anti-MYC-conjugated agarose beads and analyzed by anti-HA immunoblot.

Unlike ACT-4, a GFP::WSP-1 fusion protein is expressed in amphid sheath glia diffusely and is not localized to the sensory compartment. To determine whether *wsp-1* plays a role in amphid morphogenesis I examined *wsp-1*(*gm324*) mutants, which, unlike actin mutants, are viable despite being null for *wsp-1* (Withee et al., 2004). I did not find any defects in dye-filling in the single mutant. However, *wsp-1*(*gm324*) suppresses the *daf-6*(*n1543*) dye-filling defects (Figure 3.21). Furthermore, *daf-6* mutants homozygous for both *lit-1*(*ns132*) and *wsp-1*(*gm324*) were as dye-filling defective as *lit-1*(*ns132*); *daf-6*(*n1543*) mutants alone. These results are consistent with the hypothesis that LIT-1 and WSP-1 act within the same pathway to promote amphid channel expansion.

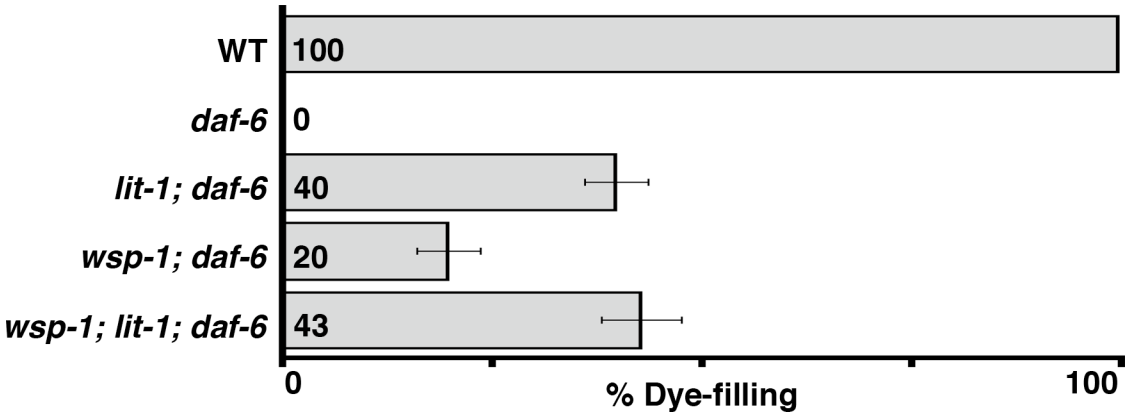

Figure 3.21. Mutation of *wsp-1* suppresses the amphid compartment defects of *daf-6* mutants. Dye-filling in animals of the indicated genotypes (n≥90). The alleles used are: *daf-6*(*n1543*), *lit-1*(*ns132*), *wsp-1*(*gm324*). *daf-6* is marked with *unc-3*(*e151*) in all strains. Error bars, s.e.m.

Chapter 4

The retromer and sensory compartment morphogenesis in *C. elegans*

Summary

In this chapter I describe the mapping, cloning and characterization of the *daf-6* suppressor *ns133*. *ns133* was isolated by Elliot A. Perens (Perens, 2006) during the screen for *daf-6* suppressors described in Chapter 3. Using SNP mapping, whole genome sequencing and transgenic rescue experiments, I show that *ns133* is an allele of *snx-1*, the gene encoding sorting nexin 1, a component of the retromer. *snx-1* acts within glia to regulate the morphogenesis of the amphid sensory compartment, and SNX-1 lines this compartment. *snx-1* enhances the suppression of *daf-6* by *lit-1*, as well as the dye-filling defects of *che-14*. These observations suggest that *snx-1* could act in amphid compartment expansion, similar to *lit-1* and *che-14*. I also show that other components of the retromer, *vps-29* and the sorting nexin *snx-3*, are involved in amphid morphogenesis. These results link amphid morphogenesis with the retromer complex, a known effector of membrane trafficking in the cell.

4.1. *ns133* is a suppressor of *daf-6*

ns133 was isolated in the *daf-6* suppressor screen conducted by Elliot Perens (Perens, 2006). Approximately 40% of *ns133*; *daf-6* animals dye-fill in comparison to 0% of *daf-6* animals (Figure 4.1A). In addition, *ns133*; *daf-6* animals have normal amphids as judged by fluorescence microscopy (Figure 4.1B). Animals that displayed normal dye-filling in one of the two amphids also had only one amphid channel that resembled a wild-type channel by EM serial reconstruction (Figure 4.1C, n=3).

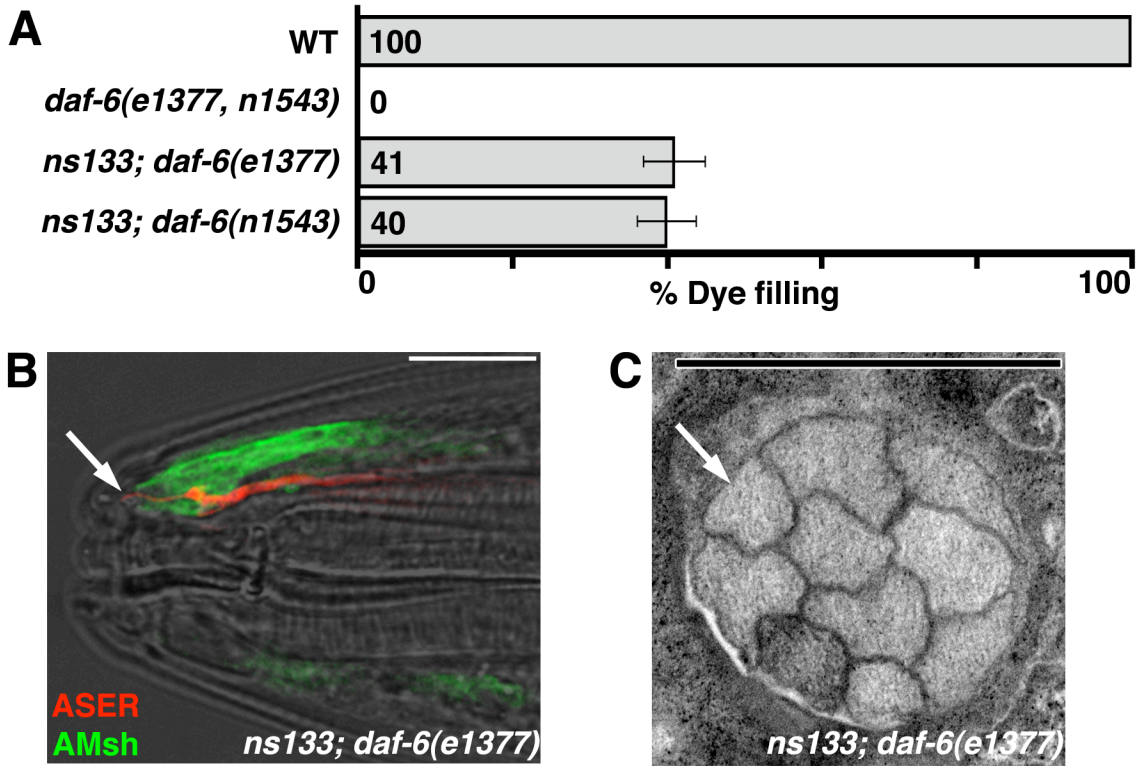

Figure 4.1. *ns133* is a suppressor of *daf-6*. (A) Dye-filling in animals of the indicated genotypes (n≥90). *daf-6*(*n1543*) was linked to *unc-3*(*e151*). (B) The ASER neuron and the amphid sheath glia, visualized with mCherry (red) and GFP (green), respectively, in an *ns133*; *daf-6*(*e1377*) animal. Arrow, ASER cilium. Left is anterior. Scale bar, 10 μm. (C) Electron micrograph of a cross-section through the amphid sheath channel of a *ns133*; *daf-6*(*e1377*) adult animal. Arrow, cilium. Scale bar, 1 μm.

4.2. *ns133* is an allele of *snx-1*

As a first step in mapping *ns133*, I asked whether the mutation is located on the X chromosome or one of the autosomal chromosomes. By the series of crosses described in Figure 4.2, I was able to compare males and hermaphrodites that were homozygous for *daf-6* but heterozygous for *ns133*. Only 3% of the hermaphrodites dye-filled compared to 33% of the males. This discrepancy between the male and hermaphrodite dye-filling results suggests that *ns133* is located on chromosome X, and that the male animals obtained from the final cross are actually hemizygous for the *ns133* suppressor. Furthermore, since hermaphrodite animals can still dye-fill with a frequency of 3%, *ns133* is either partially dominant, or there is a maternal rescue effect.

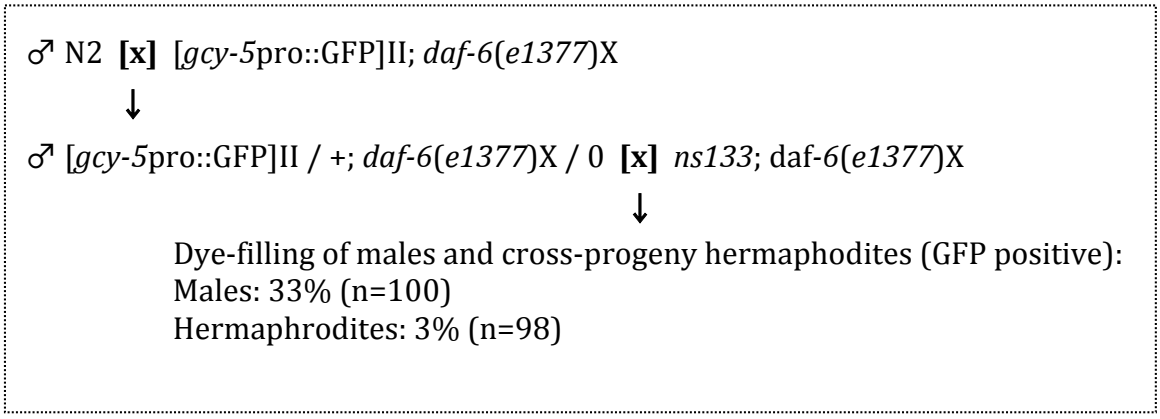

Figure 4.2. *ns133* is located on the X chromosome. Outline of a cross designed to compare male and hermaphrodite animals heterozygous for *ns133* and homozygous for *daf-6*. For details, see text.

In order to map *ns133*, I used standard SNP mapping techniques taking advantage of the polymorphisms between the N2 Bristol strain, commonly used in the lab, and the

Hawaiian strain (Wicks et al., 2001). However, due to the fact that *ns133* resides on chromosome X, the same chromosome as *daf-6*, the mapping strategy had to be modified from the one used for the mapping of autosomal suppressors such as *ns132*. As seen in Figure 4.3, I constructed a strain homozygous for the SNPs observed in the Hawaiian background on all of chromosome X, except for the region that contains the *unc-3* and *daf-6* loci; this region came from the N2 background in which the mutations were isolated. This was accomplished by repeatedly crossing Hawaiian males into *unc-3*(*e151*) *daf-6*(*n1543*) hermaphrodites, re-isolating the Unc and Dyf phenotypes, and checking for the presence of Hawaiian SNPs.

In the first step of this mapping strategy, *unc-3* allows for the identification of cross progeny (non-Unc animals). In the second step, animals that can dye-fill are selected, thus re-isolating the *ns133* suppressor. In the third and final step, these animals are allowed to give progeny that are used to verify the presence of the suppressor (through the dye-filling assay) and provide DNA for the determination of SNPs. This last step is crucial: because of the semi-dominant nature of *ns133*, animals coming from the second step could be heterozygous for *ns133* and complicate the interpretation of the SNP results.

Using this strategy, I was able to map *ns133* to the left arm of chromosome X. However, despite repeated attempts with modified versions of this strategy, narrower mapping of *ns133* using this approach was not feasible due to contradictory results from the recombinant animals. The reasons behind these contradictions include less than 100% penetrance of *daf-6* in the Hawaiian background, as well as increased semi-dominance for *ns133* in the Hawaiian background.

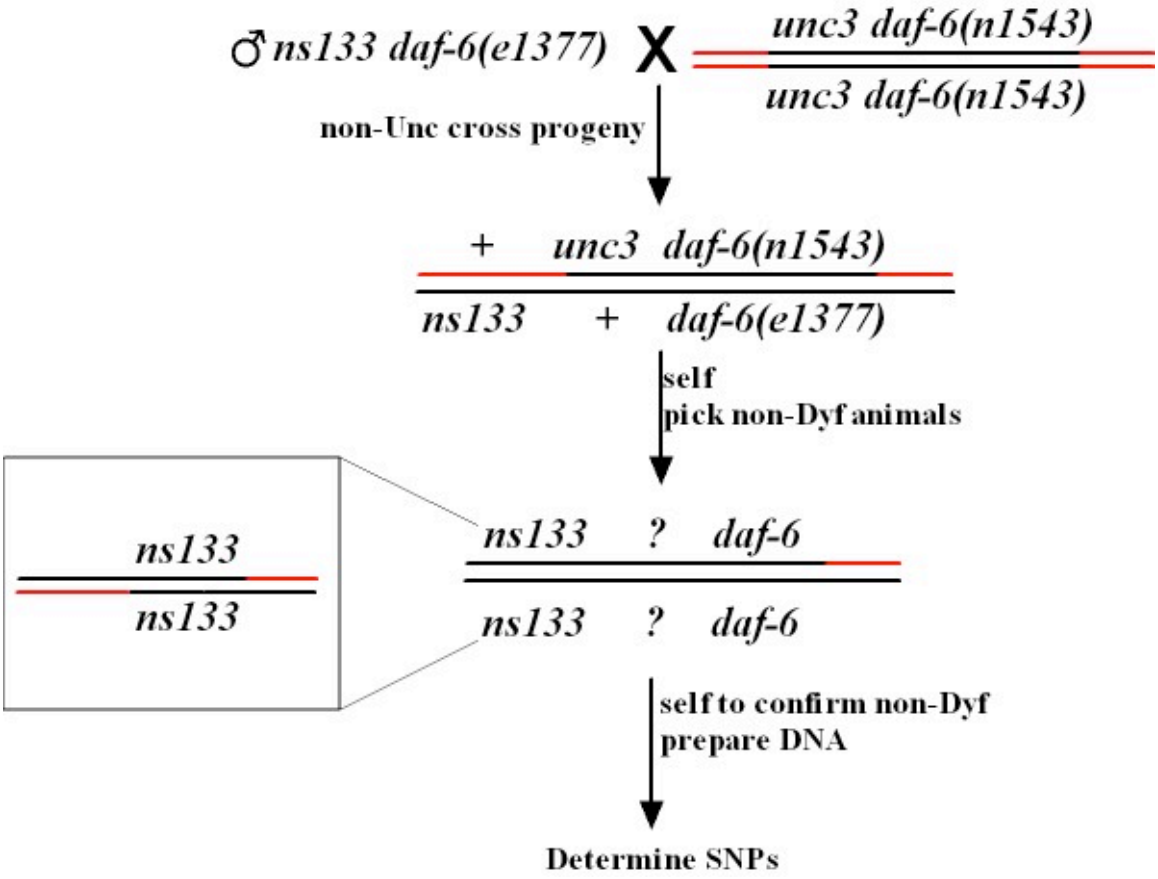

Figure 4.3. The strategy for SNP mapping of *ns133*. For details, see text.

To circumvent the issues of the SNP mapping approach, I decided to use the Solexa sequencing technology, and galign analysis software (Shaham, 2009), to identify candidate mutations on chromosome X in the *ns133 daf-6*(*e1377*) strain. This approach uncovered approximately 80 mutations on chromosome X in this strain. I used the results of the SNP mapping, the nature of the mutations (e.g. nonsense vs silent mutations), and the identity of the mutated genes to prioritize these candidates and proceeded to test whether any of them corresponded to *ns133*. Eventually, I identified a 97 nucleotide deletion in *snx-1* that was present in *ns133 daf-6*(*e1377*) as well as the out-crossed (3x) *ns133 daf-6*(*e1377*) strain (Figure 4.4A). This deletion starts 32 nucleotides before the end of exon 4 and proceeds into the following intron, thus removing the splice donor site at the end of exon 4. The suppression of *daf-6* by *ns133* can be rescued by transgenic extrachromosomal arrays carrying either the genomic region of *snx-1* or a construct in which a 0.8 kb promoter region of *snx-1* drives expression of the *snx-1* cDNA (Figure 4.4B). In addition, *tm847*, another allele of *snx-1* with a larger deletion, also suppresses *daf-6* to the same extent as *ns133* (but neither allele has an effect on dye-filling on its own). These results suggest that *ns133* is indeed an allele of *snx-1*.

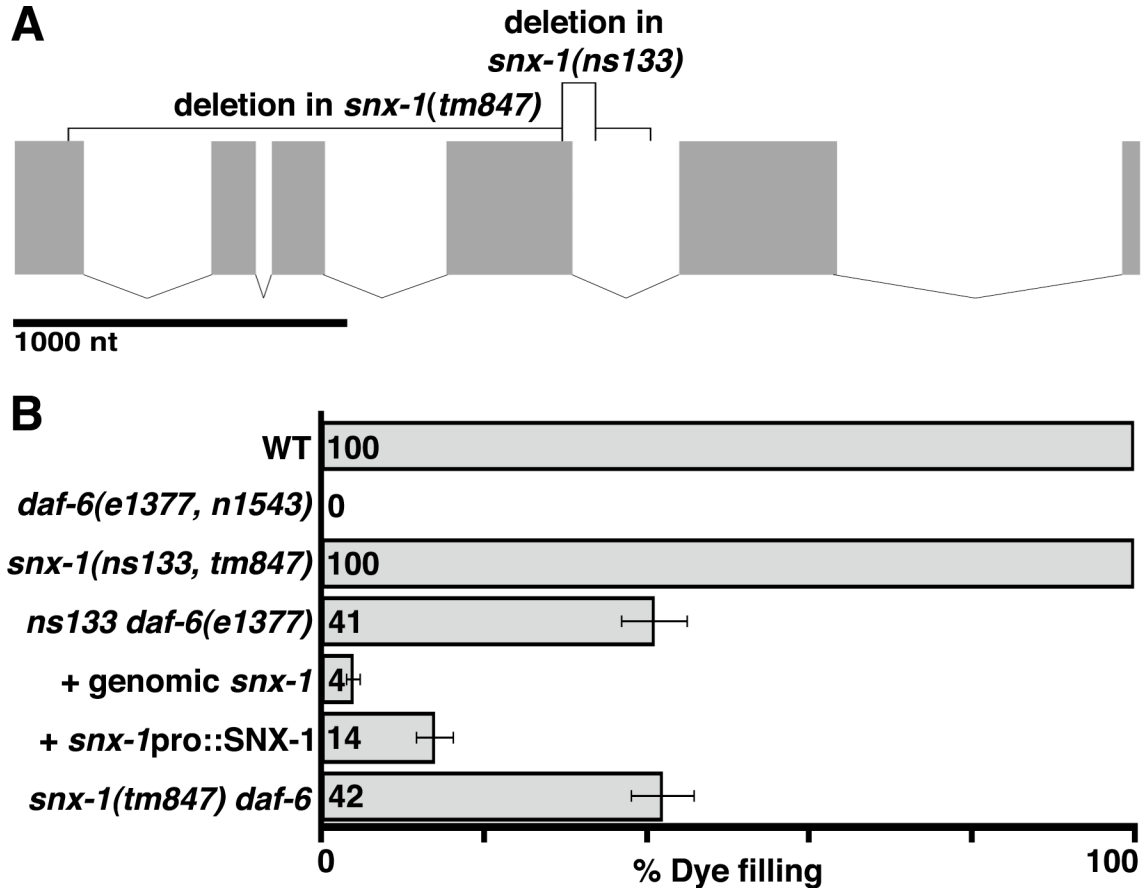

Figure 4.4. *ns133* is an allele of *snx-1*. (A) Schematic of the *snx-1* locus and the areas deleted in the alleles used in this study. (B) Dye-filling in animals of the indicated genotypes (n≥100). Unless otherwise specified, the *daf-6* allele used is *n1543*, linked to *unc-3*(*e151*). Error bars, s.e.m.

4.3. *snx-1* can act within glia to regulate amphid morphogenesis

To determine whether *snx-1* can act within glia to regulate amphid morphogenesis, I used the *lin-26* promoter fragment previously described (Landmann et al., 2004) to drive expression of the *snx-1* cDNA in glia, during the time of amphid formation. As shown in Figure 4.5A, transgenic animals were rescued, i.e. failed to dye-fill, in support of our hypothesis. Driving the same cDNA with the *T02B11.3* promoter that is expressed later in development (around the three-fold developmental stage) did not result in rescue, suggesting that *snx-1* expression is required at the time of amphid morphogenesis.

To determine the subcellular localization of SNX-1, I used the *T02B11.3* promoter to drive expression of a GFP::SNX-1 fusion protein within the sheath glia. As seen in Figure 4.5B, the protein localizes to the amphid compartment, similar to GFP::LIT-1.

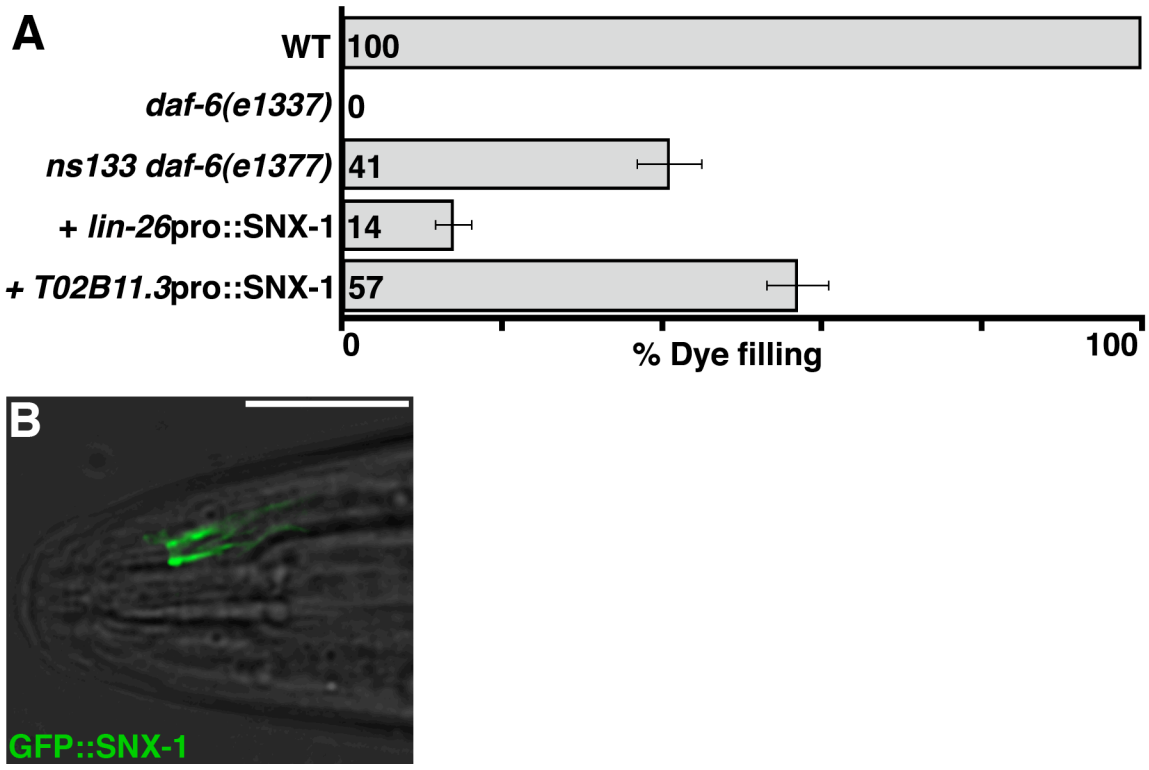

Figure 4.5. *snx-1* can act within glia and SNX-1 localizes to the amphid sensory compartment. (A) Dye-filling in animals of the indicated genotypes (n≥100). Error bars, s.e.m. (B) Amphid compartment localization of GFP::SNX-1 (expression was driven by the *T02B11.3* promoter). Left is anterior. Scale bar, 1 μm.

Having identified a role for *snx-1* in amphid morphogenesis, I decided to investigate potential interactions between this gene and other regulators of amphid sensory compartment formation, such as *lit-1* and *che-14*. As can been seen in Figure 4.6, *snx-1* enhances the suppression of *daf-6* by *lit-1*(*ns132*), suggesting that they act in the same direction (expanding the amphid compartment). No dye-filling phenotype was observed for the *lit-1*; *snx-1* double (Figure 4.6). In addition, similar to *lit-1*, *snx-1* enhances the defects of *che-14*, another gene involved in amphid pocket expansion (Figure 4.6).

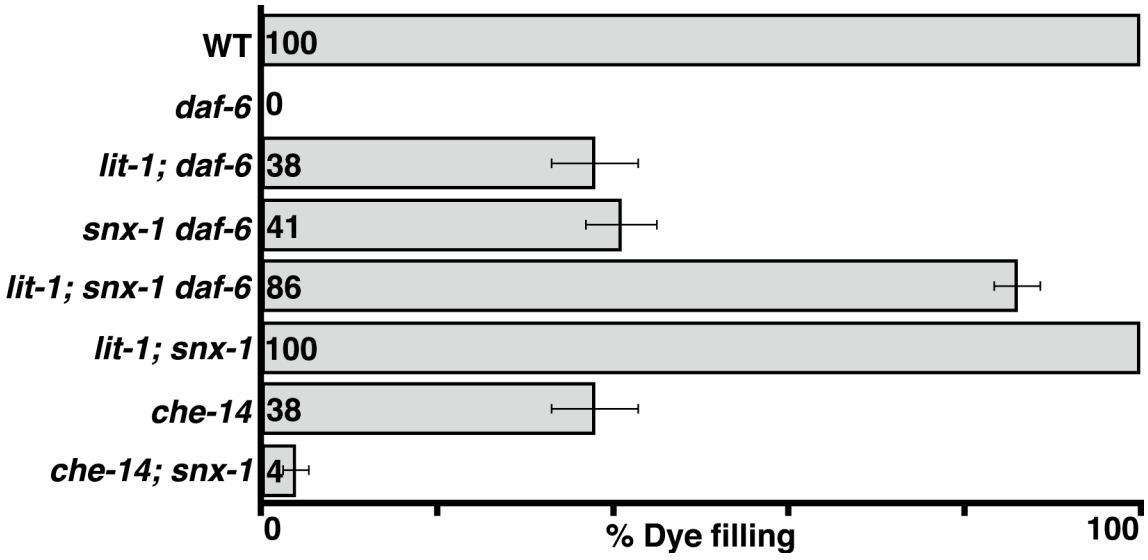

Figure 4.6. *snx-1* enhances the *lit-1* suppression of *daf-6* and the dye-filling defects of *che-14*. Dye-filling in animals of the indicated genotypes (n≥100). The alleles used are: *daf-6*(*e1377*), *lit*-1(*ns132*), snx-*1*(*ns133*), *che-14*(*ok193*). Error bars, s.e.m.

Work presented in the previous chapter suggests that the suppression of *daf-6* by *lit-1*(*ns132*) could arise by the mislocalization of the truncated version of LIT-1 encoded by the *ns132* allele. Due to the role of the retromer in protein trafficking, it is possible that the suppression of *daf-6* by *snx-1* could also be achieved through the mislocalization of LIT-1. To test this hypothesis I observed the localization of GFP::LIT-1 in the *snx-1*(*ns133*) background. GFP::LIT-1 localized normally in these animals (n>50), suggesting a different mechanism of suppression.

4.4. A role for the retromer complex in amphid channel morphogenesis

As mentioned in the introduction, *snx-1* is a member of the retromer complex that acts in retrieving membrane material and transmembrane proteins from the endosome and directing them to the Golgi. I therefore decided to investigate whether other components of the retromer complex can regulate amphid morphogenesis. As seen in Figure 4.7, mutations of the sorting nexin *snx-3*, another membrane binding protein, can also suppress *daf-6*. Construction of a strain mutant for *snx-1* and *snx-3*, as well as *daf-6*, was not feasible, suggesting that elimination of both sorting nexin genes results in lethality. Mutation of *vps-29*, a gene encoding a component of the cargo selector module of the retromer, also suppressed *daf-6*. Interestingly, *vps-35*, the gene encoding the component of the cargo selector module that is thought to directly interact with MIG-14/Wntless, does not seem to be involved. It is worth noting that, as shown in Figure 4.7, mutation of these genes affects dye-filling only in the context of a *daf-6* background.

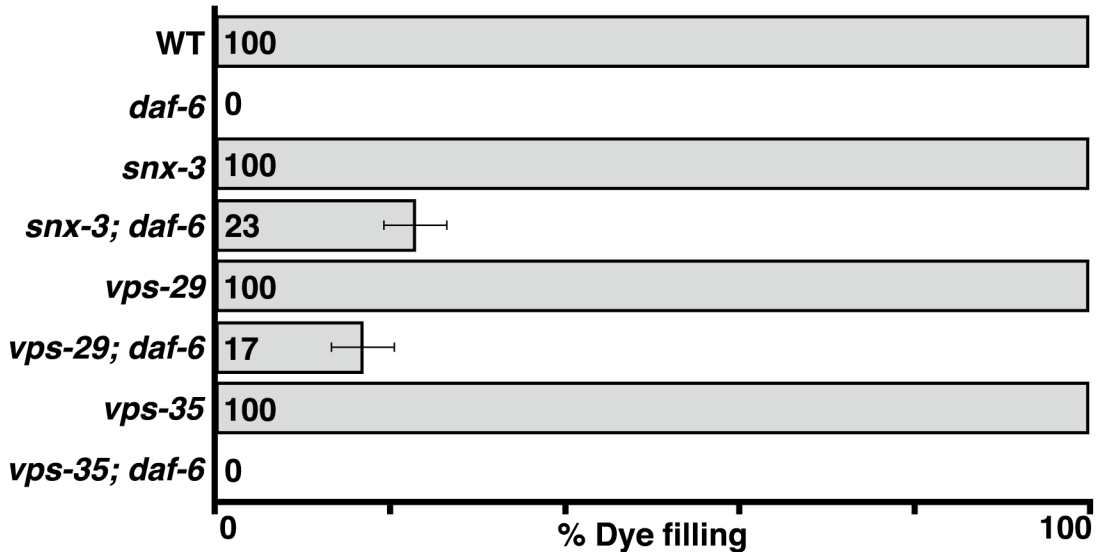

Figure 4.7. A broader role for the retromer in amphid compartment morphogenesis. Dye-filling in animals of the indicated genotypes (n≥100). The alleles used are: *daf-6*(*n1543*), *snx-3*(*tm1595*), *vps-29*(*tm1320*) and *vps-35*(*hu68*). *daf-6* was linked to *unc-3*(*e151*). Error bars, s.e.m.

Chapter 5

Discussion

5.1. *daf-6* acts in restricting the expansion of the amphid sensory compartment

daf-6 was originally identified for its role in dauer entry, with *daf-6* mutants being unable to enter this alternative developmental stage (Riddle et al., 1981). Electron microscopy reconstruction of the amphid sensilla of *daf-6* animals (Albert et al., 1981; Perkins et al., 1986; Perens and Shaham, 2005) revealed that the amphid sensory compartment is bloated and the sensory cilia become unbundled and lost within it, unable to reach the environment. This complicated phenotype seen in adult animals was explained as the consequence of either the misalignment of the sheath and socket channels (Perkins et al., 1986), or the inability of the sheath channel to open anteriorly (Perens and Shaham, 2005). The electron microscopy reconstruction of developing amphids by Yun Lu has allowed us to conclude that in *daf-6* mutants the two glial cells become properly aligned and the sheath channel opens anteriorly. However, the sensory compartment becomes bloated soon afterwards, suggesting that normally *daf-6* restricts the expansion of the compartment.

Another intriguing aspect of amphid morphogenesis, revealed by the reconstruction of its morphogenesis, is the presence of a dense network of filaments that transverse the length of the sensory compartment and appear to connect the tip of the sensory dendrites to the egg shell (Figures 2.4 and 2.6). What is the nature of these filaments? One possibility is that they are the scaffold, set up up by DEX-1 and DYF-7, that anchors the dendrites to the tip of the nose while their cell bodies migrate posteriorly (Heiman and Shaham, 2009). Ablation of the amphid sheath glia during embryogenesis results in short dendrites (Taulant Bacaj and Shai Shaham, unpublished observations); perhaps this is due to a requirement for the sheath glia in establishing such filaments.

The fact that such filaments form properly in *daf-6* mutants is in agreement with the lack of any dendrite extension defects these animals. In an alternative hypothesis, these filaments are reminiscent of the intraluminal chitin mesh that regulates the size of tracheal tubes in the developing *Drosophila* embryo (see section 1.4.3 of the introduction). Could the dendrite-to-egg shell filaments also be made of chitin and/or serving a similar role in regulating the size and shape of the amphid sensory compartment? Either scenario provides testable hypotheses: in the former case, *dex-1* and *dyf-7* mutants should show defects in filament formation; in the latter, mutants for chitin biosynthesis and/or modification should display defects in sensory compartment morphogenesis.

5.2. *lit-1* regulates the morphogenesis of a subcellular structure

LIT-1 is the *C. elegans* homolog of the Nemo-like kinase (NLK) (Brott et al., 1998), a Serine/Threonine kinase originally described in *Drosophila* (Choi and Benzer, 1994). In *C. elegans*, *lit-1* (loss of intestine) was first identified for its role in endoderm specification during early embryogenesis (Kaletta et al., 1997). Subsequent work established *lit-1* as a component of the Wnt/β-catenin asymmetry pathway that directs many cell fate decisions in *C. elegans* (Mizumoto and Sawa, 2007b; Phillips and Kimble, 2009). NLK also plays roles in control of the Wnt (Ishitani et al., 1999; Thorpe and Moon, 2004), TGFβ (Ohkawara et al., 2004), and Notch (Ishitani et al., 2010) signaling pathways in vertebrates.

In all of the examples described so far, the role of LIT-1/NLK has been to regulate cell fate determination. In my studies, I identified *lit-1* mutations as suppressors of lesions in *daf-6*, a gene that affects morphogenesis of the amphid glial sensory compartment, but not glial cell fate. Indeed, *lit-1* mutants seem to have well-specified amphid components: both neurons and glia are present and their morphology is normal, save for the smaller amphid sensory compartment observed in *lit-1*(*t1512*) mutants. Furthermore, despite an established connection between *lit-1* and the Wnt/β-catenin asymmetry pathway (a major regulator of cell fate decisions in *C. elegans*), I found no evidence linking Wnt signaling to amphid morphogenesis. These observations are consistent with the idea that the role of *lit-1* in sensory organ morphogenesis does not involve cell fate decisions, but instead reflects a novel function in cellular morphogenesis.

Within the context of cell fate decisions, LIT-1/NLK often acts by impinging upon the activity of nuclear transcription factors (Lo et al., 2004; Ohkawara et al., 2004; Ishitani et al., 2010). It is unclear whether the role of *lit-1* in sensory organ morphogenesis involves transcriptional regulation. The C-terminal domain of LIT-1 is required for its role in amphid morphogenesis and for its amphid channel localization, but it is not essential for the ability of LIT-1 to enter the nucleus. This suggests that LIT-1 may exert its primary influence on channel morphogenesis at the channel itself. However, according to the results of a yeast two-hybrid assay, the LIT-1 C-terminus can interact not only with cytoskeletal proteins (actin and WASP), but also with the transcription factors ZTF-16 and MEP-1. Thus, while it is likely that sensory

compartment localization is important for LIT-1 function, I cannot rule out the possibility that LIT-1 has independent relevant functions in the nucleus.

5.3. Opposing activities of *lit-1* and *daf-6* direct sensory compartment morphogenesis

The studies presented here suggest that *daf-6* and *lit-1* direct the morphogenesis of the sheath glia sensory compartment by exerting opposing influences. In *daf-6* mutants, neurons and glia form an amphid primordium in which all components are initially linked and aligned; however, the sensory compartment expands abnormally. Conversely, in *lit-1* mutants, the sensory compartment is too narrow. Mutations in *lit-1* can correct for the loss of *daf-6*; thus, *lit-1*; *daf-6* double mutants have relatively normal glial channels. A situation that mimics *lit-1*; *daf-6* double mutants arises in animals with mutations in genes controlling neuronal cilia development. In these animals, channel localization of LIT-1, as well as DAF-6, is perturbed. Consistent with the *lit-1*; *daf-6* phenotype, channel formation is only mildly defective in these mutants (Perens and Shaham, 2005).

The observation that *lit-1* loss-of-function mutations suppress *daf-6* null alleles argues that *lit-1* cannot function solely upstream of *daf-6* in a linear pathway leading to channel formation. The data presented here are consistent with the possibility that *daf-6* functions upstream of *lit-1*, to inhibit *lit-1* activity. Alternatively, *lit-1* and *daf-6* may act in parallel. The current studies do not allow me to distinguish between these two possibilities.

5.4. Vesicles, the actin cytoskeleton, and sensory compartment morphogenesis

How might DAF-6 restrict the size of glial sensory compartments? Electron micrographs of the *C. elegans* amphid reveal the presence of highly organized Golgi stacks near the amphid channel. These images also show vesicles, containing extracellular matrix, that appear to be released by the sheath glia into the channel (Ward et al., 1975). These studies suggest that vesicular secretion may play a role in channel morphogenesis. Interestingly, DAF-6 is related to Patched, a protein implicated in endocytosis of the Hedgehog ligand, and the *C. elegans* Patched gene *ptc-1* is proposed to regulate vesicle dynamics during germ-cell cytokinesis (Kuwabara et al., 2000). Furthermore, DAF-6 can be seen in punctate structures, which may be vesicles (Perens and Shaham, 2005), and DAF-6 and CHE-14/Dispatched function together in tubulogenesis (Michaux et al., 2000; Perens and Shaham, 2005), a process hypothesized to require specialized vesicular transport. Together, these observations raise the possibility that DAF-6 may restrict amphid sensory compartment expansion by regulating vesicle dynamics in the sheath glia (Perens and Shaham, 2005).

If indeed DAF-6 controls membrane dynamics, it is possible that LIT-1, which localizes to and functions at the sheath glia channel, also interfaces with such processes. How might LIT-1 localize to the glial sensory compartment and control vesicle dynamics? Previous studies suggest that cortical localization of LIT-1 requires it to stably interact with WRM-1/β-catenin (Takeshita and Sawa, 2005; Mizumoto and Sawa, 2007a). In the sheath glia, however, I found that *wrm-1* is not required for sensory compartment morphogenesis or for LIT-1 localization, and that LIT-1 and WRM-1 do not co-localize to the amphid sensory compartment. Instead, I found that LIT-1

physically interacts with actin, and that actin is highly enriched around the amphid sensory compartment. Thus, actin might serve as a docking site for LIT-1. The interaction between LIT-1 and actin may not be passive. Indeed, I showed that LIT-1 also binds to WASP, and mutations in *wsp-1*/WASP suppress *daf-6* similarly to mutations in *lit-1*. Furthermore, WASP activity is stimulated by phosphorylation of Serines 483 and 484 (Cory et al., 2003), suggesting that LIT-1, a Ser/Thr kinase, could activate WASP to promote actin remodeling.

Remodeling of the cortical actin cytoskeleton plays important roles in several aspects of membrane dynamics (Lanzetti, 2007). For example, WASP-dependent actin polymerization has a well-established role in promoting vesicle assembly during clathrin-mediated endocytosis (Galletta et al., 2010). Recent work has demonstrated positive roles for actin polymerization in exocytosis as well (Malacombe et al., 2006; Trifaró et al., 2008). In pancreatic acinar cells, secretory granules become coated with actin prior to membrane fusion (Valentijn et al., 2000), and in neuroendocrine cells, actin polymerization driven by WASP stimulates secretion (Gasman et al., 2004). The actin-based terminal web is required for apical secretion in the trachea and other tubular organs of *Drosophila* (Massarwa et al., 2009). During *Drosophila* myoblast fusion, actin polymerization, dependent on WASP and WASP interacting protein (WIP), is required for targeted exocytosis of prefusion vesicles (Kim et al., 2007), and antibodies against WASP inhibit fusion of purified yeast vacuoles (Eitzen et al., 2002). An attractive possibility, therefore, is that LIT-1 might regulate sensory compartment morphogenesis by altering vesicle trafficking through WASP-dependent actin polymerization (Figure 5.1).

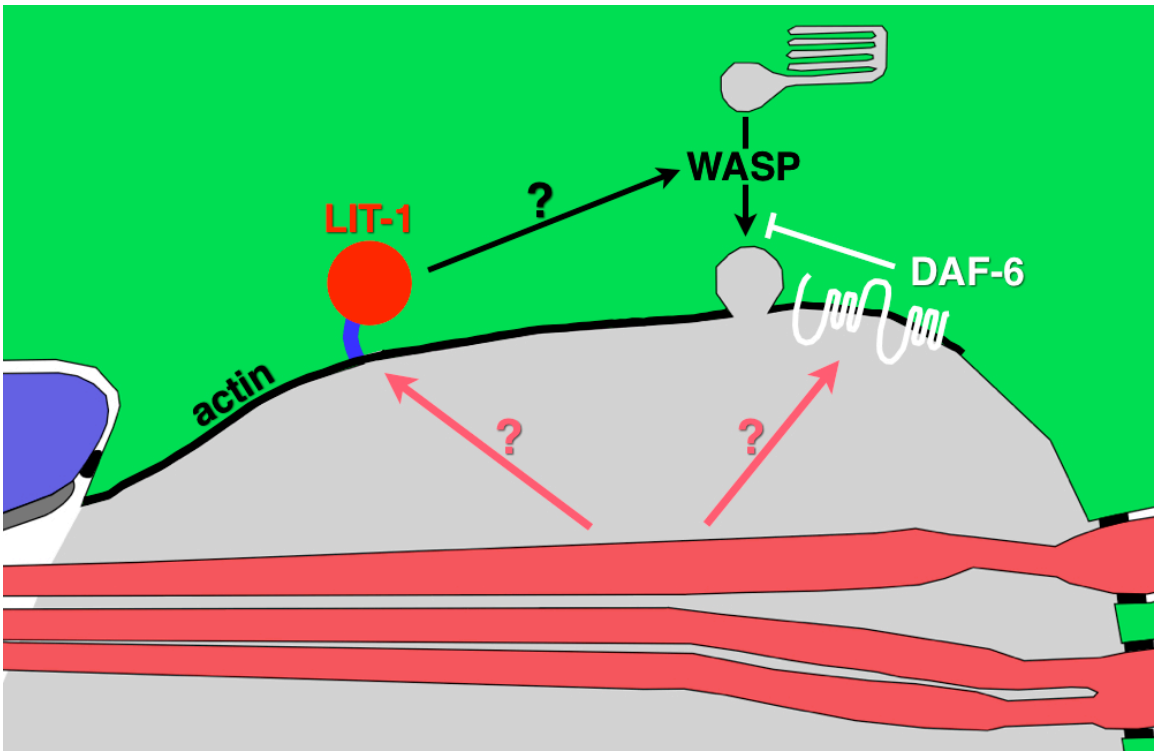

Figure 5.1. A model for size regulation of the amphid sensory compartment. LIT-1 localizes to the sensory compartment by binding to the actin-based terminal web and drives expansion of the compartment by promoting apical secretion. This could be achieved by activation of WASP and subsequent stimulation of actin polymerization, which drives vesicle secretion. DAF-6 antagonizes this process, and thus restricts amphid compartment expansion, either by inhibiting apical secretion or promoting endocytosis. Uncharacterized neuronal signals (red arrows) are important for DAF-6 and LIT-1 localization, as well as for fine-tuning the sensory compartment shape.

My studies of glial sensory compartment formation have identified new roles for LIT-1 and the glial cytoskeleton in *C. elegans*. Glial ensheathment of sensory endings is a feature of many sensory organs, and the LIT-1 MAPK complex is highly conserved.

LIT-1 was also shown recently to be required for anchor cell invasion across the basement membrane in *C. elegans* and during carcinoma cell invasion during metastasis (Matus et al., 2010), two processes that require extensive remodeling of the actin cytoskeleton. Interestingly, no components of the Wnt signaling pathway were implicated in these processes, suggesting that the contribution of *lit-1* could be Wnt-independent, similar to the observations described here. These results may thus represent a general mechanism for regulating cell shape changes using localized interactions of LIT-1/NLK with cytoskeletal proteins.

5.5. The retromer and amphid sensory organ morphogenesis

Is there a relationship between the roles of LIT-1 and the retromer complex in regulating the amphid sensory compartment? The studies presented here support the hypothesis that the retromer complex acts within glia, at the time of amphid morphogenesis, to antagonize *daf-6*, similar to *lit-1*. Indeed, *lit-1* and *snx-1* mutations synergize, and the respective proteins show similar sensory compartment localization. There is currently no evidence, however, for a direct, physical interaction between the two proteins.

Interestingly, the closely related sorting nexins Snx9, Snx18 and Snx33 (which are not considered part of the retromer) have been shown to physically interact with N-WASP and induce its activation (Yarar et al., 2007; Shin et al., 2007; Park et al., 2010; Zhang et al., 2009). All of these proteins contain, in addition to the PX and BAR domains discussed in the introduction, an SH3 domain. In the case of Snx9, this SH3

domain is necessary for the interaction between Snx9 and WASP (Yarar et al., 2007); neither *snx-1* nor *snx-3*, the genes shown here to regulate amphid morphogenesis, encode such an SH3 domain.

Given the role of the retromer in Wnt signaling (see introduction), is it possible that its role in sensory organ morphogenesis reflects the involvement of Wnt in this process? Strong evidence suggests that this is not the case. I tested, without success, whether a variety of Wnt signaling pathway mutants mimic or, alternatively, are able to suppress, the dye-filling defects of *daf-6*. Importantly, the retromer has been shown to regulate Wnt by impinging upon the stability of MIG-14/Wntless (Pan et al., 2008; Yang et al., 2008), but two alleles of the *mig-14* gene, both of which display Wnt phenotypes, do not suppress *daf-6*. In addition, a presumed null allele of *vps-35*, the gene encoding the component of the retromer that recognizes MIG-14, also fails to suppress *daf-6*.

The fact that *vps-35* does not appear to have a role in sensory compartment morphogenesis is intriguing. As mentioned in the introduction, Vps35 is the largest member of the cargo-recognition subunit of the retromer, and the one believed to actually bind to the cytoplasmic tail of the cargo proteins. The fact that *vps-26*, another cargo-recognition component, appears to be involved suggests that the cargo-recognition subunit is not simply irrelevant in this context. Instead, there is perhaps another, so far uncharacterized, retromer component that is responsible for the recycling of a protein that antagonizes DAF-6; this would account for the suppression of *daf-6* defects in retromer mutants.

Finally, the retromer could regulate sensory organ morphogenesis through its effect on membrane dynamics, independent of its role in transmembrane protein recycling. In the process of recycling proteins from the endosome, the retromer also directs a steady stream of membrane material to the Golgi network. There, this material can be used to create vesicles that can fuse with the luminal surface and expand the sensory compartment. It is possible that the aberrant expansion seen in *daf-6* mutants depends upon the availability of this membrane-supply stream. This hypothesis also explains why null alleles of retromer components do not have sensory compartment defects on their own: retromer activity becomes pertinent to amphid morphogenesis only within the context of the *daf-6* background.

5.6. Future Directions

In the studies described here, I identify the MOM-4/LIT-1 kinase module as a regulator of amphid compartment morphogenesis, which could act by regulating the actin cytoskeleton through WASP. This discovery presents new opportunities in expanding our understanding of sensory compartment formation.

One of the most exciting open questions is how LIT-1 regulates WASP. As mentioned previously, WASP can be activated by phosphorylation on two serine residues in its WCA domain (Cory et al., 2003), raising the possibility that LIT-1, a Serine/Threonine kinase, could induce its activation in such a fashion. An in vitro kinase assay with LIT-1 as the enzyme and WSP-1 as the substrate could be used as an initial test of this hypothesis. The presence of MOM-4 in the reaction might be required for the

full activation of LIT-1, as is in the case during the phosphorylation of POP-1/ TCF/LEF by LIT-1 (Shin et al., 1999). The *C. elegans* version of WASP, WSP-1, contains a serine and a threonine residue in approximately the same region that the two serine residues of mammalian WASP are found. It would be interesting to test whether mutation of these residues has an effect on the ability of WSP-1 to regulate amphid morphogenesis.

A hypothesis presented earlier suggested that LIT-1 localizes to the amphid sensory compartment by interacting with the actin of the terminal web that lines the glial channel. Testing this hypothesis with chemical destabilizers of the actin cytoskeleton was not successful, and the lack of viable alleles of actin genes precludes traditional genetic approaches. Glia specific RNAi against actin genes could be achieved either through expression of appropriate dsRNA specifically within glia (Esposito et al., 2007), or with standard RNAi methods, using animals defective in the RNAi machinery in all cells except for glia (e.g. *rde-4* mutants in which *rde-4* activity has been restored in the glia). With such approaches, the role of actin in LIT-1 localization (or sensory compartment morphogenesis in general) could potentially be investigated.

The yeast two-hybrid screen described here led to the identification of proteins that interact with the C-terminal domain of LIT-1 besides actin and WSP-1. Some of these proteins, such as ZTF-16 and MEP-1, are transcription factors; given the many instances in which LIT-1 has been shown to regulate the activity of transcription factors by phosphorylation (discussed in the introduction), it will be interesting to investigate whether these factors have a role in amphid morphogenesis. Another hit from the screen, C44B12.5, is a poorly characterized transmembrane protein. This protein was identified in multiple clones, suggesting a potentially strong interaction with LIT-1. It will be

interesting to investigate whether C44B12.5 is expressed in glia and, if so, where the protein localizes.

As described in Chapter 3, the C-terminal domain of LIT-1 is necessary and sufficient for the sensory compartment localization of the protein, with a fusion between GFP and the LIT-1 C-terminal domain localizing to the channel. This fusion protein could be used as a tool to uncover the factors required for this localization, by means of a genetic screen for mutants in which the localization of GFP::LIT-1Ct is disrupted. The region of localization is small (about 2 μm) and potential mutants will have to be identified under the high magnification provided by a compound scope (in contrast with mutants for dye-filling defects that can be readily identified using a dissecting scope). However, the sensory compartment localization of GFP::LIT-1Ct is very efficient, suggesting that such a screen could be effective despite being somewhat arduous.

Investigating the contribution of the retromer in sensory compartment morphogenesis is still in an early phase. Work should continue with addressing the potential roles of other, previously described, retromer components and sorting nexins using genetic tools. This will allow us to form a list of relevant genes. The subcellular localization of the corresponding proteins and their dynamics during development could shed some light on their roles in amphid morphogenesis. Eventually, we need to understand whether the retromer regulates sensory compartment formation by recycling a specific transmembrane protein with a critical role in morphogenesis, or by acting as a regulator of bulk membrane movement as previously discussed. Of course, these two possibilities are not mutually exclusive.

It is also important to note that at least four more suppressors of *daf-6* were identified in the screen described in Chapter 2 (Perens, 2006). Mapping and cloning of these suppressors should expand our understanding of sensory compartment formation. Initial efforts have suggested that at least some of the challenges confronted during the cloning of *lit*-1(*ns132*) and *snx-1*(*ns133*), such as low penetrance, semi-dominance, and reduced penetrance of *daf-6* in the Hawaiian background, will apply to the remaining suppressors as well. However, the fact that we already know some key players, such as *lit-1* and the retromer, combined with rapid technical advances in the field of full genome sequencing, suggests that cloning of further suppressors will be more tractable.

Understanding the morphogenesis of the amphid sensory compartment has been hampered by our inability to observe this process in real time. In the studies presented here, this problem has been partially addressed by the use of EM to capture different timepoints during the process of amphid morphogenesis. However, this approach has obvious limitations, as it can only provide a series of snapshots through development. Understanding the interactions between dendrites and glia that lead to the establishment and expansion of the sensory compartment will eventually require the establishment of a system that allows for direct, in vivo observation. The identification of molecules that line the sensory compartment (such as actin, LIT-1, MOM-4 and SNX-1, presented here), in combination with early glial (Landmann et al., 2004) and neuronal (Heiman and Shaham, 2009) promoters, provides some of the tools necessary for building such a system.

Chapter 6

Materials and methods

Strains

Strains were handled using standard methods (Brenner, 1974). All strains were maintained and scored at 20°C unless otherwise indicated. The alleles used in the studies presented here are: *daf-6*(*e1377*, *n1543*) (Riddle et al., 1981) and (Starich et al., 1995) respectively), *lit-1*(*t1512*) (Kaletta et al., 1997), *lit-1*(*ns132*) (described here), *che-14*(*ok193*) (Michaux et al., 2000), *wsp-1*(*gm324*) (Withee et al., 2004), *mom-4*(*ne1539*)(Nakamura et al., 2005), a gift from Craig Mello, *daf-19*(*m86*) (Perkins et al., 1986), *daf-16*(*mu86*)((Lin et al., 2001), *mig-14*(mu71) (Harris et al., 1996), *mig-14*(*ga62*)(Eisenmann and Kim, 2000), *lin-44*(*n1792*) (Herman and Horvitz, 1994), *egl-20*(*n585*, *mu27*) ((Trent et al., 1983) and (Harris et al., 1996) respectively), *cwn-1*(*ok546*) (Zinovyeva and Forrester, 2005), *cwn-2*(*ok895*) (Zinovyeva and Forrester, 2005), *mom-2*(*ne834*) (Nakamura et al., 2005), a gift from Craig Mello), *mom-2*(*or309*) (Thorpe et al., 1997), *lin-17*(*n671*, *n698*) (Ferguson and Horvitz, 1985), *lin-17*(*n3091*) (Sawa et al., 1996), *mig-1*(*e1787*) (Desai et al., 1988), *mom-5*(*or57*) (Thorpe et al., 1997), *mom-5*(*zu193*) (Rocheleau et al., 1997), *cfz-2*(*ok1201*) (Zinovyeva and Forrester, 2005), *mig-5*(*rh147*) (Walston et al., 2006), *lin-18*(*e620*) (Ferguson and Horvitz, 1985), *bar-1*(*ga80*) (Eisenmann and Kim, 2000), *wrm-1*(*ne1982*) (Nakamura et al., 2005) a gift from Craig Mello, *pop-1*(*q624*) (Siegfried and Kimble, 2002), *cam-1*(*ks52*) (Koga et al., 1999), *vang-1*(*ok1142*) (Green et al., 2008), *unc*-3(*e151*) (Prasad et al., 1998), *unc-32*(*e189*) (Pujol et al., 2001), *snx-1*(*ns133*) (described here), *snx-1*(*tm847*) Mitani lab, *snx-3*(*tm1595*) Mitani lab, *vps-29*(*tm1320*) Mitani lab, and *vps-35*(*hu68*) (Coudreuse et al., 2006).

Extrachromosomal arrays:

Table 6.1: Unstable extrachromosomal transgenes used in these studies

Extrachromosomal array(s)	Constructs
nsEx1933, *nsEx1934*, *nsEx1935, nsEx1936*	pGO1, pMH135
nsEx1931, *nsEx1932*	pGO2, pMH135
nsEx2136, *nsEx2137*, *nsEx2138*	pGO6, *ptr-10*pro::NLSRFP
nsEx2078, *nsEx2079*, *nsEx2080*, *nsEx2081*	pGO8, pMH135
nsEx2108, *nsEx2109*, *nsEx2110*, *nsEx2111*, *nsEx2112*, *nsEx2113*	pGO10, *vap-1*pro::GFP
nsEx2308, *nsEx2309*, *nsEx2310*	pGO17, *vap-1*pro::GFP, pRF4
nsEx2952, *nsEx2953*, *nsEx2954*	pGO18, pMH135
nsEx2541, *nsEx2542*, *nsEx2543*	pGO20, pEP51
nsEx2539, *nsEx2540*	pGO32, pEP51
nsEx2605, *nsEx2606*, *nsEx2607*, *nsEx2608*	pGO38, pRF4
nsEx2609, *nsEx2610*, *nsEx2611*, *nsEx2612*	pGO47, pRF4
nsEx2626, *nsEx2627*, *nsEx2628*, *nsEx2629*,	pGO56, pRF4
nsEx2747, *nsEx2748*, *nsEx2749*	pGO73, pRF4
nsEx2838, *nsEx2839*, *nsEx2840*	pGO91, pRF4
nsEx2874, *nsEx2875*, *nsEx2876*	pGO116, pGO93
nsEx2750, nsEx2751, nsEx2752, nsEx2760, nsEx2761, nsEx2762, nsEx2763, nsEx2764, nsEx2765, nsEx2766, nsEx2767, nsEx2768	*T02B11.3*pro::GFP, *gcy-5*pro::mCherry, pEP51
nsEx2373, nsEx2374, nsEx2375, nsEx2376	*snx-1* genomic region, pMH135
nsEx2558, nsEx2559, nsEx2560, nsEx2561	pGO35 (single digest), pMH135
nsEx2562, nsEx2563, nsEx2564, nsEx2565	pGO39, pMH135
nsEx2566, nsEx2567, nsEx2568, nsEx2569	pGO41, pMH135
nsEx2630, nsEx2631, nsEx2632	pGO54, pRF4
nsEx3006, nsEx3007, nsEx3008, nsEx3009	pGO127, pMH135

Plasmid construction

Table 6.2: Plasmids used in these studies. All pGO constructs were made using pPD95.75 (Andrew Fire) as a backbone, unless otherwise noted.

Plasmid	Description	Details
pGO1	*lit-1* genomic region	8.2 kb genomic region that includes the lit-1 locus (W06F12.1b.1 transcript) with a 2.1 kb promoter region and a 637 bp 3'UTR (SalI/AflII) Forward primer: gtcgaccgatttttttcacg Reverse primer: gtgaaagaactcggtagtattggcac
pGO2	*lit-1*(*ns132*) genomic region	Same as pGO1 but amplified from the *lit-1*(*ns132*) strain
pGO6	*lit-1*pro::NLS-GFP	*lit-1*pro consists of 2.5 kb upstream of the *lit-1* start site (W06F12.1b.1 transcript) (SphI/BamHI). Cloned in pPD95.69 (Andrew Fire)
pGO8	*lit-1*pro::LIT-1	*lit-1* cDNA (yk1457b04) a gift from Yuji Kohara (AgeI/EcoRI)
pGO10	*lin-26myo-2*pro::LIT-1	The e1 *lin-26* promoter fragment (Landmann et al., 2004) fused to the *myo-2* minpro (Okkema et al., 1993) (a gift from Maxwell G. Heiman (Heiman and Shaham, 2009) (SphI/XbaI),
pGO17	*lit-1*pro::NLS-RFP	see pGO6
pGO18	*dyf-7*pro::LIT-1	*dyf-7*pro (SphI/XmaI) a gift from Maxwell G. Heiman (Heiman and Shaham, 2009), driving the *lit-1* cDNA (see pGO10)
pGO20	*lin-26myo-2*pro::GFP::LIT-1	*lin-26myo-2*pro (see pGO10) driving a rescuing GFP::LIT-1 fusion
pGO32	*vap-1*pro::GFP::LIT-1	*vap-1*pro a gift from Leo Liu. See also (Perens and Shaham, 2005)
pGO35	*snx-1*pro::SNX-1::*snx-1* 3'UTR	0.8 kb region of promoter and 0.6 kb 3'UTR
pGO38	*T02B11.3*pro::GFP::LIT-1	*T02B11.3*pro a gift from Maya Tevlin (Wang et al., 2008)
pGO39	*T02B11.3*pro::SNX-1::*snx-1* 3'UTR	
pGO41	*lin-26myo-2*pro::SNX-1::*snx-1* 3'UTR	
pGO47	*T02B11.3*pro::GFP::LIT-1Q437Stop	The *lit-1* cDNA truncated at Q437
pGO54	*T02B11.3*pro::GFP::SNX-1::*snx-1* 3'UTR	GFP fused to SNX-1

pGO56	*T02B11.3*pro::GFP::LIT-1Ct	GFP fused to the carboxy-terminal domain of LIT-1 (last 103aa, EEGRLRFH...PPSPQAW)
pGO73	*T02B11.3*pro::GFP::LIT-1ΔCt	GFP fused to *lit-1* cDNA truncated at L359
pGO87	pLexA-N::LIT-1Ct	LexA fused to the carboxy-terminal domain of LIT-1 (last 103aa, EEGRLRFH...PPSPQAW)
pGO91	*T02B11.3*pro::GFP::MOM-4	GFP fused to *mom-4* cDNA (yk1072f05), a gift from Yuji Kohara
pGO93	*pha-4*pro::mCherry	*pha-4*pro a gift from Maxwell G. Heiman
pGO116	*T02B11.3*pro::GFP::ACT-4	GFP fused to *act-4* cDNA
pGO119	*Ac*::MYC::WSP-1	myc tagged *wsp-1* cDNA in the pAc, Drosophila actin 5c promoter vector, a gift from Michael Chiorazzi; see (Han et al., 1989)
pGO120	T02B11.3pro::mEos::ACT-4	mEos a gift from Loren L Looger. See (Mckinney et al., 2009)
pGO123	*Ac::*HA::eGFP::LIT-1	See pGO119. eGFP a gift from Maya Bader
pGO127	*lin-26myo-2*pro::LIT-1(K97G)	same as pGO10 but with the kinase activity of LIT-1 abrogated
pGO131	*T02B11.3*pro::GFP::ACT-1	
pRF4	*rol-6*(*su1006*)	from (Mello et al., 1991)
pMH135	*pha-4*pro::GFP	a gift from Maxwell G. Heiman (Heiman and Shaham, 2009)
pEP51	*unc-122*pro::GFP	coelomocyte marker
	*T02B11.3*pro::GFP	a gift from Maya Tevlin (Wang et al., 2008)
	*ptr-10*pro::NLS-RFP	from (Yoshimura et al., 2008)
	*vap-1*pro::GFP	*vap-1*pro a gift from Leo Liu. See also (Perens and Shaham, 2005)
	*gcy-5*pro::mCherry	*gcy-5*pro after (Yu et al., 1997)

Dye-filling assay

Animals were washed off NGM plates with M9 buffer, resuspended in a solution of 10µg/mL of DiI (1,1'-dioctadecyl-3,3,3',3'-tetramethylindocarbocyanine perchlorate)(Invitrogen D282), and rotated in the dark for 1.5 h at room temperature. Animals were then transferred to a fresh NGM plate, anesthetized with 20 mM sodium azide, and observed using a dissecting microscope equipped with epifluorescence.

Animals in which none of the amphid neurons filled with dye were scored as dye-filling defective (Dyf). For the sensitized dye-filling assay 1 μg/mL of DiI was used, and the incubation time was 15 min. Animals were scored as dye-filling defective (Dyf) if either one or two amphids failed to fill.

Transmission electron microscopy (EM) (performed by Yun Lu)

Previously described conventional fixation methods were used for adult animals (Perens and Shaham, 2005). High-pressure fixation was used for embryos and some adult animals. Briefly, samples were frozen using the Leica High Pressure Freezer EM-PACT2 (pressure of 18,000 bar, cooling rate of 20,000 °C/sec). Freeze substitution was performed using the Leica EM AFS2 Automatic Freeze Substitution System (McDonald, 2007). Ultrathin serial sections (60 nm) were cut using a REICHERT Ultra-Cut-E ultramicrotome and collected on Pioloform-coated single-slot copper grids. EM images for every other section were acquired using an FEI Tecnai G2 Spirit BioTwin transmission electron microscope operating at 80 kV with a Gatan 4K x 4K digital camera.

Fluorescence Electron Microscopy (fEM) (Performed by Shigeki Watanabe)

Sample preparation: *C. elegans* animals expressing mEos2::ACT-4 (Mckinney et al., 2009) were prepared for fEM as previously described (Watanabe et al., 2011). Transgenic animals were raised in the dark and adults were rapidly frozen together with bacteria, as a cryoprotectant, using a high-pressure freezer (Bal-Tec, HM010). Frozen samples were transferred under liquid nitrogen into cryovials containing 0.1% potassium

permanganate (EMS) + 0.001% osmium tetroxide (EMS, crystals) in 95% acetone. Freeze-substitution and subsequent plastic embedding were carried out in an automated freeze-substitution unit as follows: -90°C for 30 h, 5°C/h to -30°C, -30°C for 2 h for the freeze-substitution and -30°C for 48 h for the plastic embedding. Fixatives were washed out with 95% ethanol 6 times over 2 h. Animals were then infiltrated with glycol methacrylate (GMA) solutions in three steps: 30% for 5 h, 70% for 6 h, and 100% overnight. Specimens were moved to a cap of polypropylene BEEM capsules (EBSciences), and the plastic media was exchanged with freshly mixed and pre-cooled GMA three times over a period of 6 h. At the last step of the exchange, animals were separated from the bacteria using tweezers (EMS, #5), and GMA media containing 0.15% of N,N-Dimethyl-p-toluidine (Sigma-Aldrich) was added for polymerization. Polymerization was complete after 12 h. Plastic blocks were stored in a vacuum bag at -20°C until imaging.

Protein localization by fEM (Watanabe et al., 2011): Serial sections (80 nm) were collected onto pre-cleaned coverslips. For fluorescence nanoscopy, photo-activated localization microscopy (PALM; Zeiss, PAL-M, Prototype Serial No. 2701000005) was employed. The region of interest was screened using wide-field illumination. Just prior to PALM imaging, 250 nm gold nanoparticles (Microspheres-Nanospheres), which serve as fiduciary markers, were applied to the sections for 4 min. Then, 3500-5000 frames with an exposure time of 50 ms/frame were collected while stochastically photo-converting mEos signals with 1 μW of a 405 nm laser. For EM imaging, sections were then stained with 2.5% uranyl acetate (EMS) in water, and a thin layer of carbon was applied. Back-scattered electrons were collected using a scanning electron microscope

(FEI, nova nano) and a high contrast solid-state detector (FEI, vCD). Fluorescence and electron micrographs were aligned based on the gold fiduciary markers.

Fluorescence microscopy and image analysis

All images were acquired using a DeltaVision Image Restoration Microscope (Applied Precision) equipped with a 60X/NA 1.42 Plan Apo N oil immersion objective (Olympus) and a Photometrics CoolSnap camera (Roper Scientific), except for panel 3.15B for which an Upright Axioplan LSM 510 laser scanning confocal microscope (Zeiss) equipped with a C-Apochromat 40x/NA 1.2 objective was used. Acquisition, deconvolution and analysis of images from the DeltaVision system were performed with Softworx (Applied Precision); images from the confocal microscope were acquired and analyzed using LSM 510 (Zeiss).

***lit-1* cosmid rescue**

ns132 was mapped using single nucleotide polymorphism mapping ((Wicks et al., 2001)) to the right arm of Chromosome III. Transgenic *ns132*; *daf-6(e1377)* animals carrying extrachromosomal arrays of cosmids from this region provided by the Sanger Center, Cambridge, UK, were generated.

Yeast two-hybrid screen

LexA::LIT-1Ct was used as bait in a Y2H screen using the DUALhybrid kit (Dualsystems Biotech) in conjunction with the *C. elegans* Y2H cDNA library (Dualsystems Biotech), as described by the manufacturer. For the growth assay, cultures growing on Synthetic Complete Dextrose –Tryptophan, -Leucine (SCD –WL) plates

were resuspended in water to OD_{660} = 0.1. 5 µL of each culture were seeded on SCD –WL plates and SCD –WL, –Histidine (H) plates + 1 mM 3AT (3-amino-1,2,4-triazole) to select for HIS3 expression. β-galactosidase assay was performed using a yeast β-galactosidase assay kit (Thermo Scientific).

Protein Interaction Studies

Drosophila S2 cells (Invitrogen), cultured at 25°C, were tranfected with FuGene HD (Roche), incubated for 3 days, and lysed in 1 mL of IP buffer (60 mM Tris HCl, pH 8.0, 1% Tergitol type NP-40 (Sigma), 10% glycerol, 1 x Complete protease inhibitor cocktail (Roche), 1 x PhoStop phosphatase inhibitor cocktail (Roche)). 100 µL of lysate was stored on ice as input. Immunoprecipitation was performed with the remaining lysate for 2 h at 4°C, using goat anti-myc-conjugated agarose beads (Genetex). Immunoprecipitated complexes were released from the beads with 100 µL of sample buffer (same as IP buffer with the addition of 2% sodium dodecylsulfate (SDS), 0.1M Dithiothreitol (DTT) and 0.01% bromophenol blue). Samples were analyzed on NuPage 4%–12% Bis-Tris gels (Invitrogen). Immunoblotting was performed using rat monoclonal anti-HA 3F10 coupled to horseradish peroxidase (HRP) (Roche), 1:2,000; rabbit polyclonal anti-myc (AbCam) 1:5,000; goat polyclonal anti-rabbit coupled to HRP (Pierce), 1:2,000.

Appendix

Summary

This appendix includes electron micrographs at the level of the amphid sensory compartment of *daf-6*(*n1543*) adult animals. As discussed in Chapter 2, *n1543* animals display less bloating and a broader range of phenotypes than animals carrying the stronger *e1377* allele of *daf-6*; indeed the cilia being exposed to the environment in many cases. The fact that these mutants fail to dye-fill suggests that the dye-filling phenotype can be separated from the opening of the sensory compartment, and could thus reflect defects in the physiology of the neurons.

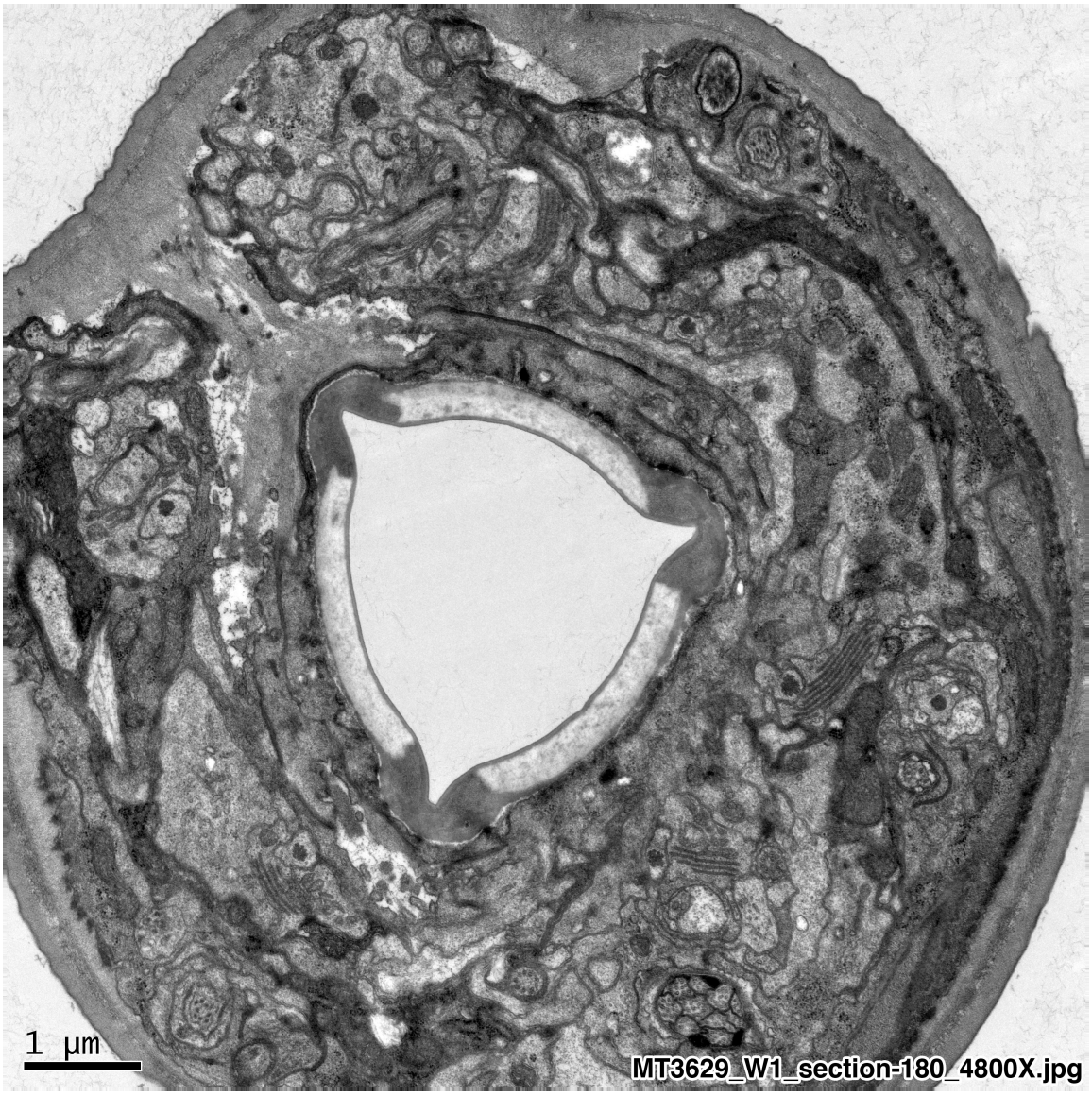
1 µm
MT3629_W1_section-180_4800X.jpg

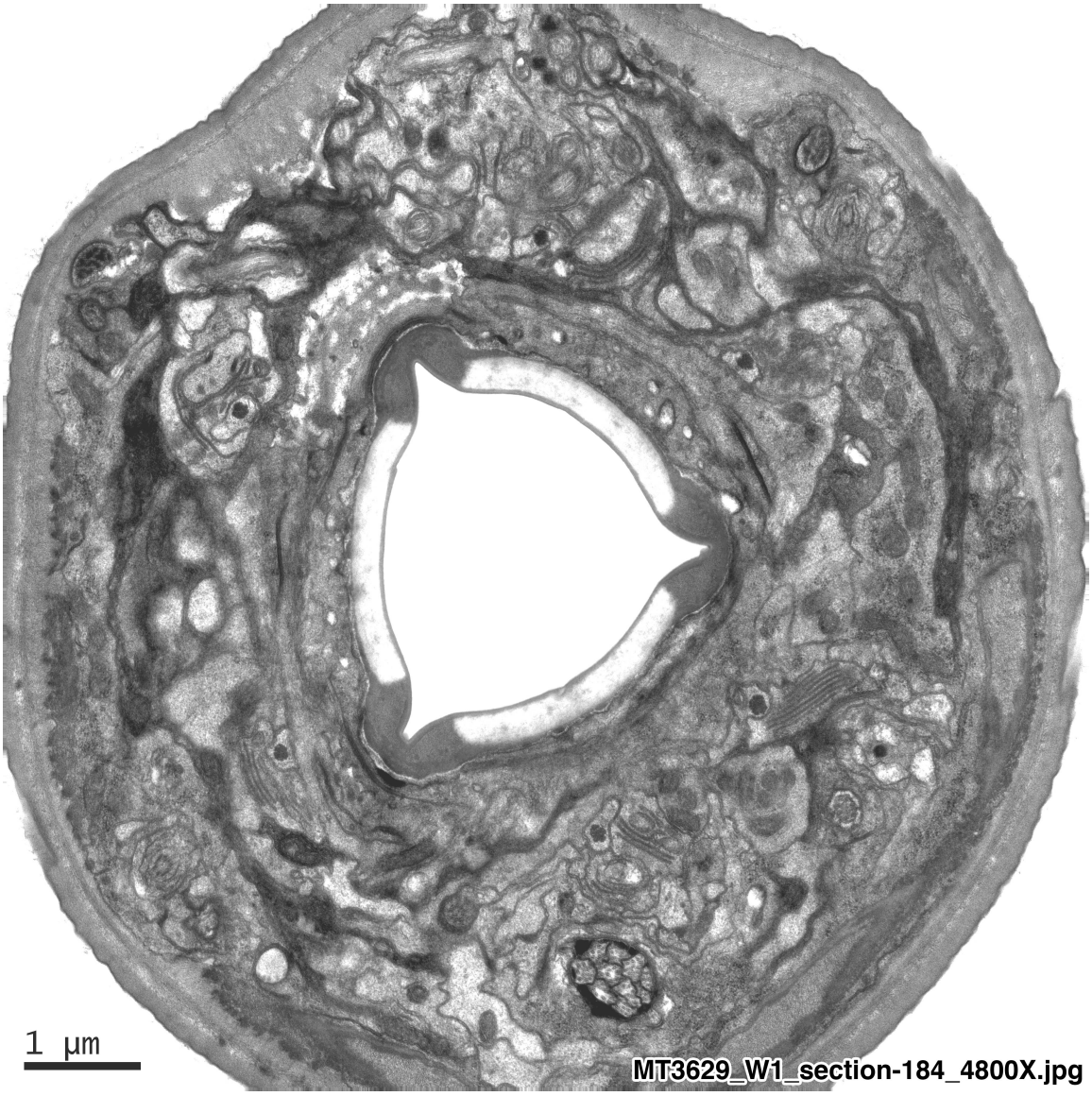
1 µm
MT3629_W1_section-184_4800X.jpg


2µm
MT3629_W1_section-174_4800X.jpg

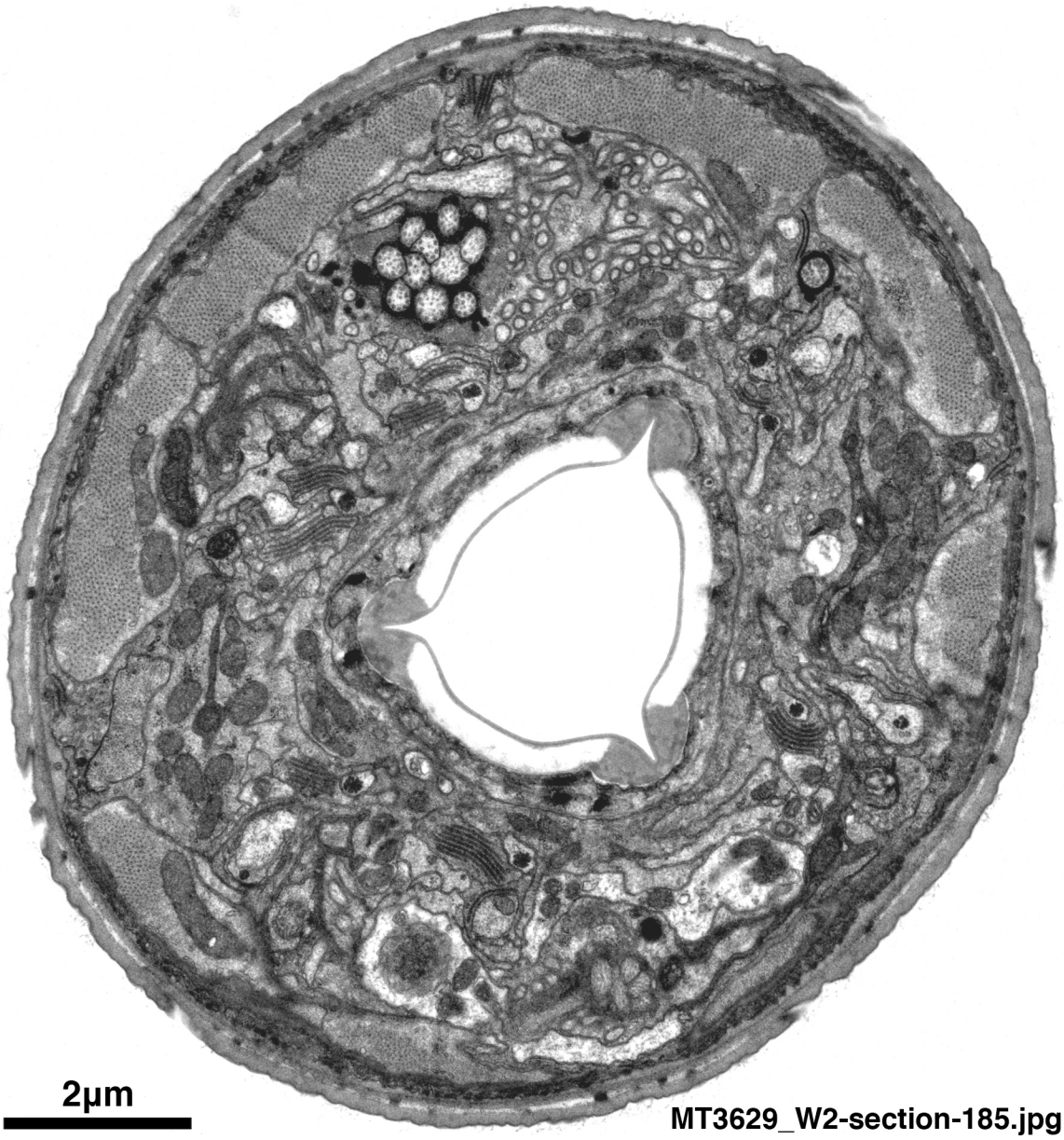
2µm
MT3629_W2-section-185.jpg

References

Albert, P. S., Brown, S. J., and Riddle, D. L. (1981). Sensory control of dauer larva formation in *Caenorhabditis elegans*. J. Comp. Neurol. *198*, 435-451.

Albert, P. S., and Riddle, D. L. (1983). Developmental alterations in sensory neuroanatomy of the *Caenorhabditis elegans* dauer larva. J Comp Neurol *219*, 461-481.

Araújo, S. J., Aslam, H., Tear, G., and Casanova, J. (2005). mummy/cystic encodes an enzyme required for chitin and glycan synthesis, involved in trachea, embryonic cuticle and CNS development--analysis of its role in *Drosophila* tracheal morphogenesis. Dev Biol *288*, 179-193.

Auld, V. J., Fetter, R. D., Broadie, K., and Goodman, C. S. (1995). Gliotactin, a novel transmembrane protein on peripheral glia, is required to form the blood-nerve barrier in *Drosophila*. Cell *81*, 757-767.

Bacaj, T., Tevlin, M., Lu, Y., and Shaham, S. (2008). Glia are essential for sensory organ function in *C. elegans*. Science *322*, 744-747.

Bacon, C., Lakics, V., Machesky, L., and Rumsby, M. (2007). N-WASP regulates extension of filopodia and processes by oligodendrocyte progenitors, oligodendrocytes, and Schwann cells-implications for axon ensheathment at myelination. Glia *55*, 844-858.

Baker, N. E., Mlodzik, M., and Rubin, G. M. (1990). Spacing differentiation in the developing *Drosophila* eye: a fibrinogen-related lateral inhibitor encoded by scabrous. Science *250*, 1370-1377.

Banerjee, S., and Bhat, M. A. (2007). Neuron-glial interactions in blood-brain barrier formation. Annu Rev Neurosci *30*, 235-258.

Bänziger, C., Soldini, D., Schütt, C., Zipperlen, P., Hausmann, G., and Basler, K. (2006). Wntless, a conserved membrane protein dedicated to the secretion of Wnt proteins from signaling cells. Cell *125*, 509-522.

Bargmann, C. I. (2006). Chemosensation in *C. elegans*. WormBook: the online review of *C. elegans* biology 1-29.

Barres, B. A. (2008). The mystery and magic of glia: a perspective on their roles in health and disease. Neuron *60*, 430-440.

Bartscherer, K., Pelte, N., Ingelfinger, D., and Boutros, M. (2006). Secretion of Wnt ligands requires Evi, a conserved transmembrane protein. Cell *125*, 523-533.

Baumgartner, S., Littleton, J. T., Broadie, K., Bhat, M. A., Harbecke, R., Lengyel, J. A., Chiquet-Ehrismann, R., Prokop, A., and Bellen, H. J. (1996). A *Drosophila* neurexin is required for septate junction and blood-nerve barrier formation and function. Cell *87*, 1059-1068.

Bayless, K. J., and Davis, G. E. (2002). The Cdc42 and Rac1 GTPases are required for capillary lumen formation in three-dimensional extracellular matrices. J Cell Sci *115*, 1123-1136.

Bayless, K. J., Salazar, R., and Davis, G. E. (2000). RGD-dependent vacuolation and lumen formation observed during endothelial cell morphogenesis in three-dimensional fibrin matrices involves the alpha(v)beta(3) and alpha(5)beta(1) integrins. Am J Pathol *156*, 1673-1683.

Behr, M., Riedel, D., and Schuh, R. (2003). The claudin-like megatrachea is essential in septate junctions for the epithelial barrier function in *Drosophila*. Dev Cell *5*, 611-620.

Belenkaya, T. Y., Wu, Y., Tang, X., Zhou, B., Cheng, L., Sharma, Y. V., Yan, D., Selva, E. M., and Lin, X. (2008). The retromer complex influences Wnt secretion by recycling wntless from endosomes to the trans-Golgi network. Dev Cell *14*, 120-131.

Bell, J., Bolanowski, S., and Holmes, M. H. (1994). The structure and function of Pacinian corpuscles: a review. Prog. Neurobiol. *42*, 79-128.

Berry, K. L., Bülow, H. E., Hall, D. H., and Hobert, O. (2003). A *C. elegans* CLIC-like protein required for intracellular tube formation and maintenance. Science *302*, 2134-2137.

Bertrand, V., and Hobert, O. (2009). Linking asymmetric cell division to the terminal differentiation program of postmitotic neurons in *C. elegans*. Dev Cell *16*, 563-575.

Bhat, M. A. (2003). Molecular organization of axo-glial junctions. Curr Opin Neurobiol *13*, 552-559.

Bilder, D., Schober, M., and Perrimon, N. (2003). Integrated activity of PDZ protein complexes regulates epithelial polarity. Nat Cell Biol *5*, 53-58.

Bonifacino, J. S., and Hurley, J. H. (2008). Retromer. Curr Opin Cell Biol *20*, 427-436.

Braid, L. R., Lee, W., Uetrecht, A. C., Swarup, S., Papaianni, G., Heiler, A., and Verheyen, E. M. (2010). Nemo phosphorylates Even-skipped and promotes Eve-mediated repression of odd-skipped in even parasegments during *Drosophila* embryogenesis. Dev Biol *343*, 178-189.

Brenner, S. (1974). The genetics of *Caenorhabditis elegans*. Genetics *77*, 71-94.

Brott, B. K., Pinsky, B. A., and Erikson, R. L. (1998). Nlk is a murine protein kinase related to Erk/MAP kinases and localized in the nucleus. Proc. Natl. Acad. Sci. USA *95*, 963-968.

Brown, K. E., and Freeman, M. (2003). Egfr signalling defines a protective function for ommatidial orientation in the *Drosophila* eye. Development *130*, 5401-5412.

Bryant, D. M., and Mostov, K. E. (2008). From cells to organs: building polarized tissue. Nat Rev Mol Cell Biol *9*, 887-901.

Buechner, M. (2002). Tubes and the single *C. elegans* excretory cell. Trends Cell Biol. *12*, 479-484.

Buechner, M., Hall, D. H., Bhatt, H., and Hedgecock, E. M. (1999). Cystic canal mutants in *Caenorhabditis elegans* are defective in the apical membrane domain of the renal (excretory) cell. Dev Biol *214*, 227-241.

Bundgaard, M., and Abbott, N. J. (2008). All vertebrates started out with a glial blood-brain barrier 4-500 million years ago. Glia *56*, 699-708.

Burkitt, G. H., Young, B., and Heath, J. W. (1993). Wheater's Functional Histology: A Text and Colour Atlas (New York: Churchill Livinstone).

Bushong, E. A., Martone, M. E., and Ellisman, M. H. (2004). Maturation of astrocyte morphology and the establishment of astrocyte domains during postnatal hippocampal development. Int J Dev Neurosci *22*, 73-86.

Bushong, E. A., Martone, M. E., Jones, Y. Z., and Ellisman, M. H. (2002). Protoplasmic astrocytes in CA1 stratum radiatum occupy separate anatomical domains. J Neurosci *22*, 183-192.

Campellone, K. G., and Welch, M. D. (2010). A nucleator arms race: cellular control of actin assembly. Nat Rev Mol Cell Biol *11*, 237-251.

Cassada, R. C., and Russell, R. L. (1975). The dauerlarva, a post-embryonic developmental variant of the nematode *Caenorhabditis elegans*. Dev. Biol. *46*, 326-342.

Chan, J. R., Jolicoeur, C., Yamauchi, J., Elliott, J., Fawcett, J. P., Ng, B. K., and Cayouette, M. (2006). The polarity protein Par-3 directly interacts with p75NTR to regulate myelination. Science *314*, 832-836.

Choi, K. W., and Benzer, S. (1994). Rotation of photoreceptor clusters in the developing *Drosophila* eye requires the *nemo* gene. Cell *78*, 125-136.

Chou, Y. H., and Chien, C. T. (2002). Scabrous controls ommatidial rotation in the *Drosophila* compound eye. Dev Cell *3*, 839-850.

Cook, B., Hardy, R. W., McConnaughey, W. B., and Zuker, C. S. (2008). Preserving cell shape under environmental stress. Nature *452*, 361-364.

Cory, G. O., Cramer, R., Blanchoin, L., and Ridley, A. J. (2003). Phosphorylation of the WASP-VCA domain increases its affinity for the Arp2/3 complex and enhances actin polymerization by WASP. Mol. Cell *11*, 1229-1239.

Cosgaya, J. M., Chan, J. R., and Shooter, E. M. (2002). The neurotrophin receptor p75NTR as a positive modulator of myelination. Science *298*, 1245-1248.

Coudreuse, D. Y., Roël, G., Betist, M. C., Destrée, O., and Korswagen, H. C. (2006). Wnt gradient formation requires retromer function in Wnt-producing cells. Science *312*, 921-924.

Cullen, P. J. (2008). Endosomal sorting and signalling: an emerging role for sorting nexins. Nat Rev Mol Cell Biol *9*, 574-582.

Datta, A., Bryant, D. M., and Mostov, K. E. (2011). Molecular regulation of lumen morphogenesis. Current Biology *21*, R126-36.

Davis, G. E., and Camarillo, C. W. (1996). An alpha 2 beta 1 integrin-dependent pinocytic mechanism involving intracellular vacuole formation and coalescence regulates capillary lumen and tube formation in three-dimensional collagen matrix. Exp Cell Res *224*, 39-51.

Derry, J. M., Ochs, H. D., and Francke, U. (1994). Isolation of a novel gene mutated in Wiskott-Aldrich syndrome. Cell *79*, following 922.

Desai, C., Garriga, G., McIntire, S. L., and Horvitz, H. R. (1988). A genetic pathway for the development of the *Caenorhabditis elegans* HSN motor neurons. Nature *336*, 638-646.

Devine, W. P., Lubarsky, B., Shaw, K., Luschnig, S., Messina, L., and Krasnow, M. A. (2005). Requirement for chitin biosynthesis in epithelial tube morphogenesis. Proc Natl Acad Sci USA *102*, 17014-17019.

Doherty, J., Logan, M. A., Taşdemir, O. E., and Freeman, M. R. (2009). Ensheathing glia function as phagocytes in the adult *Drosophila* brain. J Neurosci *29*, 4768-4781.

Drenckhahn, D., and Mannherz, H. G. (1983). Distribution of actin and the actin-associated proteins myosin, tropomyosin, alpha-actinin, vinculin, and villin in rat and bovine exocrine glands. Eur. J. Cell Biol. *30*, 167-176.

Dugas, J. C., Tai, Y. C., Speed, T. P., Ngai, J., and Barres, B. A. (2006). Functional genomic analysis of oligodendrocyte differentiation. J Neurosci *26*, 10967-10983.

Dyson, S. E., Jones, D. G., and Kendrick, W. L. (1976). Some observations on the ultrastructure of developing rat cerebral capillaries. Cell Tissue Res *173*, 529-542.

Eisenmann, D. M. (2005). Wnt signaling. WormBook: the online review of *C. elegans* biology 1-17.

Eisenmann, D. M., and Kim, S. K. (2000). Protruding vulva mutants identify novel loci and Wnt signaling factors that function during *Caenorhabditis elegans* vulva development. Genetics *156*, 1097-1116.

Eitzen, G., Wang, L., Thorngren, N., and Wickner, W. (2002). Remodeling of organelle-bound actin is required for yeast vacuole fusion. J. Cell Biol. *158*, 669-679.

Emery, B. (2010). Regulation of oligodendrocyte differentiation and myelination. Science *330*, 779-782.

Esposito, G., Di Schiavi, E., Bergamasco, C., and Bazzicalupo, P. (2007). Efficient and cell specific knock-down of gene function in targeted *C. elegans* neurons. Gene *395*, 170-176.

Etienne-Manneville, S., and Hall, A. (2002). Rho GTPases in cell biology. Nature *420*, 629-635.

Faivre-Sarrailh, C., Banerjee, S., Li, J., Hortsch, M., Laval, M., and Bhat, M. A. (2004). *Drosophila* contactin, a homolog of vertebrate contactin, is required for septate junction organization and paracellular barrier function. Development *131*, 4931-4942.

Ferguson, E. L., and Horvitz, H. R. (1985). Identification and characterization of 22 genes that affect the vulval cell lineages of the nematode *Caenorhabditis elegans*. Genetics *110*, 17-72.

Fernandez-Valle, C., Gorman, D., Gomez, A. M., and Bunge, M. B. (1997). Actin plays a role in both changes in cell shape and gene-expression associated with Schwann cell myelination. J Neurosci *17*, 241-250.

Fiehler, R. W., and Wolff, T. (2008). Nemo is required in a subset of photoreceptors to regulate the speed of ommatidial rotation. Dev Biol *313*, 533-544.

Folkman, J., and Haudenschild, C. (1980). Angiogenesis in vitro. Nature *288*, 551-556.

Franch-Marro, X., Wendler, F., Guidato, S., Griffith, J., Baena-Lopez, A., Itasaki, N., Maurice, M. M., and Vincent, J. P. (2008). Wingless secretion requires endosome-to-Golgi retrieval of Wntless/Evi/Sprinter by the retromer complex. Nat Cell Biol *10*, 170-177.

Freeman, M. R., and Doherty, J. (2006). Glial cell biology in *Drosophila* and vertebrates. Trends Neurosci *29*, 82-90.

Fuentes-Medel, Y., Logan, M. A., Ashley, J., Ataman, B., Budnik, V., and Freeman, M. R. (2009). Glia and muscle sculpt neuromuscular arbors by engulfing destabilized synaptic boutons and shed presynaptic debris. PLoS Biol *7*, e1000184.

Gaengel, K., and Mlodzik, M. (2003). Egfr signaling regulates ommatidial rotation and cell motility in the *Drosophila* eye via MAPK/Pnt signaling and the Ras effector Canoe/AF6. Development *130*, 5413-5423.

Galletta, B. J., Mooren, O. L., and Cooper, J. A. (2010). Actin dynamics and endocytosis in yeast and mammals. Curr. Opin. Biotechnol. *21*, 604-610.

Galliot, B., de Vargas, C., and Miller, D. (1999). Evolution of homeobox genes: Q50 Paired-like genes founded the Paired class. Dev Genes Evol *209*, 186-197.

Gao, J., Estrada, L., Cho, S., Ellis, R. E., and Gorski, J. L. (2001). The *Caenorhabditis elegans* homolog of FGD1, the human Cdc42 GEF gene responsible for faciogenital dysplasia, is critical for excretory cell morphogenesis. Human Molecular Genetics *10*, 3049-3062.

Gasman, S., Chasserot-Golaz, S., Malacombe, M., Way, M., and Bader, M. F. (2004). Regulated exocytosis in neuroendocrine cells: a role for subplasmalemmal Cdc42/N-WASP-induced actin filaments. Mol. Biol. Cell *15*, 520-531.

Gassama-Diagne, A., Yu, W., ter Beest, M., Martin-Belmonte, F., Kierbel, A., Engel, J., and Mostov, K. (2006). Phosphatidylinositol-3,4,5-trisphosphate regulates the formation of the basolateral plasma membrane in epithelial cells. Nat Cell Biol *8*, 963-970.

Genoud, C., Quairiaux, C., Steiner, P., Hirling, H., Welker, E., and Knott, G. W. (2006). Plasticity of astrocytic coverage and glutamate transporter expression in adult mouse cortex. PLoS Biol *4*, e343.

Ghabrial, A., Luschnig, S., Metzstein, M. M., and Krasnow, M. A. (2003). Branching morphogenesis of the *Drosophila* tracheal system. Annu Rev Cell Dev Biol *19*, 623-647.

Göbel, V., Barrett, P. L., Hall, D. H., and Fleming, J. T. (2004). Lumen morphogenesis in *C. elegans* requires the membrane-cytoskeleton linker erm-1. Dev Cell *6*, 865-873.

Goley, E. D., and Welch, M. D. (2006). The ARP2/3 complex: an actin nucleator comes of age. Nat Rev Mol Cell Biol *7*, 713-726.

Granderath, S., Stollewerk, A., Greig, S., Goodman, C. S., O'Kane, C. J., and Klämbt, C. (1999). loco encodes an RGS protein required for *Drosophila* glial differentiation. Development *126*, 1781-1791.

Green, J. L., Inoue, T., and Sternberg, P. W. (2008). Opposing Wnt pathways orient cell polarity during organogenesis. Cell *134*, 646-656.

Griffin, J. W., and Thompson, W. J. (2008). Biology and pathology of nonmyelinating Schwann cells. Glia *56*, 1518-1531.

Halassa, M. M., Fellin, T., Takano, H., Dong, J. H., and Haydon, P. G. (2007). Synaptic islands defined by the territory of a single astrocyte. J Neurosci *27*, 6473-6477.

Halassa, M. M., and Haydon, P. G. (2010). Integrated brain circuits: astrocytic networks modulate neuronal activity and behavior. Annu Rev Physiol *72*, 335-355.

Han, K., Levine, M. S., and Manley, J. L. (1989). Synergistic activation and repression of transcription by *Drosophila* homeobox proteins. Cell *56*, 573-583.

Hansel, D. E., Eipper, B. A., and Ronnett, G. V. (2001). Neuropeptide Y functions as a neuroproliferative factor. Nature *410*, 940-944.

Harris, J., Honigberg, L., Robinson, N., and Kenyon, C. (1996). Neuronal cell migration in *C. elegans*: regulation of Hox gene expression and cell position. Development *122*, 3117-3131.

Hartenstein, V., and Posakony, J. W. (1989). Development of adult sensilla on the wing and notum of *Drosophila melanogaster*. Development *107*, 389-405.

Hartline, D. K., and Colman, D. R. (2007). Rapid conduction and the evolution of giant axons and myelinated fibers. Current Biology *17*, R29-35.

Hedgecock, E. M., Culotti, J. G., and Hall, D. H. (1990). The *unc-5*, *unc-6*, and *unc-40* genes guide circumferential migrations of pioneer axons and mesodermal cells on the epidermis in *C. elegans*. Neuron *4*, 61-85.

Heiman, M. G., and Shaham, S. (2007). Ancestral roles of glia suggested by the nervous system of *Caenorhabditis elegans*. Neuron Glia Biol *3*, 55-61.

Heiman, M. G., and Shaham, S. (2009). DEX-1 and DYF-7 establish sensory dendrite length by anchoring dendritic tips during cell migration. Cell *137*, 344-355.

Herman, M. (2001). *C. elegans* POP-1/TCF functions in a canonical Wnt pathway that controls cell migration and in a noncanonical Wnt pathway that controls cell polarity. Development *128*, 581-590.

Herman, M. A., and Horvitz, H. R. (1994). The *Caenorhabditis elegans* gene *lin-44* controls the polarity of asymmetric cell divisions. Development *120*, 1035-1047.

Herman, R. K. (1987). Mosaic analysis of two genes that affect nervous system structure in *Caenorhabditis elegans*. Genetics *116*, 377-388.

Hierro, A., Rojas, A. L., Rojas, R., Murthy, N., Effantin, G., Kajava, A. V., Steven, A. C., Bonifacino, J. S., and Hurley, J. H. (2007). Functional architecture of the retromer cargo-recognition complex. Nature *449*, 1063-1067.

Higgs, H. N., and Pollard, T. D. (2001). Regulation of actin filament network formation through ARP2/3 complex: activation by a diverse array of proteins. Annu Rev Biochem *70*, 649-676.

Huang, S., Shetty, P., Robertson, S. M., and Lin, R. (2007). Binary cell fate specification during *C. elegans* embryogenesis driven by reiterated reciprocal asymmetry of TCF POP-1 and its coactivator beta-catenin SYS-1. Development *134*, 2685-2695.

Husain, N., Pellikka, M., Hong, H., Klimentova, T., Choe, K. M., Clandinin, T. R., and Tepass, U. (2006). The agrin/perlecan-related protein eyes shut is essential for epithelial lumen formation in the *Drosophila* retina. Dev Cell *11*, 483-493.

Iden, S., and Collard, J. G. (2008). Crosstalk between small GTPases and polarity proteins in cell polarization. Nat Rev Mol Cell Biol *9*, 846-859.

Ishitani, T., Hirao, T., Suzuki, M., Isoda, M., Ishitani, S., Harigaya, K., Kitagawa, M., Matsumoto, K., and Itoh, M. (2010). Nemo-like kinase suppresses Notch signalling by interfering with formation of the Notch active transcriptional complex. Nat. Cell Biol. *12*, 278-285.

Ishitani, T., Ninomiya-Tsuji, J., Nagai, S., Nishita, M., Meneghini, M., Barker, N., Waterman, M., Bowerman, B., Clevers, H., Shibuya, H., and Matsumoto, K. (1999). The TAK1-NLK-MAPK-related pathway antagonizes signalling between beta-catenin and transcription factor TCF. Nature *399*, 798-802.

Kaletta, T., Schnabel, H., and Schnabel, R. (1997). Binary specification of the embryonic lineage in *Caenorhabditis elegans*. Nature *390*, 294-298.

Kamei, M., Saunders, W. B., Bayless, K. J., Dye, L., Davis, G. E., and Weinstein, B. M. (2006). Endothelial tubes assemble from intracellular vacuoles in vivo. Nature *442*, 453-456.

Kidd, A. R., Miskowski, J. A., Siegfried, K. R., Sawa, H., and Kimble, J. (2005). A beta-catenin identified by functional rather than sequence criteria and its role in Wnt/MAPK signaling. Cell *121*, 761-772.

Kim, H. J., DiBernardo, A. B., Sloane, J. A., Rasband, M. N., Solomon, D., Kosaras, B., Kwak, S. P., and Vartanian, T. K. (2006). WAVE1 is required for oligodendrocyte morphogenesis and normal CNS myelination. J Neurosci *26*, 5849-5859.

Kim, S., Shilagardi, K., Zhang, S., Hong, S. N., Sens, K. L., Bo, J., Gonzalez, G. A., and Chen, E. H. (2007). A critical function for the actin cytoskeleton in targeted exocytosis of prefusion vesicles during myoblast fusion. Dev. Cell *12*, 571-586.

Kippert, A., Trajkovic, K., Rajendran, L., Ries, J., and Simons, M. (2007). Rho regulates membrane transport in the endocytic pathway to control plasma membrane specialization in oligodendroglial cells. J Neurosci *27*, 3560-3570.

Koga, M., Take-uchi, M., Tameishi, T., and Ohshima, Y. (1999). Control of DAF-7 TGF-(alpha) expression and neuronal process development by a receptor tyrosine kinase KIN-8 in *Caenorhabditis elegans*. Development *126*, 5387-5398.

Kortenjann, M., Nehls, M., Smith, A. J., Carsetti, R., Schüler, J., Köhler, G., and Boehm, T. (2001). Abnormal bone marrow stroma in mice deficient for nemo-like kinase, Nlk. Eur J Immunol *31*, 3580-3587.

Krause, M., Harrison, S. W., Xu, S. Q., Chen, L., and Fire, A. (1994). Elements regulating cell- and stage-specific expression of the *C. elegans* MyoD family homolog hlh-1. Dev Biol *166*, 133-148.

Kuwabara, P. E., Lee, M. H., Schedl, T., and Jefferis, G. S. (2000). A *C. elegans* patched gene, *ptc-1*, functions in germ-line cytokinesis. Genes Dev. *14*, 1933-1944.

Landmann, F., Quintin, S., and Labouesse, M. (2004). Multiple regulatory elements with spatially and temporally distinct activities control the expression of the epithelial differentiation gene *lin-26* in *C. elegans*. Dev. Biol. *265*, 478-490.

Lanzetti, L. (2007). Actin in membrane trafficking. Curr. Opin. Cell Biol. *19*, 453-458.

Lee, R. W., and Trifaró, J. M. (1981). Characterization of anti-actin antibodies and their use in immunocytochemical studies on the localization of actin in adrenal chromaffin cells in culture. Neuroscience *6*, 2087-2108.

Legan, P. K., Rau, A., Keen, J. N., and Richardson, G. P. (1997). The mouse tectorins. Modular matrix proteins of the inner ear homologous to components of the sperm-egg adhesion system. J Biol Chem *272*, 8791-8801.

Leiserson, W. M., Harkins, E. W., and Keshishian, H. (2000). Fray, a *Drosophila* serine/threonine kinase homologous to mammalian PASK, is required for axonal ensheathment. Neuron *28*, 793-806.

Liang, X., Draghi, N. A., and Resh, M. D. (2004). Signaling from integrins to Fyn to Rho family GTPases regulates morphologic differentiation of oligodendrocytes. J Neurosci *24*, 7140-7149.

Lin, K., Hsin, H., Libina, N., and Kenyon, C. (2001). Regulation of the *Caenorhabditis elegans* longevity protein DAF-16 by insulin/IGF-1 and germline signaling. Nat. Genet. *28*, 139-145.

Lin, R., Thompson, S., and Priess, J. R. (1995). pop-1 encodes an HMG box protein required for the specification of a mesoderm precursor in early *C. elegans* embryos. Cell *83*, 599-609.

Llimargas, M., Strigini, M., Katidou, M., Karagogeos, D., and Casanova, J. (2004). Lachesin is a component of a septate junction-based mechanism that controls tube size and epithelial integrity in the *Drosophila* tracheal system. Development *131*, 181-190.

Lo, M. C., Gay, F., Odom, R., Shi, Y., and Lin, R. (2004). Phosphorylation by the beta-catenin/MAPK complex promotes 14-3-3-mediated nuclear export of TCF/POP-1 in signal-responsive cells in *C. elegans*. Cell *117*, 95-106.

Lubarsky, B., and Krasnow, M. A. (2003). Tube morphogenesis: making and shaping biological tubes. Cell *112*, 19-28.

Luschnig, S., Bätz, T., Armbruster, K., and Krasnow, M. A. (2006). serpentine and vermiform encode matrix proteins with chitin binding and deacetylation domains that limit tracheal tube length in *Drosophila*. Current Biology *16*, 186-194.

Lushnikova, I., Skibo, G., Muller, D., and Nikonenko, I. (2009). Synaptic potentiation induces increased glial coverage of excitatory synapses in CA1 hippocampus. Hippocampus *19*, 753-762.

Malacombe, M., Bader, M. F., and Gasman, S. (2006). Exocytosis in neuroendocrine cells: new tasks for actin. Biochim. Biophys. Acta *1763*, 1175-1183.

Maloof, J. N., Whangbo, J., Harris, J. M., Jongeward, G. D., and Kenyon, C. (1999). A Wnt signaling pathway controls hox gene expression and neuroblast migration in *C. elegans*. Development *126*, 37-49.

Martin-Belmonte, F., Gassama, A., Datta, A., Yu, W., Rescher, U., Gerke, V., and Mostov, K. (2007). PTEN-mediated apical segregation of phosphoinositides controls epithelial morphogenesis through Cdc42. Cell *128*, 383-397.

Massarwa, R., Schejter, E. D., and Shilo, B. Z. (2009). Apical secretion in epithelial tubes of the *Drosophila* embryo is directed by the Formin-family protein Diaphanous. Dev Cell *16*, 877-888.

Matus, D. Q., Li, X. Y., Durbin, S., Agarwal, D., Chi, Q., Weiss, S. J., and Sherwood, D. R. (2010). In vivo identification of regulators of cell invasion across basement membranes. Science signaling *3*, ra35.

McDonald, K. (2007). Cryopreparation methods for electron microscopy of selected model systems. Methods Cell Biol. *79*, 23-56.

McKeown, C., Praitis, V., and Austin, J. (1998). sma-1 encodes a betaH-spectrin homolog required for *Caenorhabditis elegans* morphogenesis. Development *125*, 2087-2098.

Mckinney, S. A., Murphy, C. S., Hazelwood, K. L., Davidson, M. W., and Looger, L. L. (2009). A bright and photostable photoconvertible fluorescent protein. Nat. Methods *6*, 131.

Melendez-Vasquez, C. V., Einheber, S., and Salzer, J. L. (2004). Rho kinase regulates schwann cell myelination and formation of associated axonal domains. J Neurosci *24*, 3953-3963.

Mello, C. C., Kramer, J. M., Stinchcomb, D., and Ambros, V. (1991). Efficient gene transfer in C.elegans: extrachromosomal maintenance and integration of transforming sequences. EMBO J. *10*, 3959-3970.

Meneghini, M. D., Ishitani, T., Carter, J. C., Hisamoto, N., Ninomiya-Tsuji, J., Thorpe, C. J., Hamill, D. R., Matsumoto, K., and Bowerman, B. (1999). MAP kinase and Wnt pathways converge to downregulate an HMG-domain repressor in *Caenorhabditis elegans*. Nature *399*, 793-797.

Merino, C., Penney, J., González, M., Tsurudome, K., Moujahidine, M., O'Connor, M. B., Verheyen, E. M., and Haghighi, P. (2009). Nemo kinase interacts with Mad to

coordinate synaptic growth at the *Drosophila* neuromuscular junction. J Cell Biol *185*, 713-725.

Mi, S., Miller, R. H., Lee, X., Scott, M. L., Shulag-Morskaya, S., Shao, Z., Chang, J., Thill, G., Levesque, M., Zhang, M., Hession, C., Sah, D., Trapp, B., He, Z., Jung, V., McCoy, J. M., and Pepinsky, R. B. (2005). LINGO-1 negatively regulates myelination by oligodendrocytes. Nat Neurosci *8*, 745-751.

Michailov, G. V., Sereda, M. W., Brinkmann, B. G., Fischer, T. M., Haug, B., Birchmeier, C., Role, L., Lai, C., Schwab, M. H., and Nave, K. A. (2004). Axonal neuregulin-1 regulates myelin sheath thickness. Science *304*, 700-703.

Michaux, G., Gansmuller, A., Hindelang, C., and Labouesse, M. (2000). CHE-14, a protein with a sterol-sensing domain, is required for apical sorting in *C. elegans* ectodermal epithelial cells. Curr. Biol. *10*, 1098-1107.

Mizumoto, K., and Sawa, H. (2007a). Cortical beta-catenin and APC regulate asymmetric nuclear beta-catenin localization during asymmetric cell division in *C. elegans*. Dev. Cell. *12*, 287-299.

Mizumoto, K., and Sawa, H. (2007b). Two betas or not two betas: regulation of asymmetric division by beta-catenin. Trends Cell Biol. *17*, 465-473.

Mlodzik, M., Baker, N. E., and Rubin, G. M. (1990). Isolation and expression of scabrous, a gene regulating neurogenesis in *Drosophila*. Genes Dev *4*, 1848-1861.

Montcouquiol, M., Valat, J., Travo, C., and Sans, A. (1998). A role for BDNF in early postnatal rat vestibular epithelia maturation: implication of supporting cells. Eur J Neurosci *10*, 598-606.

Montesano, R., Matsumoto, K., Nakamura, T., and Orci, L. (1991a). Identification of a fibroblast-derived epithelial morphogen as hepatocyte growth factor. Cell *67*, 901-908.

Montesano, R., Schaller, G., and Orci, L. (1991b). Induction of epithelial tubular morphogenesis in vitro by fibroblast-derived soluble factors. Cell *66*, 697-711.

Moussian, B., Schwarz, H., Bartoszewski, S., and Nüsslein-Volhard, C. (2005). Involvement of chitin in exoskeleton morphogenesis in *Drosophila melanogaster*. J Morphol *264*, 117-130.

Mukhopadhyay, S., Lu, Y., Shaham, S., and Sengupta, P. (2008). Sensory signaling-dependent remodeling of olfactory cilia architecture in *C. elegans*. Dev Cell *14*, 762-774.

Murai, K. K., Nguyen, L. N., Irie, F., Yamaguchi, Y., and Pasquale, E. B. (2003). Control of hippocampal dendritic spine morphology through ephrin-A3/EphA4 signaling. Nat Neurosci *6*, 153-160.

Nakamura, K., Kim, S., Ishidate, T., Bei, Y., Pang, K., Shirayama, M., Trzepacz, C., Brownell, D. R., and Mello, C. C. (2005). Wnt signaling drives WRM-1/beta-catenin asymmetries in early *C. elegans* embryos. Genes Dev. *19*, 1749-1754.

Nave, K. A. (2010). Myelination and support of axonal integrity by glia. Nature *468*, 244-252.

Nelson, F. K., Albert, P. S., and Riddle, D. L. (1983). Fine structure of the *Caenorhabditis elegans* secretory-excretory system. J Ultrastruct Res *82*, 156-171.

Nelson, F. K., and Riddle, D. L. (1984). Functional study of the *Caenorhabditis elegans* secretory-excretory system using laser microsurgery. J Exp Zool *231*, 45-56.

Nestor, M. W., Mok, L. P., Tulapurkar, M. E., and Thompson, S. M. (2007). Plasticity of neuron-glial interactions mediated by astrocytic EphARs. J Neurosci *27*, 12817-12828.

Newman, E., and Reichenbach, A. (1996). The Müller cell: a functional element of the retina. Trends Neurosci *19*, 307-312.

Noordermeer, J. N., Kopczynski, C. C., Fetter, R. D., Bland, K. S., Chen, W. Y., and Goodman, C. S. (1998). Wrapper, a novel member of the Ig superfamily, is expressed by midline glia and is required for them to ensheath commissural axons in *Drosophila*. Neuron *21*, 991-1001.

Novak, N., Bar, V., Sabanay, H., Frechter, S., Jaegle, M., Snapper, S. B., Meijer, D., and Peles, E. (2011). N-WASP is required for membrane wrapping and myelination by Schwann cells. J Cell Biol *192*, 243-250.

Oberheim, N. A., Takano, T., Han, X., He, W., Lin, J. H., Wang, F., Xu, Q., Wyatt, J. D., Pilcher, W., Ojemann, J. G., Ransom, B. R., Goldman, S. A., and Nedergaard, M. (2009). Uniquely hominid features of adult human astrocytes. J Neurosci *29*, 3276-3287.

Oberheim, N. A., Wang, X., Goldman, S., and Nedergaard, M. (2006). Astrocytic complexity distinguishes the human brain. Trends Neurosci *29*, 547-553.

Ogata, K., and Kosaka, T. (2002). Structural and quantitative analysis of astrocytes in the mouse hippocampus. Neuroscience *113*, 221-233.

Ohkawara, B., Shirakabe, K., Hyodo-Miura, J., Matsuo, R., Ueno, N., Matsumoto, K., and Shibuya, H. (2004). Role of the TAK1-NLK-STAT3 pathway in TGF-beta-mediated mesoderm induction. Genes Dev. *18*, 381-386.

Okkema, P. G., Harrison, S. W., Plunger, V., Aryana, A., and Fire, A. (1993). Sequence requirements for myosin gene expression and regulation in *Caenorhabditis elegans*. Genetics *135*, 385-404.

Osterhout, D. J., Wolven, A., Wolf, R. M., Resh, M. D., and Chao, M. V. (1999). Morphological differentiation of oligodendrocytes requires activation of Fyn tyrosine kinase. J Cell Biol *145*, 1209-1218.

Pan, C. L., Baum, P. D., Gu, M., Jorgensen, E. M., Clark, S. G., and Garriga, G. (2008). *C. elegans* AP-2 and retromer control Wnt signaling by regulating mig-14/Wntless. Dev. Cell *14*, 132-139.

Park, J., Kim, Y., Lee, S., Park, J. J., Park, Z. Y., Sun, W., Kim, H., and Chang, S. (2010). SNX18 shares a redundant role with SNX9 and modulates endocytic trafficking at the plasma membrane. J Cell Sci *123*, 1742-1750.

Paul, S. M., Ternet, M., Salvaterra, P. M., and Beitel, G. J. (2003). The Na+/K+ ATPase is required for septate junction function and epithelial tube-size control in the *Drosophila* tracheal system. Development *130*, 4963-4974.

Peckol, E. L., Troemel, E. R., and Bargmann, C. I. (2001). Sensory experience and sensory activity regulate chemosensory receptor gene expression in *Caenorhabditis elegans*. Proc Natl Acad Sci USA *98*, 11032-11038.

Pereanu, W., Shy, D., and Hartenstein, V. (2005). Morphogenesis and proliferation of the larval brain glia in *Drosophila*. Dev Biol *283*, 191-203.

Perens, E. A. (2006). The roles of *daf-6* and cell-cell interactions in sensory organ morphogenesis (New York: The Rockefeller University).

Perens, E. A., and Shaham, S. (2005). *C. elegans daf-6* encodes a patched-related protein required for lumen formation. Dev. Cell *8*, 893-906.

Perkins, L. A., Hedgecock, E. M., Thomson, J. N., and Culotti, J. G. (1986). Mutant sensory cilia in the nematode *Caenorhabditis elegans*. Dev. Biol. *117*, 456-487.

Peter, B. J., Kent, H. M., Mills, I. G., Vallis, Y., Butler, P. J., Evans, P. R., and McMahon, H. T. (2004). BAR domains as sensors of membrane curvature: the amphiphysin BAR structure. Science *303*, 495-499.

Phillips, B. T., and Kimble, J. (2009). A new look at TCF and beta-catenin through the lens of a divergent *C. elegans* Wnt pathway. Dev. Cell *17*, 27-34.

Pollack, G. S., and Balakrishnan, R. (1997). Taste sensilla of flies: function, central neuronal projections, and development. Microsc Res Tech *39*, 532-546.

Pollard, T. D., and Borisy, G. G. (2003). Cellular motility driven by assembly and disassembly of actin filaments. Cell *112*, 453-465.

Port, F., Kuster, M., Herr, P., Furger, E., Bänziger, C., Hausmann, G., and Basler, K. (2008). Wingless secretion promotes and requires retromer-dependent cycling of Wntless. Nat Cell Biol *10*, 178-185.

Prasad, B. C., Ye, B., Zackhary, R., Schrader, K., Seydoux, G., and Reed, R. R. (1998). unc-3, a gene required for axonal guidance in *Caenorhabditis elegans*, encodes a member of the O/E family of transcription factors. Development *125*, 1561-1568.

Procko, C., Lu, Y., and Shaham, S. (2011). Glia delimit shape changes of sensory neuron receptive endings in *C. elegans*. Development .

Pujol, N., Bonnerot, C., Ewbank, J. J., Kohara, Y., and Thierry-Mieg, D. (2001). The *Caenorhabditis elegans unc-32* gene encodes alternative forms of a vacuolar ATPase a subunit. J. Biol. Chem. *276*, 11913-11921.

Riddle, D. L., Swanson, M. M., and Albert, P. S. (1981). Interacting genes in nematode dauer larva formation. Nature *290*, 668-671.

Rio, C., Dikkes, P., Liberman, M. C., and Corfas, G. (2002). Glial fibrillary acidic protein expression and promoter activity in the inner ear of developing and adult mice. J. Comp. Neurol. *442*, 156-162.

Rocheleau, C. E., Downs, W. D., Lin, R., Wittmann, C., Bei, Y., Cha, Y. H., Ali, M., Priess, J. R., and Mello, C. C. (1997). Wnt signaling and an APC-related gene specify endoderm in early *C. elegans* embryos. Cell *90*, 707-716.

Rocheleau, C. E., Yasuda, J., Shin, T. H., Lin, R., Sawa, H., Okano, H., Priess, J. R., Davis, R. J., and Mello, C. C. (1999). WRM-1 activates the LIT-1 protein kinase to transduce anterior/posterior polarity signals in *C. elegans*. Cell *97*, 717-726.

Rohatgi, R., Ma, L., Miki, H., Lopez, M., Kirchhausen, T., Takenawa, T., and Kirschner, M. W. (1999). The interaction between N-WASP and the Arp2/3 complex links Cdc42-dependent signals to actin assembly. Cell *97*, 221-231.

Ross, M. H., Romrell, L. J., and Kaye, G. I. (1995). Histology : A Text and Atlas (Baltimore: Williams & Wilkins).

Saher, G., Brügger, B., Lappe-Siefke, C., Möbius, W., Tozawa, R., Wehr, M. C., Wieland, F., Ishibashi, S., and Nave, K. A. (2005). High cholesterol level is essential for myelin membrane growth. Nat Neurosci *8*, 468-475.

Sawa, H., Lobel, L., and Horvitz, H. R. (1996). The *Caenorhabditis elegans* gene *lin-17*, which is required for certain asymmetric cell divisions, encodes a putative seven-transmembrane protein similar to the *Drosophila* frizzled protein. Genes Dev. *10*, 2189-2197.

Schneitz, K., Spielmann, P., and Noll, M. (1993). Molecular genetics of Aristaless, a prd-type homeo box gene involved in the morphogenesis of proximal and distal pattern elements in a subset of appendages in *Drosophila*. Genes Dev *7*, 911.

Schulte, J., Tepass, U., and Auld, V. J. (2003). Gliotactin, a novel marker of tricellular junctions, is necessary for septate junction development in *Drosophila*. J Cell Biol *161*, 991-1000.

Schwabe, T., Bainton, R. J., Fetter, R. D., Heberlein, U., and Gaul, U. (2005). GPCR signaling is required for blood-brain barrier formation in *Drosophila*. Cell *123*, 133-144.

Seaman, M. N. (2005). Recycle your receptors with retromer. Trends Cell Biol *15*, 68-75.

Seaman, M. N., McCaffery, J. M., and Emr, S. D. (1998). A membrane coat complex essential for endosome-to-Golgi retrograde transport in yeast. J Cell Biol *142*, 665-681.

Sepp, K. J., Schulte, J., and Auld, V. J. (2000). Developmental dynamics of peripheral glia in *Drosophila melanogaster*. Glia *30*, 122-133.

Shaham, S. (2005). Glia-neuron interactions in nervous system function and development. Curr Top Dev Biol *69*, 39-66.

Shaham, S. (2009). galign: a tool for rapid genome polymorphism discovery. PLoS ONE *4*, e7188.

Shanbhag, S. R., Muller, B., and Steinbrecht, R. A. (1999). Atlas of olfactory organs of *Drosophila melanogaster* 1. Types, external organization, innervation and distribution of olfactory sensilla. International Journal of Insect Morphology and Embryology *28*, 377-379.

Shanbhag, S. R., Müller, B., and Steinbrecht, R. A. (2000). Atlas of olfactory organs of *Drosophila melanogaster* 2. Internal organization and cellular architecture of olfactory sensilla. Arthropod Struct Dev *29*, 211-229.

Shin, N., Lee, S., Ahn, N., Kim, S. A., Ahn, S. G., YongPark, Z., and Chang, S. (2007). Sorting nexin 9 interacts with dynamin 1 and N-WASP and coordinates synaptic vesicle endocytosis. J Biol Chem *282*, 28939-28950.

Shin, T. H., Yasuda, J., Rocheleau, C. E., Lin, R., Soto, M., Bei, Y., Davis, R. J., and Mello, C. C. (1999). MOM-4, a MAP kinase kinase kinase-related protein, activates WRM-1/LIT-1 kinase to transduce anterior/posterior polarity signals in *C. elegans*. Mol. Cell *4*, 275-280.

Siegfried, K. R., and Kimble, J. (2002). POP-1 controls axis formation during early gonadogenesis in *C. elegans*. Development *129*, 443-453.

Simmer, F., Tijsterman, M., Parrish, S., Koushika, S. P., Nonet, M. L., Fire, A., Ahringer, J., and Plasterk, R. H. (2002). Loss of the putative RNA-directed RNA polymerase RRF-3 makes *C. elegans* hypersensitive to RNAi. Curr. Biol. *12*, 1317-1319.

Simons, M., and Mlodzik, M. (2008). Planar cell polarity signaling: from fly development to human disease. Annu Rev Genet *42*, 517-540.

Spacek, J. (1985). Three-dimensional analysis of dendritic spines. III. Glial sheath. Anat. Embryol. *171*, 245-252.

Starich, T. A., Herman, R. K., Kari, C. K., Yeh, W. H., Schackwitz, W. S., Schuyler, M. W., Collet, J., Thomas, J. H., and Riddle, D. L. (1995). Mutations affecting the chemosensory neurons of *Caenorhabditis elegans*. Genetics *139*, 171-188.

Strauss, O. (2005). The retinal pigment epithelium in visual function. Physiol Rev *85*, 845-881.

Strømme, P., Mangelsdorf, M. E., Scheffer, I. E., and Gécz, J. (2002). Infantile spasms, dystonia, and other X-linked phenotypes caused by mutations in Aristaless related homeobox gene, ARX. Brain Dev *24*, 266-268.

Strutt, H., and Strutt, D. (2003). EGF signaling and ommatidial rotation in the *Drosophila* eye. Current Biology *13*, 1451-1457.

Sulston, J. E., Albertson, D. G., and Thomson, J. N. (1980). The *Caenorhabditis elegans* male: postembryonic development of nongonadal structures. Dev Biol *78*, 542-576.

Sulston, J. E., Schierenberg, E., White, J. G., and Thomson, J. N. (1983). The embryonic cell lineage of the nematode *Caenorhabditis elegans*. Dev. Biol. *100*, 64-119.

Suzuki, N., Buechner, M., Nishiwaki, K., Hall, D. H., Nakanishi, H., Takai, Y., Hisamoto, N., and Matsumoto, K. (2001). A putative GDP-GTP exchange factor is required for development of the excretory cell in *Caenorhabditis elegans*. EMBO Rep *2*, 530-535.

Suzuki, Y., Takeda, M., and Farbman, A. I. (1996). Supporting cells as phagocytes in the olfactory epithelium after bulbectomy. J. Comp. Neurol. *376*, 509-517.

Swoboda, P., Adler, H. T., and Thomas, J. H. (2000). The RFX-type transcription factor DAF-19 regulates sensory neuron cilium formation in *C. elegans*. Mol Cell *5*, 411-421.

Symons, M., Derry, J. M., Karlak, B., Jiang, S., Lemahieu, V., Mccormick, F., Francke, U., and Abo, A. (1996). Wiskott-Aldrich syndrome protein, a novel effector for the GTPase CDC42Hs, is implicated in actin polymerization. Cell *84*, 723-734.

Takada, R., Satomi, Y., Kurata, T., Ueno, N., Norioka, S., Kondoh, H., Takao, T., and Takada, S. (2006). Monounsaturated fatty acid modification of Wnt protein: its role in Wnt secretion. Developmental Cell *11*, 791-801.

Takeshita, H., and Sawa, H. (2005). Asymmetric cortical and nuclear localizations of WRM-1/beta-catenin during asymmetric cell division in *C. elegans*. Genes Dev. *19*, 1743-1748.

Tanentzapf, G., and Tepass, U. (2003). Interactions between the crumbs, lethal giant larvae and bazooka pathways in epithelial polarization. Nat Cell Biol *5*, 46-52.

Taveggia, C., Zanazzi, G., Petrylak, A., Yano, H., Rosenbluth, J., Einheber, S., Xu, X., Esper, R. M., Loeb, J. A., Shrager, P., Chao, M. V., Falls, D. L., Role, L., and Salzer, J. L. (2005). Neuregulin-1 type III determines the ensheathment fate of axons. Neuron *47*, 681-694.

Thorpe, C. J., and Moon, R. T. (2004). nemo-like kinase is an essential co-activator of Wnt signaling during early zebrafish development. Development *131*, 2899-2909.

Thorpe, C. J., Schlesinger, A., Carter, J. C., and Bowerman, B. (1997). Wnt signaling polarizes an early *C. elegans* blastomere to distinguish endoderm from mesoderm. Cell *90*, 695-705.

Tolwani, R. J., Cosgaya, J. M., Varma, S., Jacob, R., Kuo, L. E., and Shooter, E. M. (2004). BDNF overexpression produces a long-term increase in myelin formation in the peripheral nervous system. J Neurosci Res *77*, 662-669.

Tonning, A., Hemphälä, J., Tång, E., Nannmark, U., Samakovlis, C., and Uv, A. (2005). A transient luminal chitinous matrix is required to model epithelial tube diameter in the *Drosophila* trachea. Dev Cell *9*, 423-430.

Trajkovic, K., Dhaunchak, A. S., Goncalves, J. T., Wenzel, D., Schneider, A., Bunt, G., Nave, K. A., and Simons, M. (2006). Neuron to glia signaling triggers myelin membrane exocytosis from endosomal storage sites. J Cell Biol *172*, 937-948.

Trent, C., Tsuing, N., and Horvitz, H. R. (1983). Egg-laying defective mutants of the nematode *Caenorhabditis elegans*. Genetics *104*, 619-647.

Trifaró, J. M., Gasman, S., and Gutiérrez, L. M. (2008). Cytoskeletal control of vesicle transport and exocytosis in chromaffin cells. Acta Physiol. (Oxf) *192*, 165-172.

Tsarouhas, V., Senti, K. A., Jayaram, S. A., Tiklová, K., Hemphälä, J., Adler, J., and Samakovlis, C. (2007). Sequential pulses of apical epithelial secretion and endocytosis drive airway maturation in *Drosophila*. Dev. Cell *13*, 214-225.

Tucker, M., Sieber, M., Morphew, M., and Han, M. (2005). The *Caenorhabditis elegans* aristaless orthologue, alr-1, is required for maintaining the functional and structural integrity of the amphid sensory organs. Mol Biol Cell *16*, 4695-4704.

Uv, A., Cantera, R., and Samakovlis, C. (2003). *Drosophila* tracheal morphogenesis: intricate cellular solutions to basic plumbing problems. Trends Cell Biol *13*, 301-309.

Valentijn, J. A., Valentijn, K., Pastore, L. M., and Jamieson, J. D. (2000). Actin coating of secretory granules during regulated exocytosis correlates with the release of rab3D. Proc. Natl. Acad. Sci. USA *97*, 1091-1095.

van Weering, J. R., Verkade, P., and Cullen, P. J. (2010). SNX-BAR proteins in phosphoinositide-mediated, tubular-based endosomal sorting. Semin Cell Dev Biol *21*, 371-380.

Vega-Salas, D. E., Salas, P. J., and Rodriguez-Boulan, E. (1987). Modulation of the expression of an apical plasma membrane protein of Madin-Darby canine kidney epithelial cells: cell-cell interactions control the appearance of a novel intracellular storage compartment. J Cell Biol *104*, 1249-1259.

Vega-Salas, D. E., Salas, P. J., and Rodriguez-Boulan, E. (1988). Exocytosis of vacuolar apical compartment (VAC): a cell-cell contact controlled mechanism for the establishment of the apical plasma membrane domain in epithelial cells. J. Cell Biol. *107*, 1717-1728.

Ventura, R., and Harris, K. M. (1999). Three-dimensional relationships between hippocampal synapses and astrocytes. J. Neurosci. *19*, 6897-6906.

Verheyen, E. M., Mirkovic, I., MacLean, S. J., Langmann, C., Andrews, B. C., and MacKinnon, C. (2001). The tissue polarity gene *nemo* carries out multiple roles in patterning during *Drosophila* development. Mech Dev *101*, 119-132.

Vowels, J. J., and Thomas, J. H. (1994). Multiple chemosensory defects in *daf-11* and *daf-21* mutants of *Caenorhabditis elegans*. Genetics *138*, 303-316.

Walston, T., Guo, C., Proenca, R., Wu, M., Herman, M., Hardin, J., and Hedgecock, E. (2006). *mig-5*/Dsh controls cell fate determination and cell migration in *C. elegans*. Dev. Biol. *298*, 485-497.

Wang, S., Jayaram, S. A., Hemphälä, J., Senti, K. A., Tsarouhas, V., Jin, H., and Samakovlis, C. (2006). Septate-junction-dependent luminal deposition of chitin deacetylases restricts tube elongation in the *Drosophila* trachea. Current Biology *16*, 180-185.

Wang, Y., Apicella, A., Lee, S. K., Ezcurra, M., Slone, R. D., Goldmit, M., Schafer, W. R., Shaham, S., Driscoll, M., and Bianchi, L. (2008). A glial DEG/ENaC channel functions with neuronal channel DEG-1 to mediate specific sensory functions in *C. elegans*. EMBO J. *27*, 2388-2399.

Ward, R. E., Schweizer, L., Lamb, R. S., and Fehon, R. G. (2001). The protein 4.1, ezrin, radixin, moesin (FERM) domain of *Drosophila Coracle*, a cytoplasmic component of the septate junction, provides functions essential for embryonic development and imaginal cell proliferation. Genetics *159*, 219-228.

Ward, S., Thomson, N., White, J. G., and Brenner, S. (1975). Electron microscopical reconstruction of the anterior sensory anatomy of the nematode *Caenorhabditis elegans*. J. Comp. Neurol. *160*, 313-337.

Watanabe, S., Punge, A., Hollopeter, G., Willig, K. I., Hobson, R. J., Davis, M. W., Hell, S. W., and Jorgensen, E. M. (2011). Protein localization in electron micrographs using fluorescence nanoscopy. Nat. Methods *8*, 80-84.

Wenzel, J., Lammert, G., Meyer, U., and Krug, M. (1991). The influence of long-term potentiation on the spatial relationship between astrocyte processes and potentiated synapses in the dentate gyrus neuropil of rat brain. Brain Res *560*, 122-131.

Werner, H. B., and Jahn, O. (2010). Myelin matters: proteomic insights into white matter disorders. Expert Rev Proteomics *7*, 159-164.

Wheeler, S. R., Banerjee, S., Blauth, K., Rogers, S. L., Bhat, M. A., and Crews, S. T. (2009). Neurexin IV and Wrapper interactions mediate *Drosophila* midline glial migration and axonal ensheathment. Development *136*, 1147-1157.

White, J. G., Southgate, E., Thomson, J. N., and Brenner, S. (1986). The structure of the nervous system of the nematode *C. elegans*. Philosophical Transactions of the Royal Society of London - Series B: Biological Sciences *314*, 1-340.

Wicks, S. R., Yeh, R. T., Gish, W. R., Waterston, R. H., and Plasterk, R. H. (2001). Rapid gene mapping in *Caenorhabditis elegans* using a high density polymorphism map. Nat. Genet. *28*, 160-164.

Willert, K., Brown, J. D., Danenberg, E., Duncan, A. W., Weissman, I. L., Reya, T., Yates, J. R., and Nusse, R. (2003). Wnt proteins are lipid-modified and can act as stem cell growth factors. Nature *423*, 448-452.

Withee, J., Galligan, B., Hawkins, N., and Garriga, G. (2004). *Caenorhabditis elegans* WASP and Ena/VASP Proteins Play Compensatory Roles in Morphogenesis and Neuronal Cell Migration. Genetics *167*, 1165.

Wolff, J. R., and Bär, T. (1972). 'Seamless' endothelia in brain capillaries during development of the rat's cerebral cortex. Brain Res *41*, 17-24.

Woodhoo, A., and Sommer, L. (2008). Development of the Schwann cell lineage: from the neural crest to the myelinated nerve. Glia *56*, 1481-1490.

Wu, M., and Herman, M. A. (2006). A novel noncanonical Wnt pathway is involved in the regulation of the asymmetric B cell division in *C. elegans*. Dev Biol *293*, 316-329.

Wu, V. M., and Beitel, G. J. (2004). A junctional problem of apical proportions: epithelial tube-size control by septate junctions in the *Drosophila* tracheal system. Curr Opin Cell Biol *16*, 493-499.

Wu, V. M., Schulte, J., Hirschi, A., Tepass, U., and Beitel, G. J. (2004). Sinuous is a *Drosophila* claudin required for septate junction organization and epithelial tube size control. J Cell Biol *164*, 313-323.

Yang, P. T., Lorenowicz, M. J., Silhankova, M., Coudreuse, D. Y., Betist, M. C., and Korswagen, H. C. (2008). Wnt signaling requires retromer-dependent recycling of MIG-14/Wntless in Wnt-producing cells. Dev Cell *14*, 140-147.

Yarar, D., Waterman-Storer, C. M., and Schmid, S. L. (2007). SNX9 couples actin assembly to phosphoinositide signals and is required for membrane remodeling during endocytosis. Dev Cell *13*, 43-56.

Yoshimura, S., Murray, J. I., Lu, Y., Waterston, R. H., and Shaham, S. (2008). *mls-2* and *vab-3* Control glia development, hlh-17/Olig expression and glia-dependent neurite extension in *C. elegans*. Development *135*, 2263-2275.

Young, R. W., and Bok, D. (1969). Participation of the retinal pigment epithelium in the rod outer segment renewal process. J. Cell Biol. *42*, 392-403.

Yu, R. Y., Nguyen, C. Q., Hall, D. H., and Chow, K. L. (2000). Expression of *ram-5* in the structural cell is required for sensory ray morphogenesis in *Caenorhabditis elegans* male tail. EMBO J *19*, 3542-3555.

Yu, S., Avery, L., Baude, E., and Garbers, D. L. (1997). Guanylyl cyclase expression in specific sensory neurons: a new family of chemosensory receptors. Proc. Natl. Acad. Sci. USA *94*, 3384-3387.

Yu, W., O'Brien, L. E., Wang, F., Bourne, H., Mostov, K. E., and Zegers, M. M. (2003). Hepatocyte growth factor switches orientation of polarity and mode of movement during morphogenesis of multicellular epithelial structures. Mol Biol Cell *14*, 748-763.

Zelhof, A. C., Hardy, R. W., Becker, A., and Zuker, C. S. (2006). Transforming the architecture of compound eyes. Nature *443*, 696-699.

Zeng, Y. A., Rahnama, M., Wang, S., Sosu-Sedzorme, W., and Verheyen, E. M. (2007). *Drosophila* Nemo antagonizes BMP signaling by phosphorylation of Mad and inhibition of its nuclear accumulation. Development *134*, 2061-2071.

Zeng, Y. A., and Verheyen, E. M. (2004). Nemo is an inducible antagonist of Wingless signaling during *Drosophila* wing development. Development *131*, 2911-2920.

Zhang, J., Zhang, X., Guo, Y., Xu, L., and Pei, D. (2009). Sorting nexin 33 induces mammalian cell micronucleated phenotype and actin polymerization by interacting with Wiskott-Aldrich syndrome protein. J Biol Chem *284*, 21659-21669.

Zheng, L., Zhang, J., and Carthew, R. W. (1995). *frizzled* regulates mirror-symmetric pattern formation in the *Drosophila* eye. Development *121*, 3045-3055.

Zinovyeva, A. Y., and Forrester, W. C. (2005). The *C. elegans* Frizzled CFZ-2 is required for cell migration and interacts with multiple Wnt signaling pathways. Dev. Biol. *285*, 447-461.

Zipursky, S. L., Venkatesh, T. R., Teplow, D. B., and Benzer, S. (1984). Neuronal development in the *Drosophila* retina: monoclonal antibodies as molecular probes. Cell *36*, 15-26.